POST-MODIFICATION OF THERMOSENSITIVE MICROGELS IN BLEACH

POST-MODIFICATION OF THERMOSENSITIVE MICROGELS IN BLEACH

By

ZUOHE WANG, B. Eng., M. Eng.

A Thesis

Submitted to the School of Graduate Studies

in Partial Fulfillment of the Requirements

for the Degree

Doctor of Philosophy

McMaster University

DOCTOR OF PHILOSOPHY (2013) McMaster University

(Chemical Engineering) Hamilton, Ontario

TITLE: Post-Modification of Thermosensitive Microgels in Bleach

AUTHOR: Zuohe Wang

B. Eng. (Zhejiang University)

M. Eng. (Zhejiang University)

SUPERVISOR: Professor Robert H. Pelton

NUMBER OF PAGES: viii, 103

Abstract

N-chloramide containing and primary amine-containing microgels were prepared by post-modification of thermosensitive microgels in alkaline bleach. The objective of this project was to develop simple strategies for preparation of functionalized microgels.

N-chlorination of linear poly(N-isopropylacrylamide) (PNIPAM) in bleach at high pH resulted in a novel N-chloramide containing copolymer: poly(NIPAM-co-NIPAMCl). The chlorinated PNIPAM showed controlled phase transition temperature and oxidative ability. The N-chlorination of linear PNIPAM inspired the preparation of N-chloramide containing PNIPAM microgels in a similar way. The phase transition temperature of the resulted chlorinated microgels, which corresponds to the extent of N-chlorination, was affected by the reaction temperature and salt concentration. The reaction between the chlorinated microgels and glutathione is proposed as diffusion controlled.

The N-chlorination of poly(N-isopropylmethacrylamide) (PNIPMAM) microgels in bleach was restricted, in comparison with PNIPAM microgels. The active chlorine content of chlorinated PNIPMAM microgels was about one-tenth of that of chlorinated PNIPAM microgels under the same N-chlorination condition. It is proposed that the high stability of PNIPMAM in bleach is a result of the electron-donating effect of methyl groups on PNIPMAM backbone. Hence, core-shell microgels with PNIPAM cores and poly(NIPAM-co-NIPMAM) shells showed improved colloidal stability after N-chlorination because the shell was less chlorinated and served as a steric stabilizer.

Finally, primary amine-containing microgels were prepared via Hofmann rearrangement of copolymers of methacrylamide, which decomposed to give amines, and NIPMAM, which did not react. The method was further extended to give amphoteric microgels by including acrylic acid in the starting microgels. Although other approaches to aminated and amphoteric microgels have been developed, this approach is particularly attractive because of the ease of the reaction and the ability to control the microgel isoelectric points.

Acknowledgements

First, I would like to express my deepest thanks to my supervisor, Prof. Robert Pelton. I wish to thank him for priceless guidance and help in this project. I also appreciate all the opportunities Prof. Pelton provided to attend academic conferences.

I would like to thank my supervisory committee members, Prof. Shiping Zhu, and Prof. Yingfu Li, for their valuable advice and help in this project.

I would also like to thank Prof. Michael Brook, Prof. Harald Stover and Prof. Todd Hoare for their useful discussion in this project.

I would like to thank Ms. Merica West for her help with TEM, Ms. Marnie Timleck for her help with confocal microscopy, Dr. Nick Burke for his help with GPC, Dr. Hilary A. Jenkins for training of nuclear magnetic resonance, Prof. Harald Stover and Prof. Alex Adronov for the access to their instruments. I would also like thank summer students Miles Montgomery, Kyle Lefebvre, Wing Yan Lam, Jill McKenna and Yue Zhang for their hard work.

I would like to acknowledge my colleagues in McMaster Interfacial Technologies Group for their support and friendship. Specifically, I would like to thank Dr. Wei Chen for training of microelectrophoresis, Dr. Yuguo Cui for training of dynamic light scattering and conductometric titration, Dr. Quan Wen for training of microgel preparation, Dr. Songtao Yang for training of spectrophotometer.

I would like to thank our laboratory manager Mr. Doug Keller and administrative sectary Ms. Sally Watson for their help. I am indebted to Ms. Kathy Goodram, Ms. Lynn Falkiner, Ms. Nanci Cole, Ms. Melissa Vasi and Ms. Cathie Roberts for their administrative assistance, Mr. Paul Gatt, Ms. Justyna Derkach and Mr. Dan Wright for their technical assistance.

I would like to acknowledge Natural Sciences and Engineering Research Council of Canada and BASF Canada for their financial support.

Finally, I would like to thank my parents and my brother for their love and support.

Table of content

Abbreviations

AA	acrylic acid
APS	ammonium persulfate
t-BuOK	potassium *tert*-butoxide
CFT	critical flocculation temperature
CPT	cloud point temperature
DLS	dynamic light scattering
DS	degrees of substitution
EGDMA	ethylene glycol dimethacrylate
GPC	gel permeation chromatography
GSH	glutathione; γ-L-Glutamyl-L-cysteinylglycine
IEP	isoelectric point
LCST	lower critical solution temperature
MAA	methacrylic acid
MAM	methacrylamide
MBA	N,N-methylenebisacrylamide
MW	molecular weight
MWCO	molecular weight cut-off
NaClO	sodium hypochlorite, bleach
$Na_2S_2O_3$	sodium thiosulfate
NIPAM	N-isopropylacrylamide

NIPMAM	N-isopropylmethacrylamide
NMR	nuclear magnetic resonance
PBS	phosphate buffered saline
PNIPAM	poly(N-isopropylacrylamide)
PNIPMAM	poly(N-isopropylmethacrylamide)
Poly(NIPAM-co-NIPAMCl)	N-chlorinated PNIPAM
SDS	sodium dodecyl sulfate
TEM	transmission electron microscopy
TEMPO	2,2,6,6-tetramethyl-1-piperidinyloxy
VAA	vinylacetic acid
VPTT	volume phase transition temperature

Chapter 1 Introduction

1.1 Literature Review

1.1.1 Poly(N-isopropylacrylamide)

Poly(N-isopropylacrylamide), PNIPAM, has been widely investigated as thermosensitive materials.[1] Aqueous PNIPAM has a lower critical solution temperature (LCST) of 32 ^{o}C. Heskins and Guillet[2] first reported a phase diagram of aqueous PNIPAM (Figure 1), which demonstrates a reversible temperature-induced switching of PNIPAM chains. At low temperature, PNIPAM chains are highly hydrated and behave as random coils. As a result, the aqueous suspension is homogenous and transparent. In contrast, PNIPAM chains collapse into globules at high temperature, resulting in a turbid suspension. It should be noted that the stability of the collapsed globules is affected by polymer concentration. Chan et al.[3] showed that colloidally stable nanoparticles were found in dilute PNIPAM solution at temperature higher than LCST.

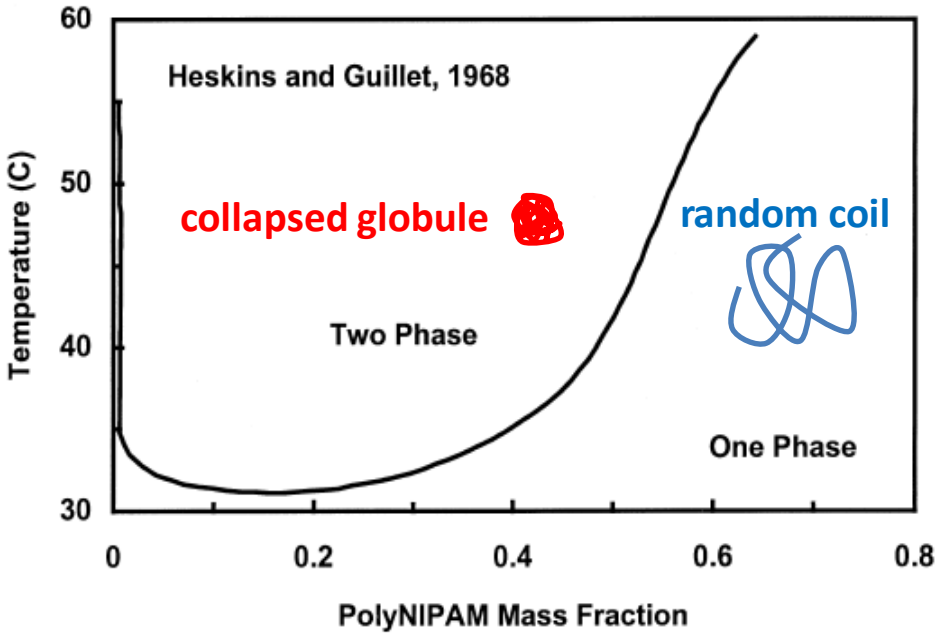

Figure 1 The phase diagram for aqueous PNIPAM, adapted from Heskins and Guillet[2].

The thermosensitive behavior of aqueous PNIPAM can be explained by the competition between hydrogen bonding and hydrophobic interaction.[1] As shown in Figure 2, the pendant amides of PNIPAM can form hydrogen bonds with water molecules, and the isopropyl groups induce hydrophobic interaction (intra-chain and inter-chain). Below LCST, the hydrogen bonding between polymer chains and water molecules dominates the

solubility of PNIPAM in water, resulting in a homogenous and transparent suspension. Increasing temperature breaks the hydrogen bonds, leading to the decrease of PNIPAM-water interaction. Therefore the hydrophobic interaction dominates, inducing phase separation of aqueous PNIPAM. In an extended study, Katsumoto et al.[4] revealed that PNIPAM chains formed intra-chain hydrogen bonds even in good solvents (e.g. cold water), via infrared spectroscopy and the quantum chemical calculations. The authors argued that the intra-chain hydrogen bond played an important role in phase separation of PNIPAM.

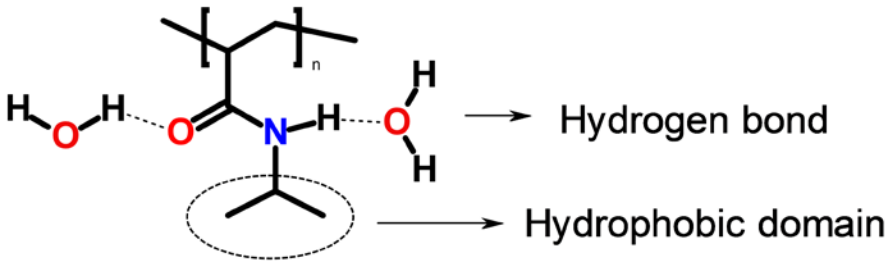

Figure 2 Hydrogen bonds and hydrophobic domain of PNIPAM in water

Although aqueous PNIPAM phase-separates due to hydrophobic interaction above LCST, it is important to point out that PNIPAM is never hydrophobic.[5] It has been found that the collapsed globule is still hydrated. Heskins and Guillet[2] reported a 52% water content and Kujawa et al.[6] suggested a 60% water content of polymer aggregates above LCST.

It is noticeable that the LCST of aqueous PNIPAM is not always 32 ^{o}C. Stöver and coworkers found that the LCST was affected by molecule weight (MW)[7] and end chain groups[8]. They successfully prepared a serial of linear PNIPAM with various MW and end groups via atom transfer radical polymerization. They found that PNIPAM with lower MW and more hydrophilic end groups had higher LCST. However, it is impractical to tune LCST via MW and end chain groups.

The most used method to tune the LCST is copolymerization of NIPAM with comonomers. PNIPAM copolymers with hydrophilic comonomers, such as acrylamide, 1-vinyl-2-pyrrolidinone and *N*, *N*- dimethylacrylamide, have LCST higher than 32 ^{o}C.[9-10] PNIPAM with high LCST can be used as drug carriers.[11] In contrast, copolymers prepared from copolymerization of NIPAM and hydrophobic comonomers exhibit LCST lower than 32 ^{o}C.[12] For example, the copolymerization of NIPAM and *n*-dodecyl- and adamantyl-containing monomers[13-14] has been reported. The hydrophobically modified PNIPAM can be used as rheology modifiers in oilfield.[1]

1.1.2 Thermosensitive Microgels

PNIPAM has been fabricated into block copolymers[15-16], brushes[17-19], gel[20] and microgels[21-22]. This project focuses on PNIPAM microgels, with diameters in a range of

50 nm to 5 μm[21]. PNIPAM microgels were first prepared by Pelton and Chibante[23], following a precipitation polymerization mechanism, as schematically described in Figure 3A. Briefly, NIPAM monomers are dissolved in water at the reaction temperature (e.g. 70 ^{o}C), and the reaction starts upon adding persulfate initiators. The formed PNIPAM phase-separates from the reaction solution, resulting in precursor particles. The precursor particles, which are colloidally unstable, aggregate into stable primary particles. Further growth of the primary particles results in the final collapsed microgels. The microgels prepared from this method are nearly monodisperse, as shown in the TEM image (Figure 3B).

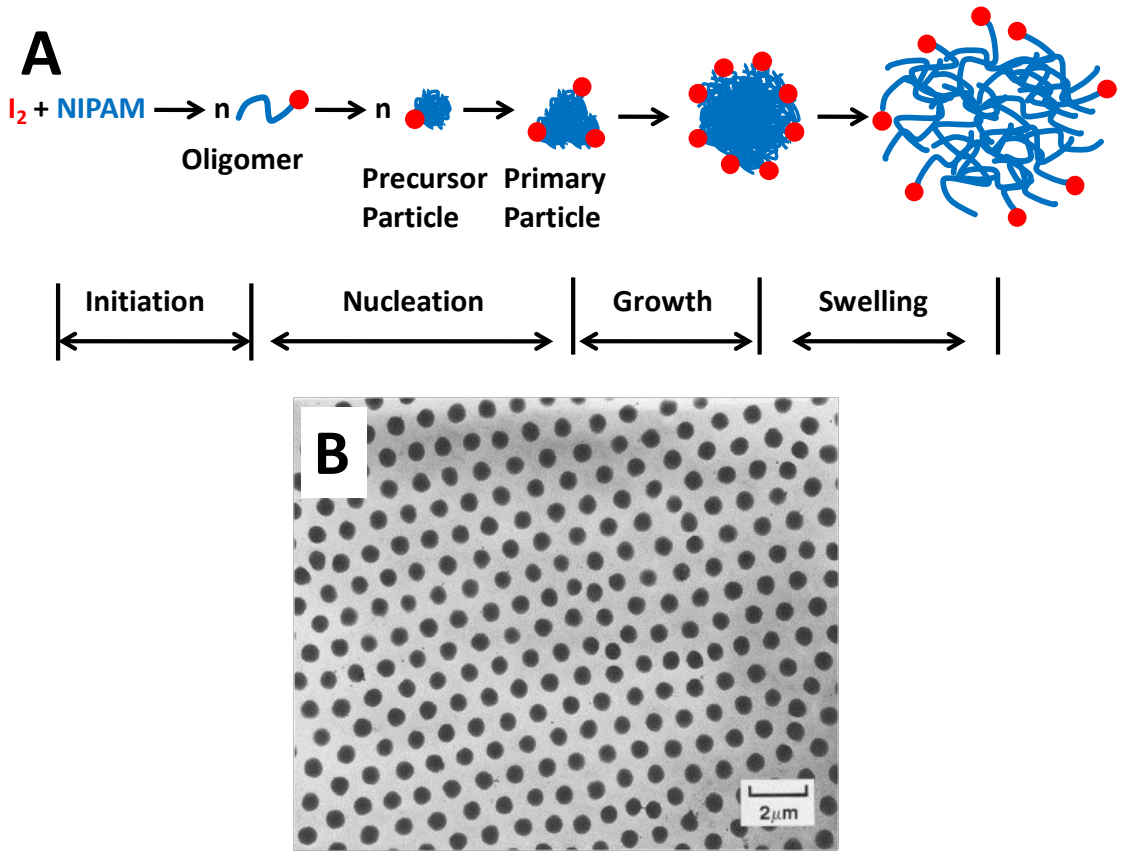

Figure 3 A) Formation mechanism of PNIPAM microgels, adapted from Pelton and Hoare.[24] B) TEM image of PNIPAM microgels, adapted from Pelton and Chibante.[23]

In a typical recipe, bifunctional monomers (e.g. *N*,*N'*-methylenebisacrylamide) were added to the reaction solution as crosslinkers, which prevents PNIPAM chains from departing at a low temperature after polymerization.[23] However, one should note that bifunctional monomers are not essential to give crosslinking to PNIPAM microgels. Gao and Frisken have reported the preparation of PNIPAM microgels in the absence of crosslinker.[25-26] The resulted microgels did not dissolve below the LCST, due to self-crosslinking between PNIPAM chains induced by chain transfer reaction. Another

important component for the formation of PNIPAM microgels is ionic surfactants (e.g. SDS), which can reduce particle size and increase colloidal stability during polymerization.[27]

PNIPAM microgels display a temperature-induced reversible shrinking/swelling behavior, as shown in Figure 4. PNIPAM microgel has a volume phase transition temperature (VPTT) between 32 to 35 ^{o}C[21], which is close to the LCST of linear PNIPAM. The microgels are shrunken above VPTT and fully swollen below VPTT. The physical properties of PNIPAM microgels are very different at shrunken state and swollen state:

1. *Water content* - PNIPAM microgels are highly swollen with ~90% water below VPTT, while the water content decreases to ~25% above VPTT.[21] Therefore the particle size significantly decreases upon increasing temperature.

2. *The molecular self-diffusion coefficient* of shrunken microgels is lower than that of swollen microgels. It has been determined that self-diffusion coefficient of water in PNIPAM microgels is 4.3×10^{-10} m^2 s^{-1} in swollen microgels, while it decreases to 1.7×10^{-11} m^2 s^{-1} in shrunken microgels.[28]

3. *Hamaker constant* - Vincent and coworkers showed that the Hamaker constant of the shrunken microgels was larger than the constant of swollen microgels.[29] As a result, the van der Waals attraction between the shrunken microgels is stronger than that between swollen microgels, which could lead to homoaggregation of microgel particles.[30]

4. *The Young's modulus* of single PNIPAM microgel has been investigated with atomic force microscopy.[31-32] It has been found that the microgel modulus in the shrunken state is about 10~15-folds higher than that in the swollen state, indicating the shrunken microgels are much stiffer than the swollen microgels.

5. *Refractive index* - It has been argued that the refractive index of the shrunken microgels is higher than that of swollen microgels.[33-34]

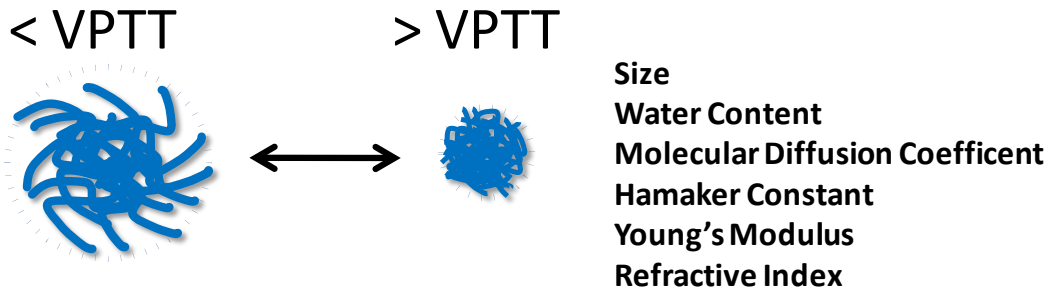

Figure 4 Thermosensitivity of PNIPAM microgels and physical properties affected in different states.

Poly(N-isopropylmethacrylamide) (PNIPMAM) is another important thermosensitive polymer. PNIPMAM has methyl group on the backbone, instead of alpha hydrogen on PNIPAM backbone (Figure 5). PNIPMAM has a LCST around 44 ^{o}C, which is higher than PNIPAM.[35] This is because the polymer chain of PNIPMAM is stiffer than PNIPAM chain, which requires higher energy for PNIPMAM chain collapse and association.[36] Microgels based on PNIPMAM have also been prepared following the precipitation polymerization mechanism.[37-38] Due to its high phase transition temperature, PNIPMAM microgel is swollen at physiological temperature, which is likely to reduce adsorption of proteins under the physiological condition. Thus PNIPMAM microgels have been used as carrier for siRNA delivery.[39]

PNIPAM PNIPMAM

Figure 5 Chemical structures of PNIPAM and PNIPMAM.

1.1.3 Synthesis of Copolymer Microgels

PNIPAM (or PNIPMAM) microgels are thermosensitive, soft and deformable, which are very different from silica and polystyrene and other hard particles. Hence these microgels have applications in many fields: such as drug delivery[40], nanocomposite[41-42], biosensing[43-44], optical devices[34, 45], and separation[46]. In most applications, copolymer microgels with specific functional groups are required. Many efforts have been made to prepare functionalized PNIPAM microgels with various functional groups, including phenylboronic[43], carboxyl[47], azido and terminal alkyne[48], glycidyl[49], amine[50] and thiol[51], etc. These groups offer either additional stimuli-responsive property, reactivity or conjugation sites for further modification.

Copolymer microgels can be prepared by inverse emulsion polymerization[52-53], reversed suspension polymerization[54], or microfluidic process[55-56]. Polymerization of NIPAM is conducted in dispersed aqueous phase in these methods, giving microgels with uniform crosslinker distribution. However, inverse emulsion and suspension polymerization require organic solvents as continuous phase, and surfactants. Microfluidic process requires both organic solvents and special microfluidic devices. These drawbacks limit the application of such methods in preparation of copolymer microgels. To date, the most used way to functionalized PNIPAM microgels is the precipitation copolymerization in water.

Hoare and Pelton systematically investigated the precipitation copolymerization of NIPAM with carboxyl-containing comonomers.[47, 57-59] They found the distribution of

carboxyl in microgel was strongly affected by the chemistry and reactivity of the comonomers. Carboxyl groups were concentrated in the microgel core when methacrylic acid was used as comonomers, while the carboxyl distribution was much more uniform by using acrylic acid as comonomers. This is because methacrylic acid was consumed much faster than NIPAM during precipitation copolymerization. In contrast, most carboxyl groups were located on the periphery of microgels when vinylacetic acid was used as comonomers, due to the low reactivity ratio and high chain transfer constant of vinylacetic acid. A kinetic model has been developed by Hoare and McLean[59] to predict the carboxyl group distribution in PNIPAM microgels. The model verified the experimental results that the carboxyl group distribution is indeed controlled by the reactivity ratio and chemistry of carboxyl comonomers[58], as shown in Figure 6. Hoare and Pelton also found that the carboxyl distribution strongly affected the property and application of microgels, such as swelling[60], drug uptake[61] and glucose sensing[43].

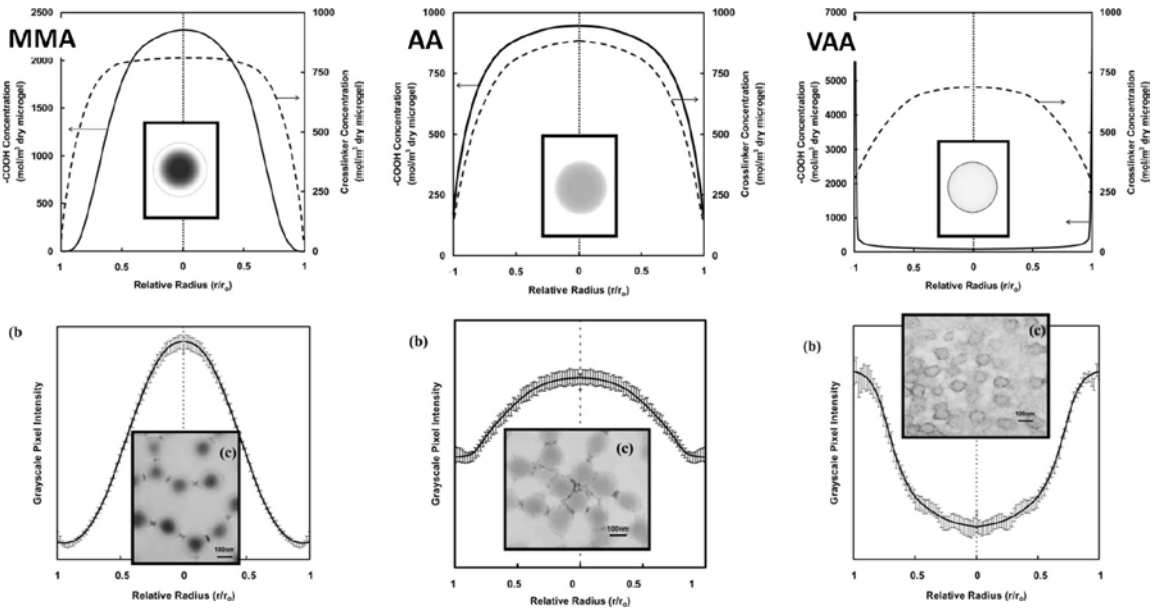

Figure 6 Axial distribution of carboxyl group in PNIPAM microgels with different comonomers (MMA, AA and VAA): model calculation (upper) and experimental results (bottom).[58]

It should be noted that some active groups cannot be directly incorporated in PNIPAM microgels via precipitation copolymerization. In this case, a post-modification method should be introduced to convert stable functional groups into active groups after polymerization. For example, thiol group is a strong chain transfer agent, which is unstable under the polymerization condition. Therefore, Gaulding et al.[51] prepared PNIPMAM microgels with disulfide crosslinkers, and then reduced disulfide into thiol groups with dithiothreitol. Also, primary amine-containing PNIPAM microgels can be prepared in a post-modification manner, such as hydrolysis of formamide-containing microgels[62].

1.1.4 Modification on Pure PNIPAM

As presented in previous sections, comonomers are required to prepare functionalized PNIPAM linear polymer and microgels. The possibility of modification on pure PNIPAM is considered here. An obvious option is hydrolysis of amides in PNIPAM, introducing carboxyls to PNIPAM. However, the hydrolysis of pendant amides is restrained. Hoare and Pelton[57] showed that the hydrolysis of PNIPAM microgels in both acidic and basic conditions, resulting in carboxylic-containing copolymer microgels, was slow and inefficient. Only 1% hydrolysis of PNIPAM was obtained after 120 h treatment at pH 10.

To efficiently modify pure PNIPAM, strong bases are required to deprotonate the pendant amides. Zhao et al.[63] used phosphazene base (*t*-BuP_4) converting the secondary amides into initiation sites for anionic polymerization. PNIPAM-g-PEO was obtained by adding ethylene oxide monomers to the polymeric initiators. The grafted copolymer PNIPAM-g-PEO prepared in this way is proposed with the "true" random distribution of PEO chains. Dou et al.[64] used *t*-BuOK to modify the secondary amides into agents for reversible addition-fragmentation transfer polymerization. Comb-like block copolymers were then obtained by adding monomers for side chains (e.g. vinyl acetate or *N*-vinyl-2-pyrrolidone). Both methods are summarised in Figure 7. Compared with the copolymerization method, the modification on pure PNIPAM does not require specific comonomers, and true random distribution could be achieved. However, the methods mentioned above require harsh reaction conditions, such as very high pH, low temperature and organic solvents. The simple and facile preparation of functional copolymers from pure PNIPAM is still a challenge.

A

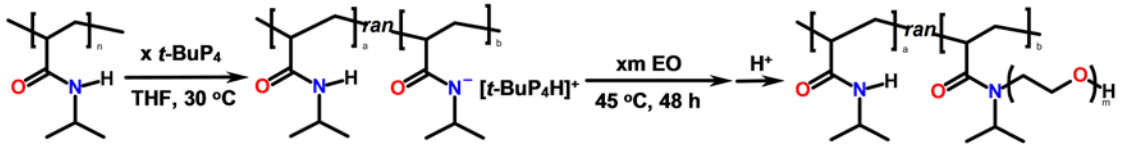

B

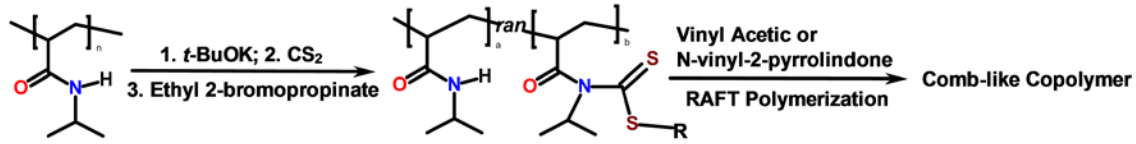

Figure 7 Modification on pure PNIPAM; adapted from A) Zhao and Schlaad[63] and B) Dou et al.[64]

1.1.5 Synthesis and Property of N-chloramide

Sodium hypochlorite (NaClO), or its aqueous solution bleach, has been widely used as a disinfectant or a bleaching agent. Nowadays, bleach is produced by reacting chlorine gas with cold and dilute NaOH solution. Hence the both NaCl and NaClO are present in aqueous bleach. The reaction is shown as follow:

$$Cl_2 + 2\ NaOH \rightarrow NaCl + NaClO + H_2O$$

NaClO is a strong oxidizer, involved in many reactions and applications. In a preliminary experiment, we found that PNIPAM microgels were unstable in bleach. This observation suggests a potential method to modify pure PNIPAM with bleach. The reactions between bleach and amides, N-chlorination and Hofmann rearrangement, are briefly introduced in the following sections.

N-halamines and N-halamides are compounds with nitrogen-halogen bonds.[65] The halogen can be chlorine, bromine or iodine. However, N-chloramines and N-chloramides are most used, due to their high stability. It has been reported[66] that the dissociation constant of N-chloramines and N-chloramides is in the range of 10^{-4} to 10^{-12}. Organic N-chloramines and N-chloramides can be prepared by reacting amines or amides with NaClO, as shown in Figure 8.

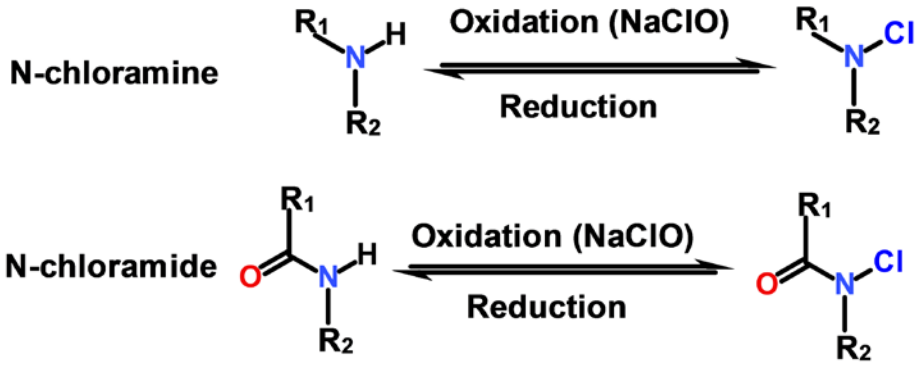

Figure 8 Formation and reduction of N-chloramines and N-chloramides

The N-Cl bonds make N-chloramines and N-chloramides oxidative. It has been reported by Prütz[67] that N-chlorinated dipeptides react with several biological substrates, such as glutathione, ascorbate, methionine, NADH and glutathione disulfide. The reactivity depends on the substrate chemical structures. The highest reaction rate was found with glutathione, and the least rate was obtained with glutathione disulfide. A mechanism was proposed for the reaction between N-chloramines and thiol compounds by Peskin and Winterbourn[68], as shown in Figure 9.

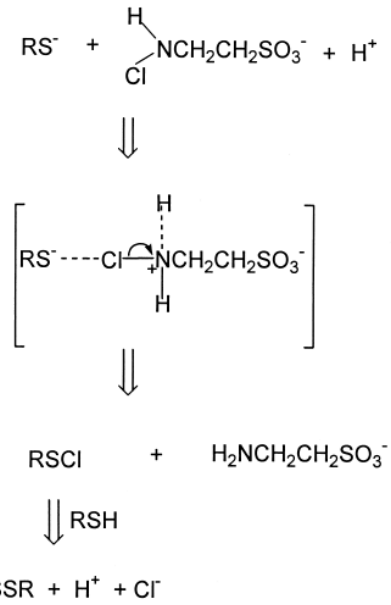

Figure 9 Mechanism for the reaction between N-chloramines and thiol compounds, taken from Peskin and Winterbourn[68].

Polymeric N-chloramides are prepared from N-chlorination of polymer precursors, such as polyamides[69], polyacrylamide[70-71] and polymers with cyclic amides[72-75]. Due to the activity of N-Cl bonds, polymeric N-chloramides have been used to prevent growth of a wide range of microorganisms, including both gram-negative and gram-positive bacteria, viruses and fungi.[76] It has been argued that biocide action of N-chloramides follows a combined mode.[77-78] The first mode is direct contact between cell membrane and N-chloramides. Another mode is the release of active chlorine from N-chloramines to the environment, which results in cell death. It has also been shown that active chlorine can transfer from polymeric N-chloramides to culture constituents.[78]

Since amides can be N-chlorinated in bleach, an idea in this project is to apply N-chlorination to PNIPAM. One can image the N-chlorinated PNIPAM combines the properties of N-chloramides and PNIPAM.

1.1.6 Primary Amine-containing PNIPAM Microgels from Hofmann Rearrangement

Another NaClO involved reaction studied in this project is Hofmann rearrangement. Hofmann rearrangement is to convert unsubstituted amides into primary amines with the aid of halogen compounds. The mechanism of the Hofmann rearrangement with NaClO is shown in Figure 10. It should be noticed that side reactions are involved in Hofmann rearrangement, such as formation of carboxylic acid and urea (RNHCONHR)[79].

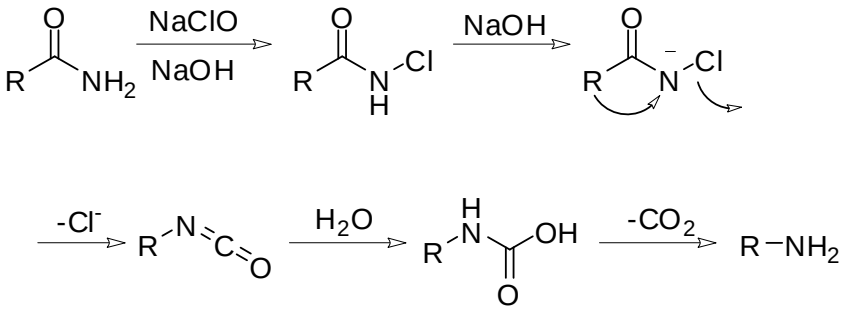

Figure 10 Hofmann rearrangement of unsubstituted amides with NaClO/NaOH.

The Hofmann rearrangement has been applied to prepare PNIPAM microgels with primary amines. Shiroya et al.[80] synthesized primary amine-containing microgels by Hofmann rearrangement of PNIPAM-acrylamide microgels in alkaline bleach at 4 ^{o}C. The PNIPAM-acrylamide copolymer microgels were prepared by precipitation copolymerization prior to the Hofmann rearrangement. Horecha et al.[81] prepared PNIPAM microgels containing primary amines in a similar method by conducting Hofmann rearrangement with diacetoxyiodobenzene in water/acetonitrile solution at 0 ^{o}C. However, both methods require low temperature and/or organic solvents.

Hofmann rearrangement conducted in alkaline bleach at room temperature has also been reported[82-83]. Hence one challenge in this project is to synthesize primary amine-containing microgels via aqueous Hofmann rearrangement at ambient temperature.

1.2 Objectives

This project is inspired by the observation in a preliminary experiment that PNIPAM microgels aggregated in alkaline bleach. It is proposal that PNIPAM microgels are chemically modified by bleach. The overall objective of this project is to develop simple strategies for synthesis of functionalized microgels based on chemical reactions induced by aqueous NaClO (bleach). The specific objectives are as follow:

1. To characterize the reaction between PNIPAM and bleach.

2. To investigate the effect of reaction conditions on the chlorination of thermosensitive microgels. The reaction conditions include reaction time, temperature, pH, salt concentration and polymer chemical structure.

3. To investigate the properties of chlorinated PNIPAM microgels possibly identifying new applications.

4. To extend the application of bleach to the preparation of primary amine-containing microgels via the Hofmann rearrangement in bleach at ambient temperature, giving new simplified routes to complex microgels.

1.3 Thesis Outline

Chapter 1: This chapter presents the background of this project, including the relevant literature review, research objectives and thesis outline.

Chapter 2: This chapter investigates the chemical structure of chlorinated linear PNIPAM. The chemical structure was studied via ^{1}H-NMR and mass spectrometry. The effect of reaction conditions (pH and temperature) on the cloud point temperature and active chlorine content in the product was studied by turbidity measurements and iodometric titration. The thermosensitivity and oxidizing ability of N-chlorinated PNIPAM was also studied. This chapter has been published in *European Polymer Journal*.

Chapter 3: This chapter presents the N-chlorination of PNIPAM microgels in bleach. The effect of reaction temperature and salt concentration on the volume phase transition temperature of chlorinated microgels was studied. The reduction of chlorinated microgels with glutathione was studied by turbidity and DLS. This chapter is in preparation for publication.

Chapter 4: This chapter compares the reactivity of PNIPAM and PNIPMAM microgels in alkaline bleach. The stability difference is discussed based on the results from turbidity and iodometric titration. A mechanism is proposed to explain the low reactivity of PNIPMAM in alkaline bleach. Furthermore, core-shell microgels with PNIPAM cores and poly(NIPAM-co-NIPMAM) shells were prepared. The core-shell microgels show improved colloidal stability after N-chlorination. This chapter is in preparation for publication.

Chapter 5: This chapter shows the synthesis of primary amine-containing microgels via Hofmann rearrangement in bleach at room temperature. The amine content of the resulted microgels was studied as a function of reaction time. In a similar way, amphoteric microgels with both primary amines and carboxyls were prepared. The isoelectric points of amphoteric microgels were studied as a function of Hofmann rearrangement time. This chapter is in preparation for publication.

Chapter 6: This chapter summarises the major contributions of this study.

1.4 References

1. Schild, H. G., Poly(N-isopropylacrylamide) - Experiment, Theory and Application. *Progress in Polymer Science* **1992,** 17, (2), 163-249.
2. Heskins, M.; Guillet, J. E., solution properties of poly(N-isopropylacrylamide). *Journal of Macromolecular Science: Part A - Chemistry* **1968,** A2, (8), 1441-1455.
3. Chan, K.; Pelton, R.; Zhang, J., On the formation of colloidally dispersed phase-separated poly(N-isopropylacrylamide). *Langmuir* **1999,** 15, (11), 4018-4020.
4. Katsumoto, Y.; Tanaka, T.; Ihara, K.; Koyama, M.; Ozaki, Y., Contribution of intramolecular C=O...H-N hydrogen bonding to the solvent-induced Reentrant phase separation of Poly(N-isopropylacrylamide). *Journal of Physical Chemistry B* **2007,** 111, (44), 12730-12737.
5. Pelton, R., Poly (N-isopropylacrylamide)(PNIPAM) is never hydrophobic. *Journal of Colloid and Interface Science* **2010,** 348, (2), 673-674.
6. Kujawa, P.; Aseyev, V.; Tenhu, H.; Winnik, F. M., Temperature-sensitive properties of poly (N-isopropylacrylamide) mesoglobules formed in dilute aqueous solutions heated above their demixing point. *Macromolecules* **2006,** 39, (22), 7686-7693.
7. Xia, Y.; Yin, X. C.; Burke, N. A. D.; Stover, H. D. H., Thermal response of narrow-disperse poly(N-isopropylacrylamide) prepared by atom transfer radical polymerization. *Macromolecules* **2005,** 38, (14), 5937-5943.
8. Xia, Y.; Burke, N. A. D.; Stover, H. D. H., End group effect on the thermal response of narrow-disperse poly(N-isopropylacrylamide) prepared by atom transfer radical polymerization. *Macromolecules* **2006,** 39, (6), 2275-2283.
9. Siu, M.; Zhang, G. Z.; Wu, C., Effect of comonomer distribution on the coil-to-globule transition of a single AB copolymer chain in dilute solution. *Macromolecules* **2002,** 35, (7), 2723-2727.
10. Yoshino, K.; Kadowaki, A.; Takagishi, T.; Kono, K., Temperature sensitization of liposomes by use of N-isopropylacrylamide copolymers with varying transition endotherms. *Bioconjugate Chemistry* **2004,** 15, (5), 1102-1109.
11. Zintchenko, A.; Ogris, M.; Wagner, E., Temperature dependent gene expression induced by PNIPAM-based copolymers: Potential of hyperthermia in gene transfer. *Bioconjugate Chemistry* **2006,** 17, (3), 766-772.
12. Bergbreiter, D. E.; Case, B. L.; Liu, Y. S.; Caraway, J. W., Poly(N-isopropylacrylamide) soluble polymer supports in catalysis and synthesis. *Macromolecules* **1998,** 31, (18), 6053-6062.
13. Mizusaki, M.; Kopek, N.; Morishima, Y.; Winnik, F. M., Interactions of amphiphilic polyelectrolytes and neutral polymeric micelles: A study by nonradiative energy transfer. *Langmuir* **1999,** 15, (23), 8090-8099.
14. Ritter, H.; Sadowski, O.; Tepper, E., Influence of cyclodextrin molecules on the synthesis and the thermoresponsive solution behavior of N-isopropylacrylamide copolymers with adamantyl groups in the side-chains. *Angewandte Chemie-International Edition* **2003,** 42, (27), 3171-3173.

15. Zhang, W. Q.; Shi, L. Q.; Wu, K.; An, Y. G., Thermoresponsive micellization of poly(ethylene glycol)-b-poly(N-isopropylacrylamide) in water. *Macromolecules* **2005,** 38, (13), 5743-5747.
16. Li, C. M.; Madsen, J.; Armes, S. P.; Lewis, A. L., A new class of biochemically degradable, stimulus-responsive triblock copolymer gelators. *Angewandte Chemie-International Edition* **2006,** 45, (21), 3510-3513.
17. Sun, T. L.; Wang, G. J.; Feng, L.; Liu, B. Q.; Ma, Y. M.; Jiang, L.; Zhu, D. B., Reversible switching between superhydrophilicity and superhydrophobicity. *Angewandte Chemie-International Edition* **2004,** 43, (3), 357-360.
18. Ionov, L.; Stamm, M.; Diez, S., Reversible switching of microtubule motility using thermoresponsive polymer surfaces. *Nano Letters* **2006,** 6, (9), 1982-1987.
19. Chen, L.; Liu, M. J.; Bai, H.; Chen, P. P.; Xia, F.; Han, D.; Jiang, L., Antiplatelet and Thermally Responsive Poly(N-isopropylacrylamide) Surface with Nanoscale Topography. *Journal of the American Chemical Society* **2009,** 131, (30), 10467-10472.
20. Juodkazis, S.; Mukai, N.; Wakaki, R.; Yamaguchi, A.; Matsuo, S.; Misawa, H., Reversible phase transitions in polymer gels induced by radiation forces. *Nature* **2000,** 408, (6809), 178-181.
21. Pelton, R., Temperature-sensitive aqueous microgels. *Advances in Colloid and Interface Science* **2000,** 85, (1), 1-33.
22. Nayak, S.; Lyon, L. A., Soft nanotechnology with soft nanoparticles. *Angewandte Chemie-International Edition* **2005,** 44, (47), 7686-7708.
23. Pelton, R. H.; Chibante, P., Preparation of Aqueous Lattices with N-Isopropylacrylamide. *Colloids and Surfaces* **1986,** 20, (3), 247-256.
24. Pelton, R.; Hoare, T., Microgels and Their Synthesis: An Introduction. In *Microgel Suspensions: Fundamentals and Applications*, Fernandez-Nieves, A.; Wyss, H. M.; Mattsson, J.; Weitz, D. A., Eds. Wiley-VCH: Weinheim, 2011.
25. Gao, J.; Frisken, B. J., Cross-linker-free N-isopropylacrylamide gel nanospheres. *Langmuir* **2003,** 19, (13), 5212-5216.
26. Gao, J.; Frisken, B. J., Influence of reaction conditions on the synthesis of self-cross-linked N-isopropylacrylamide microgels. *Langmuir* **2003,** 19, (13), 5217-5222.
27. Mcphee, W.; Tam, K. C.; Pelton, R., Poly(N-Isopropylacrylamide) Latices Prepared with Sodium Dodecyl-Sulfate. *Journal of Colloid and Interface Science* **1993,** 156, (1), 24-30.
28. Sierra-Martin, B.; Romero-Cano, M. S.; Cosgrove, T.; Vincent, B.; Fernandez-Barbero, A., Solvent relaxation of swelling PNIPAM microgels by NMR. *Colloids and Surfaces a-Physicochemical and Engineering Aspects* **2005,** 270, 296-300.
29. Rasmusson, M.; Routh, A.; Vincent, B., Flocculation of microgel particles with sodium chloride and sodium polystyrene sulfonate as a function of temperature. *Langmuir* **2004,** 20, (9), 3536-3542.
30. Routh, A. F.; Vincent, B., Salt-induced homoaggregation of poly(N-isopropylacrylamide) microgels. *Langmuir* **2002,** 18, (14), 5366-5369.
31. Wiedemair, J.; Serpe, M. J.; Kim, J.; Masson, J. F.; Lyon, L. A.; Mizaikoff, B.; Kranz, C., In-situ AFM studies of the phase-transition behavior of single thermoresponsive hydrogel particles. *Langmuir* **2007,** 23, (1), 130-137.

32. Tagit, O.; Tomczak, N.; Vancso, G. J., Probing the morphology and nanoscale mechanics of single poly(N-isopropylacrylamide) microgels across the lower-critical-solution temperature by atomic force microscopy. *Small* **2008,** 4, (1), 119-126.
33. Nerapusri, V.; Keddie, J. L.; Vincent, B.; Bushnak, I. A., Swelling and deswelling of adsorbed microgel monolayers triggered by changes in temperature, pH, and electrolyte concentration. *Langmuir* **2006,** 22, (11), 5036-5041.
34. Sorrell, C. D.; Serpe, M. J., Reflection Order Selectivity of Color-Tunable Poly(N-isopropylacrylamide) Microgel Based Etalons. *Advanced Materials* **2011,** 23, (35), 4088-+.
35. Fujishige, S.; Kubota, K.; Ando, I., Phase transition of aqueous solutions of poly (N-isopropylacrylamide) and poly (N-isopropylmethacrylamide). *The Journal of Physical Chemistry* **1989,** 93, (8), 3311-3313.
36. Tang, Y. C.; Ding, Y. W.; Zhang, G. Z., Role of methyl in the phase transition of poly(N-isopropylmethacrylamide). *Journal of Physical Chemistry B* **2008,** 112, (29), 8447-8451.
37. Duracher, D.; Elaissari, A.; Pichot, C., Preparation of poly(N-isopropylmethacrylamide) latexes kinetic studies and characterization. *Journal of Polymer Science Part a-Polymer Chemistry* **1999,** 37, (12), 1823-1837.
38. Duracher, D.; Elaissari, A.; Pichot, C., Characterization of cross-linked poly(N-isopropylmethacrylamide) microgel latexes. *Colloid and Polymer Science* **1999,** 277, (10), 905-913.
39. Blackburn, W. H.; Dickerson, E. B.; Smith, M. H.; McDonald, J. F.; Lyon, L. A., Peptide-Functionalized Nanogels for Targeted siRNA Delivery. *Bioconjugate Chemistry* **2009,** 20, (5), 960-968.
40. Oh, J. K.; Drumright, R.; Siegwart, D. J.; Matyjaszewski, K., The development of microgels/nanogels for drug delivery applications. *Progress in Polymer Science* **2008,** 33, (4), 448-477.
41. Zhang, J. G.; Xu, S. Q.; Kumacheva, E., Polymer microgels: Reactors for semiconductor, metal, and magnetic nanoparticles. *Journal of the American Chemical Society* **2004,** 126, (25), 7908-7914.
42. Bai, S.; Nguyen, T. L.; Mulvaney, P.; Wang, D. Y., Using Hydrogels to Accommodate Hydrophobic Nanoparticles in Aqueous Media via Solvent Exchange. *Advanced Materials* **2010,** 22, (30), 3247-+.
43. Hoare, T.; Pelton, R., Engineering glucose swelling responses in poly(N-isopropylacrylamide)-based microgels. *Macromolecules* **2007,** 40, (3), 670-678.
44. Su, S. X.; Ali, M.; Filipe, C. D. M.; Li, Y. F.; Pelton, R., Microgel-based inks for paper-supported biosensing applications. *Biomacromolecules* **2008,** 9, (3), 935-941.
45. Tsuji, S.; Kawaguchi, H., Colored thin films prepared from hydrogel microspheres. *Langmuir* **2005,** 21, (18), 8439-8442.
46. Parasuraman, D.; Serpe, M. J., Poly (N-Isopropylacrylamide) Microgels for Organic Dye Removal from Water. *ACS Applied Materials & Interfaces* **2011,** 3, (7), 2732-2737.
47. Hoare, T.; Pelton, R., Highly pH and temperature responsive microgels functionalized with vinylacetic acid. *Macromolecules* **2004,** 37, (7), 2544-2550.

48. Meng, Z. Y.; Hendrickson, G. R.; Lyon, L. A., Simultaneous Orthogonal Chemoligations on Multiresponsive Microgels. *Macromolecules* **2009,** 42, (20), 7664-7669.
49. Suzuki, D.; Kawaguchi, H., Hybrid microgels with reversibly changeable multiple brilliant color. *Langmuir* **2006,** 22, (8), 3818-3822.
50. Hu, X. B.; Tong, Z.; Lyon, L. A., Synthesis and physicochemical properties of cationic microgels based on poly(N-isopropylmethacrylamide). *Colloid and Polymer Science* **2011,** 289, (3), 333-339.
51. Gaulding, J. C.; Smith, M. H.; Hyatt, J. S.; Fernandez-Nieves, A.; Lyon, L. A., Reversible Inter- and Intra-Microgel Cross-Linking Using Disulfides. *Macromolecules* **2012,** 45, (1), 39-45.
52. Lin, C. L.; Chiu, W. Y.; Don, T. M., Superparamagnetic thermoresponsive composite latex via W/O miniemulsion polymerization. *Journal of Applied Polymer Science* **2006,** 100, (5), 3987-3996.
53. Fernandez, V.; Tepale, N.; Sanchez-Diaz, J.; Mendizabal, E.; Puig, J.; Soltero, J., Thermoresponsive nanostructured poly (N-isopropylacrylamide) hydrogels made via inverse microemulsion polymerization. *Colloid and Polymer Science* **2006,** 284, (4), 387-395.
54. Yang, J.; Hu, D.; Fang, Y.; Bai, C.; Wang, H., Novel method for preparation of structural microspheres poly (N-isopropylacrylamide-co-acrylic acid)/SiO2. *Chemistry of Materials* **2006,** 18, (20), 4902-4907.
55. Kim, J. W.; Utada, A. S.; Fernández‐Nieves, A.; Hu, Z.; Weitz, D. A., Fabrication of monodisperse gel shells and functional microgels in microfluidic devices. *Angewandte Chemie* **2007,** 119, (11), 1851-1854.
56. Shah, R. K.; Kim, J.-W.; Agresti, J. J.; Weitz, D. A.; Chu, L.-Y., Fabrication of monodisperse thermosensitive microgels and gel capsules in microfluidic devices. *Soft Matter* **2008,** 4, (12), 2303-2309.
57. Hoare, T.; Pelton, R., Functional group distributions in carboxylic acid containing poly(N-isopropylacrylamide) microgels. *Langmuir* **2004,** 20, (6), 2123-2133.
58. Hoare, T.; McLean, D., Kinetic prediction of functional group distributions in thermosensitive microgels. *Journal of Physical Chemistry B* **2006,** 110, (41), 20327-20336.
59. Hoare, T.; McLean, D., Multi-component kinetic modeling for controlling local compositions in thermosensitive polymers. *Macromolecular Theory and Simulations* **2006,** 15, (8), 619-632.
60. Hoare, T.; Pelton, R., Functionalized microgel swelling: Comparing theory and experiment. *The Journal of Physical Chemistry B* **2007,** 111, (41), 11895-11906.
61. Hoare, T.; Pelton, R., Impact of microgel morphology on functionalized microgel-drug interactions. *Langmuir* **2008,** 24, (3), 1005-1012.
62. Xu, J. J.; Timmons, A. B.; Pelton, R., N-Vinylformamide as a route to amine-containing latexes and microgels. *Colloid and Polymer Science* **2004,** 282, (3), 256-263.
63. Zhao, J. P.; Schlaad, H., Controlled Anionic Graft Polymerization of Ethylene Oxide Directly from Poly(N-isopropylacrylamide). *Macromolecules* **2011,** 44, (15), 5861-5864.

64. Dou, H. Q.; Zhang, X. M.; Shen, W.; Zhu, J.; Zhang, Z. B.; Zhu, X. L., Synthesis of comb-like block copolymer with poly(N-isopropylacrylamide) backbone and poly(vinyl acetate) or poly(N-vinyl-2-pyrrolidone) side chains by reversible addition-fragmentation chain transfer polymerization. *Journal of Polymer Science Part a-Polymer Chemistry* **2013,** 51, (10), 2125-2130.
65. Worley, S. D.; Williams, D. E., Halamine Water Disinfectants. *Crc Critical Reviews in Environmental Control* **1988,** 18, (2), 133-175.
66. Qian, L.; Sun, G., Durable and regenerable antimicrobial textiles: Synthesis and applications of 3-methylol-2,2,5,5-tetramethylimidazolidin-4-one (MTMIO). *Journal of Applied Polymer Science* **2003,** 89, (9), 2418-2425.
67. Prutz, W. A., Consecutive halogen transfer between various functional groups induced by reaction of hypohalous acids: NADH oxidation by halogenated amide groups. *Archives of Biochemistry and Biophysics* **1999,** 371, (1), 107-114.
68. Peskin, A. V.; Winterbourn, C. C., Kinetics of the reactions of hypochlorous acid and amino acid chloramines with thiols, methionine, and ascorbate. *Free Radical Biology and Medicine* **2001,** 30, (5), 572-579.
69. Sun, Y. Y.; Sun, G., Novel refreshable N-halamine polymeric biocides: N-chlorination of aromatic polyamides. *Industrial & Engineering Chemistry Research* **2004,** 43, (17), 5015-5020.
70. Sun, J.; Sun, Y. Y., Acyclic N-halamine-based fibrous materials: Preparation, characterization, and biocidal functions. *Journal of Polymer Science Part a-Polymer Chemistry* **2006,** 44, (11), 3588-3600.
71. Liu, S.; Sun, G., New Refreshable N-Halamine Polymeric Biocides: N-Chlorination of Acyclic Amide Grafted Cellulose. *Industrial & Engineering Chemistry Research* **2009,** 48, (2), 613-618.
72. Sun, Y. Y.; Chen, T. Y.; Worley, S. D.; Sun, G., Novel refreshable N-halamine polymeric biocides containing imidazolidin-4-one derivatives. *Journal of Polymer Science Part a-Polymer Chemistry* **2001,** 39, (18), 3073-3084.
73. Chen, Z. B.; Sun, Y. Y., N-halamine-based antimicrobial additives for polymers: Preparation, characterization, and antimicrobial activity. *Industrial & Engineering Chemistry Research* **2006,** 45, (8), 2634-2640.
74. Kocer, H. B.; Cerkez, I.; Worley, S. D.; Broughton, R. M.; Huang, T. S., N-Halamine Copolymers for Use in Antimicrobial Paints. *ACS Applied Materials & Interfaces* **2011,** 3, (8), 3189-3194.
75. Kocer, H. B.; Cerkez, I.; Worley, S. D.; Broughton, R. M.; Huang, T. S., Polymeric antimicrobial N-halamine epoxides. *ACS Applied Materials & Interfaces* **2011,** 3, (8), 2845-50.
76. Sun, G.; Wheatley, W. B.; Worley, S. D., A New Cyclic N-Halamine Biocidal Polymer. *Industrial & Engineering Chemistry Research* **1994,** 33, (1), 168-170.
77. Chen, Z.; Luo, J.; Sun, Y., Biocidal efficacy, biofilm-controlling function, and controlled release effect of chloromelamine-based bioresponsive fibrous materials. *Biomaterials* **2007,** 28, (9), 1597-1609.

78. Ahmed, A. E. S. I.; Hay, J. N.; Bushell, M. E.; Wardell, J. N.; Cavalli, G., Optimizing Halogenation Conditions of N-Halamine Polymers and Investigating Mode of Bactericidal Action. *Journal of Applied Polymer Science* **2009,** 113, (4), 2404-2412.
79. Elachari, A.; Coqueret, X.; Lablachecombier, A.; Loucheux, C., Preparation of Polyvinylamine from Polyacrylamide - a Reinvestigation of the Hofmann Reaction. *Makromolekulare Chemie-Macromolecular Chemistry and Physics* **1993,** 194, (7), 1879-1891.
80. Shiroya, T.; Tamura, N.; Yasui, M.; Fujimoto, K.; Kawaguchi, H., Enzyme Immobilization on Thermosensitive Hydrogel Microspheres. *Colloids and Surfaces B-Biointerfaces* **1995,** 4, (5), 267-274.
81. Horecha, M.; Senkovskyy, V.; Synytska, A.; Stamm, M.; Chervanyov, A. I.; Kiriy, A., Ordered surface structures from PNIPAM-based loosely packed microgel particles. *Soft Matter* **2010,** 6, (23), 5980-5992.
82. Wirsen, A.; Ohrlander, M.; Albertsson, A. C., Bioactive heparin surfaces from derivatization of polyacrylamide-grafted LLDPE. *Biomaterials* **1996,** 17, (19), 1881-1889.
83. Xu, Z. K.; Yang, Q.; Tian, J.; Dai, Z. W.; Hu, M. X., Novel photoinduced grafting-chemical reaction sequence for the construction of a glycosylation surface. *Langmuir* **2006,** 22, (24), 10097-10102.

Chapter 2 Chloramide Copolymers from Reacting PNIPAM with Bleach

In chapter 2, most experiments were conducted by myself. The iodometric titration was conducted by myself with the help of summer student Wing Yan Lam, and the GPC measurements were conducted with the help of Dr. Nick Burke in Chemistry Department. I plotted all experimental data and wrote the first draft. Dr. Pelton helped to analyze data, modify some figures and rewrite the first draft into the final version.

European Polymer Journal xxx (2013) xxx–xxx

Contents lists available at SciVerse ScienceDirect

European Polymer Journal

journal homepage: www.elsevier.com/locate/europolj

Chloramide copolymers from reacting poly(N-isopropylacrylamide) with bleach

Zuohe Wang, Robert Pelton *

Department of Chemical Engineering, McMaster University, 1280 Main Street West, Hamilton, Ontario, Canada L8S 4L7

ARTICLE INFO

Article history:
Received 31 December 2012
Received in revised form 10 March 2013
Accepted 21 April 2013
Available online xxxx

Keywords:
Polyamides
Stimuli-sensitive polymer
Water-soluble polymers
Chloramide
LCST
Bleach

ABSTRACT

Poly(N-isopropylacrylamide), PNIPAM, when reacted with aqueous NaClO at pH 10.5 gives a stable N-chloramide copolymer, poly(NIPAM-co-NIPAMCl) with little reduction in molecular weight. The copolymer is more hydrophobic than PNIPAM, and chlorination proceeded until the copolymer phase separated. Thus, the reaction temperature determined the extent of chlorination and the product cloud-point temperatures. Chlorination was reversed by reduction with $Na_2S_2O_3$. NaClO treatment of PNIPAM at the lower pH of 8 gave extensive chain degradation.

1. Introduction

Our interest in poly(N-isopropylacrylamide), PNIPAM, interactions with bleach arose while working with polymer-supported TEMPO (2,2,6,6-tetramethyl-1-piperidinyloxy) catalysts for the selective oxidation of cellulose and other carbohydrates [1]. TEMPO mediated oxidation schemes require a primary oxidant and sodium hypochlorite (NaClO, bleach) at alkaline pH is one of the most common oxidants. Recently, while evaluating a poly(N-isopropylacrylamide) (PNIPAM) microgel [2] with grafted TEMPO, it became clear that NaClO induced changes in microgel behavior. To understand these changes, we undertook a study of the properties of linear PNIPAM homopolymer in the presence of NaClO, and have identified reaction conditions leading to interesting, reversible changes in polymer composition, possibly leading to new applications. In view of the very large number of papers and patents exploring applications of PNIPAM materials, we feel that an understanding of the interactions of PNIPAM with active chlorine species should be of interest.

We have found only one publication involving mixtures of PNIPAM and NaClO (bleach). Fu et al. reported that the cloud point temperature of TEMPO-derivatized PNIPAM varied depending on the presence of oxidizing or reducing agents [3]. They explained all the behaviors in NaClO by changes in redox state of the TEMPO. They did not specify the pH, temperature or time of NaClO exposure, nor did they consider reactions with the PNIPAM backbone. Herein we provide evidence that Fu's observations can be explained by the formation of chloramide derivatives of PNIPAM – see Scheme 1.

Chloramides and chloramines have received much attention because they slowly dissociate, releasing active chlorine for bacterial control. For example, Sun's group at the University of California, Davis has published a number of papers describing various N nitrogen rich chemicals, grafted to textile fibers [4]. Upon exposure to bleach, chloramines formed on the fiber surfaces and acted as a slow release source of antibacterial reactive species. The dissociation constants of low molecular weight chloramides are low 10^{-8}–10^{-9}, indicating significant stability in water [4,5].

* Corresponding author.
E-mail address: peltonrh@mcmaster.ca (R. Pelton).

0014-3057/$ - see front matter © 2013 Elsevier Ltd. All rights reserved.
http://dx.doi.org/10.1016/j.eurpolymj.2013.04.018

Please cite this article in press as: Wang Z, Pelton R. Chloramide copolymers from reacting poly(N-isopropylacrylamide) with bleach. Eur Polym J (2013), http://dx.doi.org/10.1016/j.eurpolymj.2013.04.018

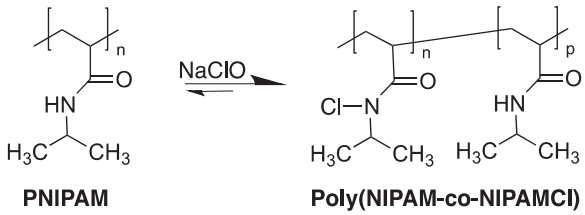

Scheme 1. Chlorination of PNIPAM with NaClO.

Zengel's 1982 patent that discloses the preparation of chloramide derivatives of polyacrylamide and polymethyacrylamide polymers and copolymers, not including PNIPAM [6]. With un-substituted amides, the Hofmann degradation to the corresponding amine is a possible side reaction [7].

Sun patented the use of polymethacrylamide polymers, grafted onto cellulose, to give antibacterial textiles after activation by exposure to bleach [8]. Polymethacrylamide, unlike polyacrylamide or PNIPAM, does not have a proton alpha to the carbonyl explaining why polymethacrylamide does not quickly degrade with exposure to bleach.

Polymer chain scission is another possible result from NaClO exposure. Chlorine-induced degradation is a problem with water treatment membranes, and there have been publications and patents claiming that PNIPAM coating protected the membranes [9,10]. However, no information was provided regarding the chemical changes in PNIPAM induced by exposure to bleach. The bleach-induced decomposition of other water-soluble polymers has been studies in some detail. For example, the molecular weight of poly(vinyl pyrrolidone) decreased by a factor of 5 when exposed to NaClO at pH 11.5 [11]. The authors proposed that scission was initiated by free radical induced hydrogen abstraction of the proton alpha to the carbonyl – similar protons are present in PNIPAM.

Herein we show that NaClO treatment of PNIPAM gives chain scission at pH 8, whereas the predominant reaction at pH 10.5 is chloramide formation (Scheme 1). In addition, we show that the chloramide content in poly(NIPAM-co-NIPAMCl) is easily controlled by the reaction temperature and that the results copolymers are stable in water.

2. Experimental

2.1. Materials

Poly(N-isopropylacrylamide) (PNIPAM) with viscosity-average molecular weight 122 kDa and PDI 2.50 was purchased from Polymer Source Inc. (Canada). The PNIPAM was dialyzed for 1 week against water using cellulose membranes (MEMBRA-CEL®, MWCO 12–14 kDa). The concentration of NaClO was determined by titration with KI/$Na_2S_2O_3$/starch before use. Type I water with a resistivity of 18 MΩ cm from Barnstead Nanopure Diamond system was used in all experiments in this paper.

2.2. PNIPAM reaction with NaClO

Typically, 10 mL PNIPAM solution (1.13 g/L) and 10 mL NaClO (40 mM) were mixed in a beaker. The solution pH was adjusted to a desired value between 7 and 12 with 1 M HCl or 1 M NaOH. The beaker was placed in an oil bath or water bath with the desired temperature. When phase separation was observed, diluting the solution with about 200 mL of water stopped the reaction. The solution was then dialyzed in cellulose membrane tubes against water. During the dialysis, the water was changed twice every day for 3 days. The poly(NIPAM-co-NIPAMCl) PNIPAM was isolated by freeze-drying and stored at 4 °C.

Some experiments were conducted in a spectrophotometer to record the turbidity changes. Typically, 1 mL polymer solution (1.13 g/L) was mixed with 1 mL NaClO (40 mM) in a polystyrene cuvette. After adjusting the pH to the desired value, transmittance at 500 nm was measured at 25 °C with a DU800 visible–UV spectrophotometer (Beckman Coulter) using a water blank.

2.3. Cloud point temperature measurements

Solutions of PNIPAM and its purified reaction products (1 g/L) were placed in polystyrene cuvettes. The transmittance at 500 nm was recorded during the temperature scan (0.5 °C/10 min). The cloud point is defined as the temperature corresponding to 50% in the normalized transmittance curves.

2.4. Iodometric titration

The oxidizing chlorine content in modified PNIPAM was determined by KI/starch/thiosulfate titration [6]. Modified PNIPAM (5 mg) was dissolved in water to make a 1 g/L solution. An excess amount of KI (~100 mg) was added to the solution. The solution pH was adjusted to around 3. Then 2 mL starch indicator (1%) was added. The solution was titrated with sodium thiosulfate (8.83 mM) until the solution turned colorless. The concentration of sodium thiosulfate was calibrated against sodium thiosulfate pentahydrate.

2.5. Gel permeation chromatography (GPC)

The GPC elution curves were obtained with a Waters GPC system consisting of a Waters 515 HPLC pump, and a Waters 717plus Autosampler. The columns used were Waters Styragel HR 2 (500–20,000 Da), HR 3 (500–30,000 Da), and HR 4 (5000–600,000). The columns were maintained at 40 °C and a Waters 2414 refractive index detector maintained at 35 °C. THF was used as the mobile phase (1.0 mL/min). The molecular weight (MW) corresponding to the peaks of the elution curves was estimated with polystyrene standards.

2.6. Nuclear magnetic resonance (NMR)

^{1}H NMR spectra were recorded on Bruker AV-200 spectrometers (200 MHz) with samples dissolved in $CDCl_3$ or DMSO-d6.

Please cite this article in press as: Wang Z, Pelton R. Chloramide copolymers from reacting poly(N-isopropylacrylamide) with bleach. Eur Polym J (2013), http://dx.doi.org/10.1016/j.eurpolymj.2013.04.018

3. Results and discussion

Aqueous solutions of 122 kDa PNIPAM were treated with NaClO, and the solution turbidity was measured as functions of time and treatment pH. The results in Fig. 1 show little change in turbidity for treatments at pH 7–9. By contrast, at higher pH values the solutions slowly became more turbid, ultimately displaying macroscopic precipitation. Therefore the bleach-induced chemical changes in PNIPAM above pH 9 resulted in a more hydrophobic polymer. Note that PNIPAM displays negligible hydrolysis under these conditions [12].

Gel permeation chromatography was used to determine the extent of polymer chain scission with NaClO treatment, and the results are summarized in Fig. 2. At pH 8, the number average molecular weight plummeted from about 150–7 kDa. Under these conditions, there was no change in turbidity (see Fig. 1) suggesting the degradation products were water soluble at 25 °C. By contrast, at pH 10.5 there was only a slight loss in molecular weight with NaClO treatment. NaClO chemistry is pH dependent [13]. The pKa of hydrochlorous acid is 7.5. At pH 10 and above, the dominant species is ClO^-, whereas below pH 6 HClO dominates. Prütz has shown that HClO does not form chloramides whereas amide exposure to ClO^- does produce chloramides [14].

To summarize, at pH 7–9 the PNIPAM chains in NaClO were degraded into water-soluble products, whereas at higher pH values the bleach treatment produced a water-insoluble product with little change in molecular weight. Because the pH 10.5 NaClO treatment seemed to produce a new polymer with little chain scission, we extended our investigation into the reaction. The introduction included a brief summary of the reactions of sodium hypochlorite with polyacrylamide and other amides. Based on this literature, we propose that the major reaction at pH 10.5 is the conversion of N-isopropylacrylamide groups to the corresponding N-chloramide derivative – see Scheme 1. Proton NMR was performed to give support for the proposed chloramide structure.

Fig. 3 compares the NMR of PNIPAM before and after treatment with bleach at 15 °C. Replacement of N–H with N–Cl caused the alpha proton (b) to shift from 3.8 ppm to 4.8 ppm. To give further support for this assignment, the small molecule analogue N-isopropylisobutyramide was prepared [15] and reacted with bleach; the mass spectrum

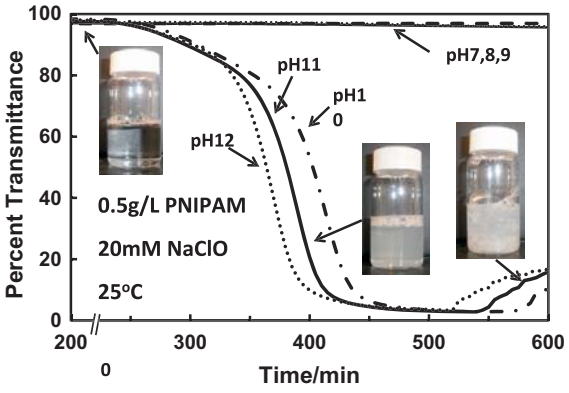

Fig. 1. PNIPAM phase separation with NaClO treatment. From pH 7 to 9 both HClO and ClO^- species are present whereas pH >10 the active species is predominately ClO^-.

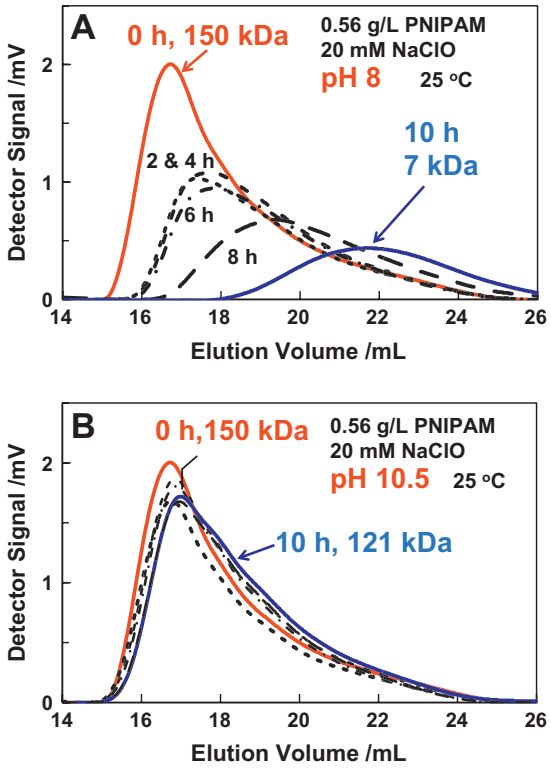

Fig. 2. GPC elution curves of PNIPAM after treated with NaClO at pH 8 or pH 10.5 at 25 °C. The molecular weight assignments are based on polystyrene standards.

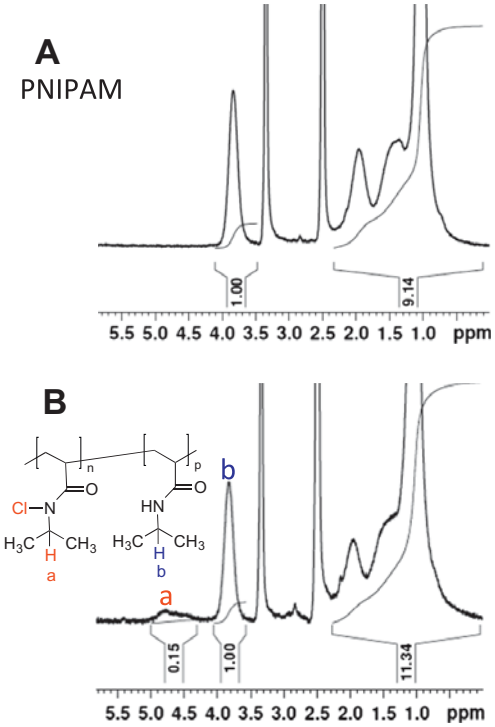

Fig. 3. ^{1}H NMR spectra of (A) PNIPAM, and, (B) poly(NIPAM-co-NIPAMCl) in DMSO-D6.

Please cite this article in press as: Wang Z, Pelton R. Chloramide copolymers from reacting poly(N-isopropylacrylamide) with bleach. Eur Polym J (2013), http://dx.doi.org/10.1016/j.eurpolymj.2013.04.018

of the chlorinated product is shown in the Supplementary Information file. Fig. 4 compares the NMR spectra of N-isopropylisobutyramide with N-chloro-N-isopropylisobutyramide. The N-α–hydrogen shifted from 4.0 ppm before chlorination to 4.9 ppm to after chlorination, supporting the assignments in Fig. 3. Note that N-isopropylisobutyramide was water-soluble whereas the chloramide adduct, N-chloro-N-isopropylisobutyramide, was insoluble in water. Replacing the amide proton with chlorine produced a much more hydrophobic material.

3.1. Influence of reaction time

PNIPAM solutions were treated with 20 mM NaClO at 25 °C for various times, and the transformation of PNIPAM to poly(NIPAM-co-NIPAMCl) was followed by measuring the cloud point temperatures. Fig. 5A shows turbidity versus temperature curves for each reaction time product. Also shown are the corresponding cloud point temperatures, Fig. 5B, taken as the temperature at which the transmittance was reduced to 50% of the initial value. The error bars denote the temperatures corresponding to 5% and 95% transmittance and serve as a measure of the sharpness of the clouding transition. For PNIPAM, the breadth of the cloud point transition is approximately independent of molecular weights above 50 kDa whereas 10.5 kDa PNIPAM shows a much broader transition [16].

Longer reaction times gave lower cloud point temperatures because of increased NIPAMCl content in the copolymer. Note the lowest cloud point achieved was near the reaction temperature of 25 °C. Presumably, once the copolymer phase separated, its reaction rate with ClO^- was greatly diminished. This observation prompted us to propose that the extent of chloramide formation could be controlled simply the reaction temperature. This approach is now illustrated.

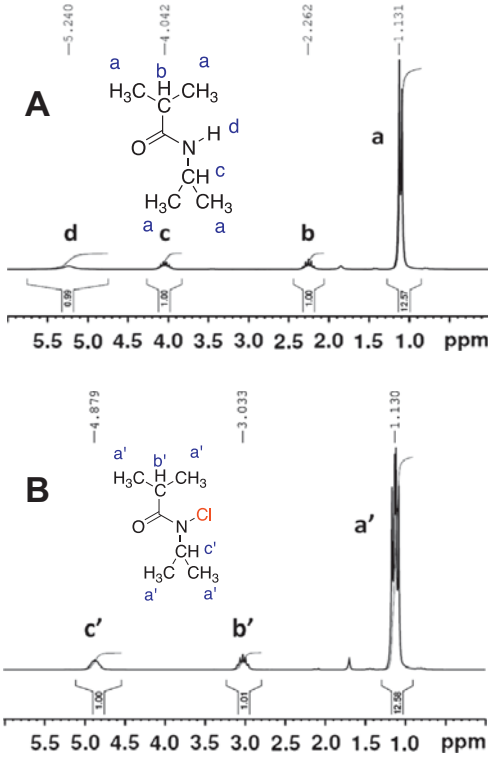

Fig. 4. ^1H NMR spectra of N-isopropylisobutyramide in CD_3Cl before (A) and after (A) NaClO treatment (pH 12; 1.11 M NaClO; 25 °C). N-isopropylisobutyramide was water-soluble whereas N-chloro-N-isopropylisobutyramide was not.

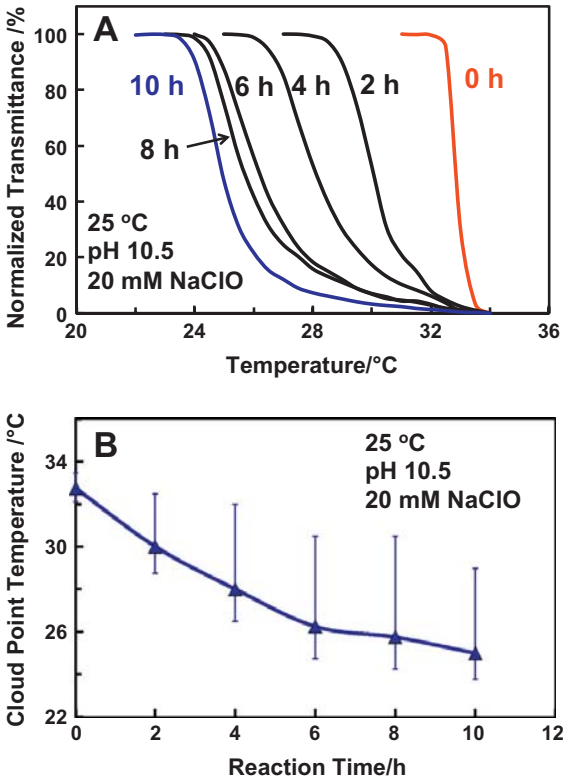

Fig. 5. Cloud point temperatures of poly(NIPAM-co-NIPAMCl) copolymers resulting from reaction with NaClO for various reaction times. Cloud point temperatures were defined to correspond to 50% relative transmittance. The error bars on the cloud points reflect the temperatures corresponding to 5% and 95% normalized transmittance.

3.2. Effect of reaction temperature

A series of NaClO treatments was conducted at various temperatures, and the reactions were terminated when

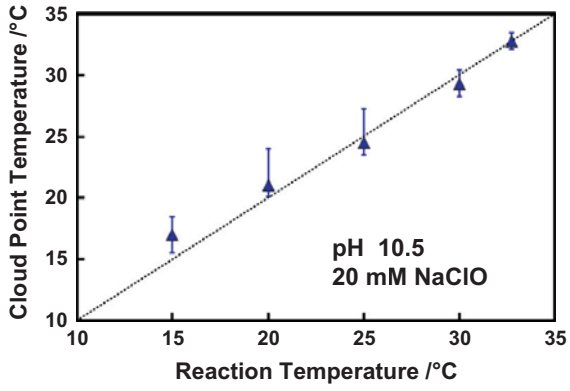

Fig. 6. Cloud point temperatures of poly(NIPAM-co-NIPAMCl) as functions of reaction temperature with NaClO. The error bars reflect the temperature range between 5% and 95% transmittance. The chlorination reaction stops when the polymer phase separates. Therefore the reaction temperature corresponds to the phase separation temperature.

Please cite this article in press as: Wang Z, Pelton R. Chloramide copolymers from reacting poly(N-isopropylacrylamide) with bleach. Eur Polym J (2013), http://dx.doi.org/10.1016/j.eurpolymj.2013.04.018

macroscopic phase separation was observed. The lowest reaction temperature was 15 °C, and a reaction time of about 50 h was required for sufficient substitution to induce phase separation. By contrast, the 30 °C reaction phase separated after a couple of hours.

The reaction products were purified by exhaustive dialysis and were freeze-dried for storage. Turbidity versus temperature plots for the product polymers in water were recorded and are available in the Supplementary Information file. The corresponding cloud point temperatures for the reaction products are shown in Fig. 6. The cloud point temperatures of the products increased linearly with chlorination reaction temperature. Therefore, the product cloud point temperature can be predetermined simply by carrying out the reaction at the desired temperature.

The chloramide content in the product copolymers was measured by iodometric titration [6,17]. Fig. 7 shows the chloramide content, expressed as a degree of substitution, versus the cloud point temperature of the polymer. The highest degree of substitution was 13%, obtained at the lowest reaction temperature of 15 °C.

3.3. Poly(NIPAM-co-NIPAMCl) stability

As mentioned in the introduction, the dissociation constant for chloramides is typically 10^{-9}, suggesting that poly(NIPAM-co-NIPAMCl) should be quite stable in water [4,5]. We used changes in the cloud point temperature to probe the stability of poly(NIPAM-co-NIPAMCl) in water, and as a dry powder; the results are summarized in Table 1. Poly(NIPAM-co-NIPAMCl) was unchanged over a month's storage as a dry solid at 23 °C, whereas there was a slight

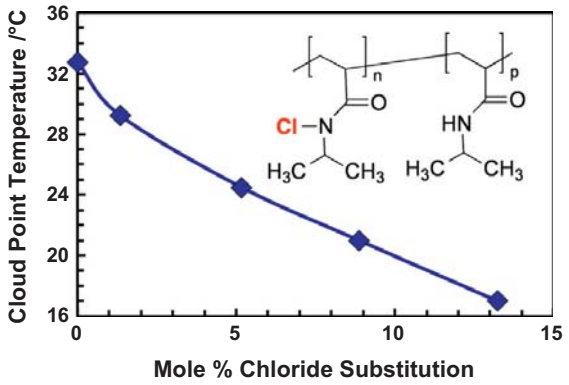

Fig. 7. The cloud point temperature of poly(NIPAM-co-NIPAMCl) as a function of the molar percentage chlorination.

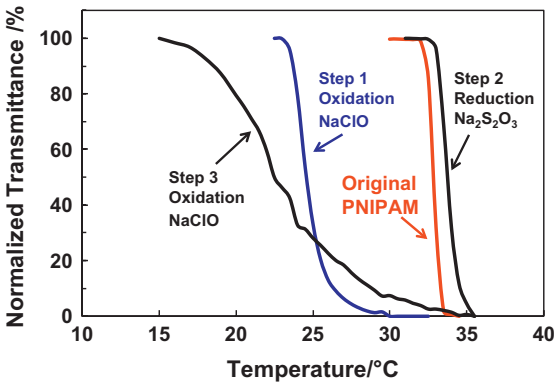

Fig. 8. Transmittance curves for PNIPAM following chlorination and reduction cycles. Oxidation: 0.56 g/L polymer, 20 mM NaClO, pH 10.5, 25 °C for 10 h; reduction: 1 g/L polymer, 1 mM $Na_2S_2O_3$, pH 7, 25 °C for 12 h. The polymers were dialyzed and freeze dried before each cloud point measurement.

increase cloud point temperature with 1 month storage in aqueous solution at 23 °C, suggesting a slight loss of chloride.

3.4. Regenerating PNIPAM

Poly(NIPAM-co-NIPAMCl) prepared at 25 °C with 20 mM NaClO at pH 10.5, was subsequently exposed to 1 mM $Na_2S_2O_3$ at pH 7 overnight. After each step the polymer was exhaustively dialyzed and freeze dried. Fig. 8 shows turbidity/temperature curves for the purified polymers after the various treatments. Sodium thiosulfate reduction restored the original cloud point. However, re-exposure to NaClO gave a much broader turbidity/temperature curve, possibly because of the introduction charged groups from the slow hydrolysis of isopropyl amide groups. Hoare and Pelton showed that 120 h treatment at pH 10 induced about 1% hydrolysis of PNIPAM [12]. Chain scission is also a possible explanation, however the results in Fig. 2B suggest only limited chain degradation should occur. Nevertheless, the results in Fig. 8 suggest that PNIPAM would not be ideal applications involving repeated exposure to bleach.

4. Conclusions

PNIPAM undergoes two reaction pathways in bleach, depending upon the pH. At pH 8, NaClO exposure causes PNIPAM chain cleavage and degradation giving water-soluble products. Based on the literature, chain scission is

Table 1
Cloud point temperatures for poly(NIPAM-co-PNIPAMCl) as functions of storage time as a dry solid or aqueous solution at 23 °C. Chloride contents were measured by iodometric titration.

NaClO reaction temperature (°C)	Initial degree of substitution (%)	Cloud point temperatures (°C)		
		Fresh polymer	1 month dry storage	1 month wet storage
15	13	17	17.5	18
20	9	21	22.5	23
25	5	24.5	25	27
30	1.3	29.3	30	33.3

Please cite this article in press as: Wang Z, Pelton R. Chloramide copolymers from reacting poly(N-isopropylacrylamide) with bleach. Eur Polym J (2013), http://dx.doi.org/10.1016/j.eurpolymj.2013.04.018

probably initiated by free radical induced hydrogen abstraction of the main chain proton alpha to the carbonyl. At pH 10.5 there was little chain scission, however the cloud point temperature of the reaction product decreases with the extent of reaction. We propose the major reaction is the conversion of N-isopropylamide groups to N-isopropyl chloramide (see Scheme 1) giving poly(NIPAM-co-NIPAMCl).

The cloud point temperature of poly(NIPAM-co-NIPAMCl) decreases approximately linearly with the chlorine content. The extent of chlorination, and thus the product cloud point, can be controlled by conducting the NaClO reaction at the desired cloud point temperature. Upon reaching the desired degree of reaction, the copolymer phase separates, inhibiting further reaction.

The chlorination of PNIPAM is somewhat reversible. Reducing conditions ($Na_2S_2O_3$) regenerate PNIPAM with some evidence of degradation. Poly(NIPAM-co-NIPAMCl) aqueous solutions slowly (i.e. weeks) dissociate to PNIPAM. Phase separated or dry poly(NIPAM-co-NIPAMCl) is more stable.

Acknowledgements

Professors Michael Brook, John Brennan and Harald Stover, McMaster Chemistry, are thanked for useful discussions. Also acknowledged are Wing Yan Lam and Dr. Nick Burke for technical assistance. The authors acknowledge the Natural Sciences and Engineering Research Council of Canada for funding. R.P. holds the Canada Research Chair in Interfacial Technologies.

Appendix A. Supplementary material

Supplementary data associated with this article can be found, in the online version, at http://dx.doi.org/10.1016/j.eurpolymj.2013.04.018.

References

[1] Pelton R, Ren PR, Liu J, Mijolovic D. Polyvinylamine-graft-tempo adsorbs onto, oxidizes and covalently bonds to wet cellulose. Biomacromolecules 2011;12:942–8.
[2] Pelton R. Temperature-sensitive aqueous microgels. Adv Colloid Interface Sci 2000;85:1–33.
[3] Fu H, Policarpio DM, Batteas JD, Bergbreiter DE. Redox-controlled 'smart' polyacrylamide solubility. Polym Chem 2010;1:631–3.
[4] Qian L, Sun G. Durable and regenerable antimicrobial textiles: synthesis and applications of 3-methylol-2,2,5,5-tetramethylimidazolidin-4-one (Mtmio). J Appl Polym Sci 2003;89:2418–25.
[5] Akdag A, Okur S, Mckee ML, Worley SD. The stabilities of N–Cl bonds in biocidal materials. J Chem Theory Comput 2006;2:879–84.
[6] Zengel HG, Bergfeld M, Zielke R. Polymeric N-halogenoamides on the basis of acrylamide and methacrylamide. US Pat. 4,356,289; October 26, 1982.
[7] Tanaka H, Ödberg L. Preparation of cationic polyacrylamides by a modified Hofmann reaction: fluorescent labeling of cationic polyacrylamides. J Polym Sci Part A: Polym Chem 1989;27:4329–39.
[8] Sun Y, Luo J. Compositions and methods for making and using acyclic N-halamine-based biocidal polymeric materials and articles. Pat; 2006.
[9] Musale DA. Method of cleaning fouled and/or scaled membranes. Pat. US 7,674,382 B2; March 9, 2010.
[10] Liu M, Chen Z, Yu S, Wu D, Gao C. Thin-film composite polyamide reverse osmosis membranes with improved acid stability and chlorine resistance by coating N-isopropylacrylamide-co-acrylamide copolymers. Desalination 2011;270:248–57.
[11] Wienk IM, Meuleman EEB, Borneman Z, Vandenboomgaard T, Smolders CA. Chemical treatment of membranes of a polymer blend – mechanism of the reaction of hypochlorite with poly(vinyl pyrrolidone). J Polym Sci Part A – Polym Chem 1995;33:49–54.
[12] Hoare T, Pelton R. Functional group distributions in carboxylic acid containing poly(N-isopropylacrylamide) microgels. Langmuir 2004;20:2123–33.
[13] Singer PC, Reckhow DA. Chemical oxidation. In: Letterman RD, editor. Water quality and treatment. New York: America Water Works Association; 1999.
[14] Prütz WA. Consecutive halogen transfer between various functional groups induced by reaction of hypohalous acids: NADH oxidation by halogenated amide groups. Arch Biochem Biophys 1999;371:107–14.
[15] Winter CH, Knisley TJ, Mahesh PKD, Karunarathne C. Thermially stable film precursors. US Pat. 20120058270A1; 2012.
[16] Schild HG. Poly(N-Isopropylacrylamide): experiment, theory and application. Prog Polym Sci 1992;17:163–249.
[17] Dickerson MB, Lyon W, Gruner WE, Mirau PA, Slocik JM, Naik RR. Sporicidal/bactericidal textiles via the chlorination of silk. ACS Appl Mater Interfaces 2012;4:1724–32.

Please cite this article in press as: Wang Z, Pelton R. Chloramide copolymers from reacting poly(N-isopropylacrylamide) with bleach. Eur Polym J (2013), http://dx.doi.org/10.1016/j.eurpolymj.2013.04.018

Appendix: Supporting Information for Chapter 2

Preparation of N-isopropylisobutyramide. Isopropylamine (>99.5%), triethylamine (>99.5%), isobutyryl chloride (98%), NaClO (10-15%) were purchased from Sigma-Aldrich and used without further purification. Isopropylamine (4.5mL) and triethylamine (7.45mL) were added in a 500mL round-bottom flask with 250mL diethyl ether. [1] The flask was cooled to 0 °C and isobutytyl chloride (5.4mL) was slowly added with magnetic stirring. The product precipitated as white crystals were filtered and dried under reduced pressure.

Reaction of N-isopropylisobutyramide with NaClO. N-isopropylisobutyramide was reacted with NaClO to confirm the formation of the corresponding chloramide. 300 mg N-isopropylisobutyramide was dissolved in 20 mL NaClO (~1.11M). The solution pH was adjusted to 12. The reaction mixture was stirred for 2 days at ambient temperature. The product was insoluble in water and formed an oil layer on top of the solution. Product composition was confirmed by NMR and mass spectroscopy. ESI-MS/MS of N-chloro-N-isopropylisobutyramide was performed on a Micromass Q-TOF Ultima Global. The theoretical isotope model was predicted by the software Masslynx.

A

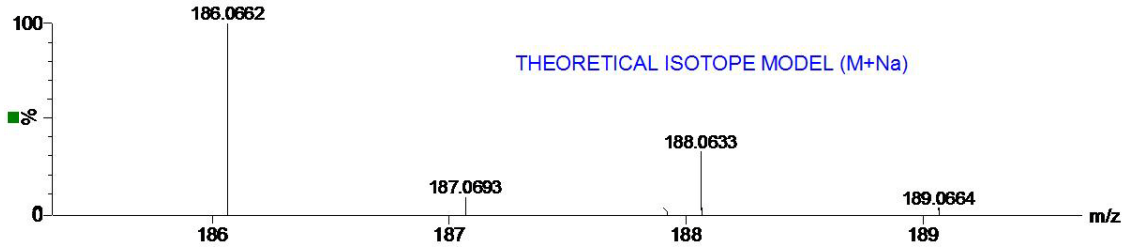

B

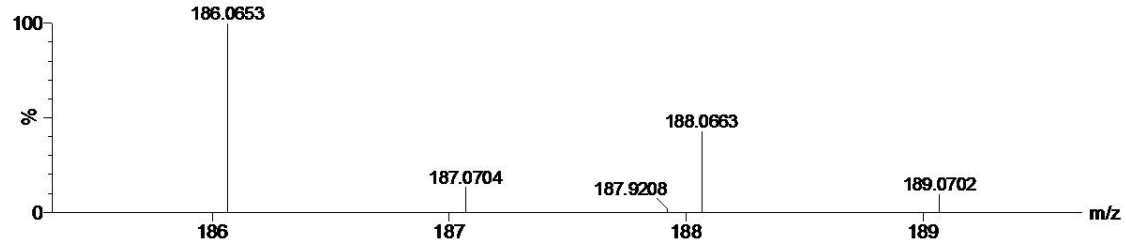

S 1 Mass spectra of theoretical isotope model ($C_7H_{14}NOClNa$) and N-chloro-N-isopropylisobutyramide.

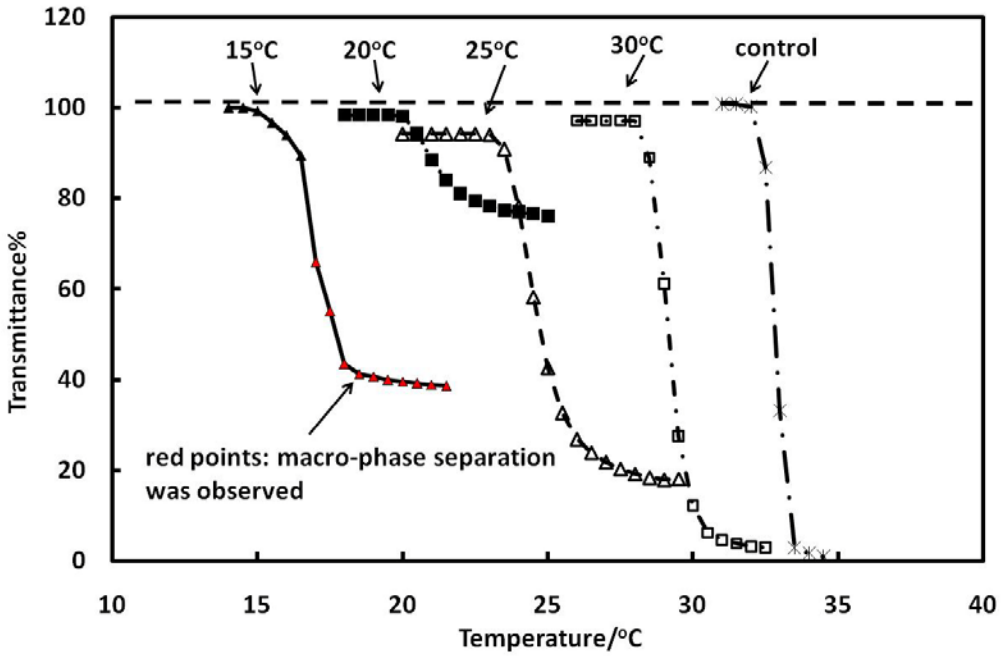

S 2 Raw transmittance data corresponding to the cloud point values in Figure 6.

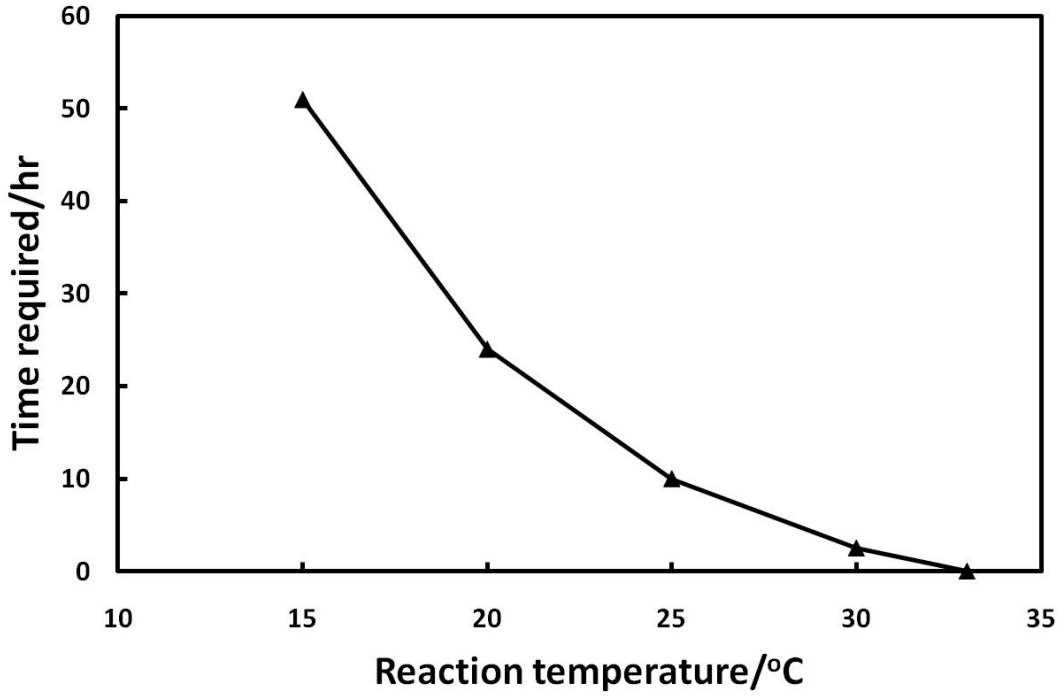

S 3 Time needed for the macroscopic precipitation of PNIPAM in 20mM NaClO as a function of reaction temperature

1. Winter, C. H.; Knisley, T. J.; Mahesh, P. K. D.; Karunarathne, C. Thermially stable film precursors. 20120058270A1, 2012.

Chapter 3 N-Chlorinated Poly(N-isopropylacrylamide) Microgels

In chapter 3, all experiments were conducted by myself, with the help of summer students Yue Zhang and Wing Yan Lam. I plotted the experiment data and wrote the first draft. Dr. Pelton helped the data analysis, suggested some experiment setup and revised the first draft.

N-Chlorinated Poly(N-isopropylacrylamide) Microgels

Zuohe Wang, Robert Pelton*, Wing Yan Lam, Yue Zhang

Department of Chemical Engineering, McMaster University, Hamilton, Canada, 1280 Main Street, West Hamilton, Ontario, Canada, L8S 4L7.

* Corresponding author email: peltonrh@mcmaster.ca

Abstract

Modification of poly(N-isopropylacrylamide) microgels carried out in aqueous bleach (NaClO) at pH 10.5 and resulted in chlorinated microgels with nitrogen-chlorine bonds (active chlorine). The N-chlorinated microgels have a volume phase transition temperature (VPTT) lower than 32 ^{o}C and show oxidative ability. The reaction was easily conducted by mixing microgels with 20 mM NaClO at pH 10.5 until the microgels phase separated. The effects of reaction temperature and salt concentration on active chlorine content and VPTT were clarified. Finally, the oxidative ability of N-chlorinated microgels was demonstrated by reduction with glutathione. The reduction was rapid at high pH (>7), and much slower under acidic pH. A core/shell structure was found for partially reduced microgels suggesting that the reduction at pH 7 is diffusion-controlled.

3.1 Introduction

Compounds with nitrogen-halogen covalent bonds, known as N-halamines, have been studied as biocides since 1980s.[1] The halogen in N-halamines can be chlorine, bromine or iodine. Among these N-halamines, organic N-chloramine with nitrogen-chlorine bond(s) is the most popular. N-chloramines are more stable than other N-halamines, with a dissociation constant from 10^{-4} to 10^{-12}.[2] Besides, N-chloramines are rechargeable by treating with aqueous bleach.

Recently, polymeric N-chloramines have been getting more attention. Polyamides[3], polyacrylamide[4-5] and polymers with cyclic amides[6-9] have been studied as the precursors, since amide has been shown suitable for chlorination/dechlorination[10]. The precursors were then N-chlorinated into polymeric N-chloramines. Polymeric N-chloramines have been used to prevent growth of a wide range of microorganisms.[11] It has been argued that biocide action of N-chloramines follows a combined mode.[12-13] The first mode is directly contact between cell membrane and N-chloramines. Another mode is releasing of active chlorine from N-chloramines to environment, which results in cell death. It has also been shown that active chlorine can transfer from N-chloramines to culture constituents.[13]

We are interested in polymeric N-chloramines releasing active chlorine slowly, which offer long-term antimicrobial efficacy. So far, however, most studies focused on polymeric N-halamines coating[9, 14-17]. Thus, most active chlorines are located on material surface, which results in low active chlorine content. One can image that hydrogel with amide groups can give high active chlorine content after N-chlorination, since all amide groups can be chlorinated theoretically.

Poly(N-isopropylacrylamide), PNIPAM, is a well-known thermosensitive polymer with a lower critical solution temperature 32 ^{o}C.[18] A new N-chloramine-containing copolymer based on PNIPAM, referred to as poly(NIPAM-co-NIPAMCl), has been prepared in our laboratory.[19] The copolymers were prepared by simply mixing commercialized linear PNIPAM with bleach at high pH (> 9), as described in Scheme 1. The reaction proceeded until the polymer phase separated. Some of the nitrogen-hydrogen bonds in PNIPAM were converted into nitrogen-chlorine bonds. The newly formed nitrogen-chlorine bonds give the new copolymer oxidative and potential antimicrobial ability. Besides, N-chloramines are more hydrophobic than amides, which leads resulting poly(NIPAM-co-NIPAMCl) with controlled lower cloud point temperature (CPT). The CPT of poly(NIPAM-co-NIPAMCl)is almost equal to the reaction temperature after the reaction in 20 mM NaClO. Thus, the active chlorine content, which corresponds to the CPT, could be easily controlled via the reaction temperature.

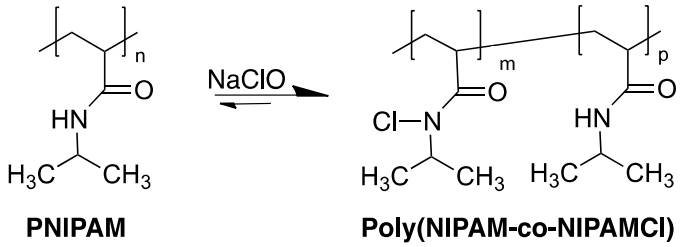

Scheme 1 Chlorination of PNIPAM in NaClO Solution (n=m+p).

Crosslinked poly(N-isopropylacrylamide) (PNIPAM) spheres, referred to as microgels, can be prepared via precipitation polymerization firstly developed by Pelton and Chibante.[20] PNIPAM microgels display a reversible swelling-shrinking transition with a volume phase transition temperature (VPTT) of ~32 ^{o}C.[21] PNIPAM microgel is a suitable candidate as chlorine-releasing agent due to the networking structure.

This paper describes the synthesis of N-chlorinated microgels by reacting the PNIPAM microgels with aqueous bleach at pH 10.5. It is found that the active chlorine content (also VPTT) is controlled by the reaction temperature and salt concentration. The oxidative ability of the N-chlorinated microgels is also demonstrated by reacting with glutathione at room temperature.

3.2 Experiments

All chemicals were purchased from Sigma-Aldrich (Canada). N-isopropylacrylamide (NIPAM, 97%) was purified from re-crystallization with a mixture of toluene and hexane (60:40) prior to use. Ethylene glycol dimethacrylate (EGDMA, 98%), sodium dodecyl sulfate (SDS, 99%), ammonium persulfate (APS, 98%), glutathione (GSH, 98%), sodium thiosulfate ($Na_2S_2O_3$, 98%) and sodium hypochlorite (bleach, NaClO, 10-15%) were used as received. Type I water (with a resistivity of 18.2 MΩ·cm) from a Barnstead Nanopure Diamond system was used in all experiments. The concentration of NaClO was determined by iodometric titration.[22]

Synthesis of Microgels. PNIPAM microgels were prepared by precipitation polymerization.[23] EGDMA, which was found to be more stable in bleach at pH 10.5, was used for crosslinkers instead of *N*,*N*'-methylenebisacrylamide. Crosslinker stability measurements are given in the Supporting Information. In a typical experiment, 1.4 g NIPAM, 0.13 g EGDMA and 0.05 g SDS were added to 150 mL water in a 250 mL flask reactor. The flask was equipped with a mechanical stirrer, a nitrogen inlet/outlet and a condenser. After deoxygenation of the solution with nitrogen for 30 min at 70 ^{o}C, 0.025 g APS (dissolved in 5 mL water) was added. The polymerization was conducted at 70 ^{o}C under nitrogen atmosphere for another 6 hr. After polymerization, microgels were purified by ultracentrifugation (Beckman L-80 XP), decantation and suspension in water

for several cycles until the conductivity of the supernatant was less than 5 μS/cm. The obtained microgels were dried in a freeze-dryer.

N-Chlorination of Microgels. A suspension with 0.56 g/L PNIPAM microgels and 20 mM NaClO was prepared in a beaker. The solution pH was adjusted to 10.5 by adding 1 M HCl. The beaker was placed in a water bath with the desired reaction temperature. The reaction was conducted until phase separation was observed. The solution pH was checked every hour and re-adjusted to 10.5 if necessary. Then the suspension was diluted with water (about 200 mL) for dialysis in cellulose membrane tubes against water for one day. The microgels were collected by ultracentrifugation and stored at 4 ^{o}C.

Some experiments were conducted in a spectrophotometer to record the turbidity changes. Typically, 1 mL microgel suspension (1.13 g/L) was mixed with 1mL NaClO (40 mM) in a cuvette. After adjusting pH to 10.5, transmittance at 500 nm was measured at 25 ^{o}C with a DU800 visible-UV spectrophotometer (Beckman Coulter) using water as a blank.

N-chlorinated Microgels Reacting with GSH. Suspensions of N-chlorinated microgels and GSH were prepared in 1 mM NaCl in polystyrene cuvettes. The N-chlorinated microgels had a VPTT of 20 ^{o}C and active chlorine content of ~0.8 mmol/g. The microgel concentration was fixed at 0.25 g/L. Thus, the active chlorine content in the suspension was kept at ~0.2 mM. GSH concentration was varied from 0.1 mM to 1 mM. The suspension pH was adjusted with 0.01 M HCl or NaOH. The change of suspension turbidity was recorded with a DU800 visible-UV spectrophotometer.

Iodometric Titration. The active chlorine content in microgels was determined by iodometric titration. N-chlorinated PNIPAM microgels (around 5 mg) were dispersed in water to make a 1 g/L solution. An excess amount of KI (~100 mg) was added to the solution. The solution pH was adjusted to 3. Then 2 mL starch indicator (1%) was added. The solution was titrated with sodium thiosulfate (10 mM) until the solution turned colorless.

Critical Flocculation Temperature (CFT). A suspension with a concentration of 1 g/L of microgels and varying concentrations of NaCl was kept in a water bath with controlled temperatures for 12 hr. Then the absorbance of the suspension (or supernatant if aggregated) was determined at a wavelength of 500 nm using a DU800 visible-UV spectrophotometer (Beckman Coulter). The CFT was defined as the temperature where the absorbance started decreasing.

Dynamic Light Scattering (DLS). Hydrodynamic diameters of microgels were measured by DLS with a detection angle of 90^{o}. The laser source was a Melles Griot HeNe laser with a wavelength of 633 nm. The scattering intensity was between 100 and 250 kcps for all measurements. Each sample was measured for at least three runs with 2 min for each run.

Microelectrophoresis. Electrophoretic mobilities of microgels under various temperatures were determined, using a Brookhaven ZetaPlus zeta potential analyzer operating in phase analysis light scattering mode with BIC Pals Zeta Potential Analyzer software (V 2.5). Data were averaged over 10 cycles, with 15 scans for each cycle.

3.3 Results

The following experiments involve following the changes in PNIPAM microgels upon exposure to bleach. Based on our previous investigations of linear PNIPAM in bleach, it can be anticipated that the N-chlorination reaction (Scheme 2) required pH values greater than 9. [19]

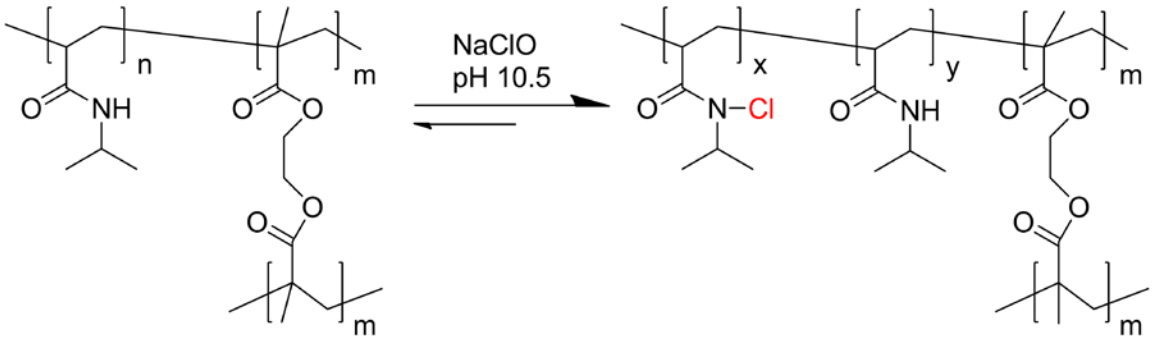

Scheme 2 Schematic description of chlorination on PNIPAM microgels by reacting with bleach at pH 10.5 (n=x+y).

A series of microgel suspensions were prepared by mixing purified PNIPAM microgels with aqueous bleach under conditions of varying pH, and the optical transmittance was recorded as a function of time. The results, shown in Figure 1, indicate two regimes of pH behavior. For pH values 7-9, the microgels slowly degraded, ultimately giving a transparent solution. By contrast, at pH 10-11 the dispersion transmittance decreased with time until the microgels phase separated. Our earlier work showed that poly(NIPAM-co-NIPAMCl) had a lower cloud point temperature than PNIPAM.[24] Therefore it is reasonable to attribute the decreasing transmittance with time (see pH 10, 11 curves in Figure 1) to the shrinkage of the microgels. However, along with shrinkage, there was a loss in colloidal stability under the relatively high ionic strength conditions.

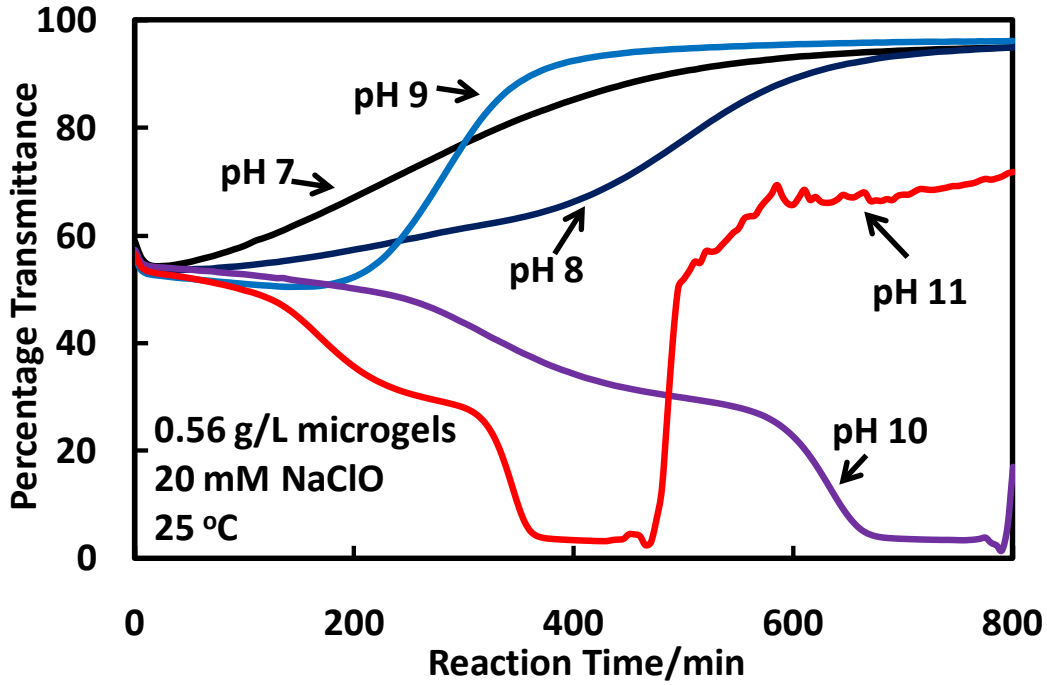

Figure 1 Suspension transmittance vs reaction time curves for chlorination of PNIPAM microgels with different pH.

3.3.1 Reaction Temperature Effect on Volume Phase Transition Temperature

Figure 2 shows photographs of PNIPAM microgel suspensions with 20 mM NaClO at pH 10.5. Macroscopic separation was observed after about 10 hour reaction at 25 ^{o}C. The aggregates were redispersed by decreasing the suspension temperature to a level lower than the reaction temperature (25 ^{o}C in Figure 2). The suspension was phase separated again by increasing the temperature higher than 25 ^{o}C. This reversibility also indicates a lower VPTT due to formation of nitrogen-chlorine bonds, which make microgels more hydrophobic.

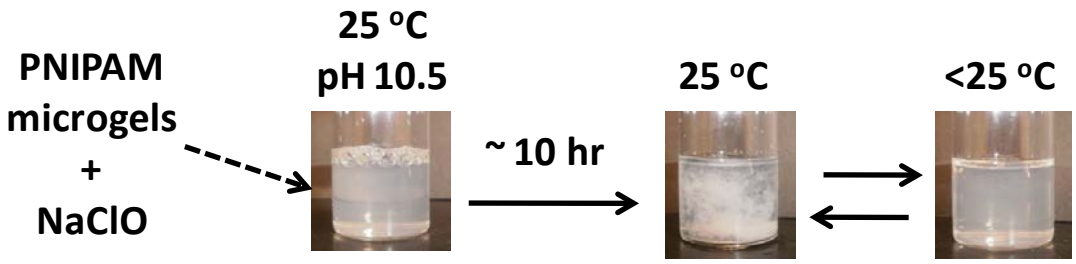

Figure 2 Photographs of PNIPAM microgels in bleach. The solution was prepared at pH 10.5 with 0.56 g/L microgels and 20 mM NaClO.

The reaction temperature was varied from 20 ^{o}C to 30 ^{o}C. Macroscopic separation was observed under all temperatures, although different reaction times were required. It took 2 hr at 30 ^{o}C, and 24 hr at 20 ^{o}C. The diameters of purified N-chlorinated microgels in water were determined by DLS, as shown in Figure 3A. N-chlorinated microgels were also thermosensitive, and lower reaction temperature led to lower VPTT. The relationship between VPTT and reaction temperature is shown in Figure 3B. It shows that the VPTT is almost identical to the reaction temperature, which provides a very simple way to predict microgel VPTT. The results in Figure 3 also suggest that N-chlorinated microgels disperse in water when the measurement temperature is higher than VPTT, although they aggregated in 20 mM NaClO at VPTT during chlorination.

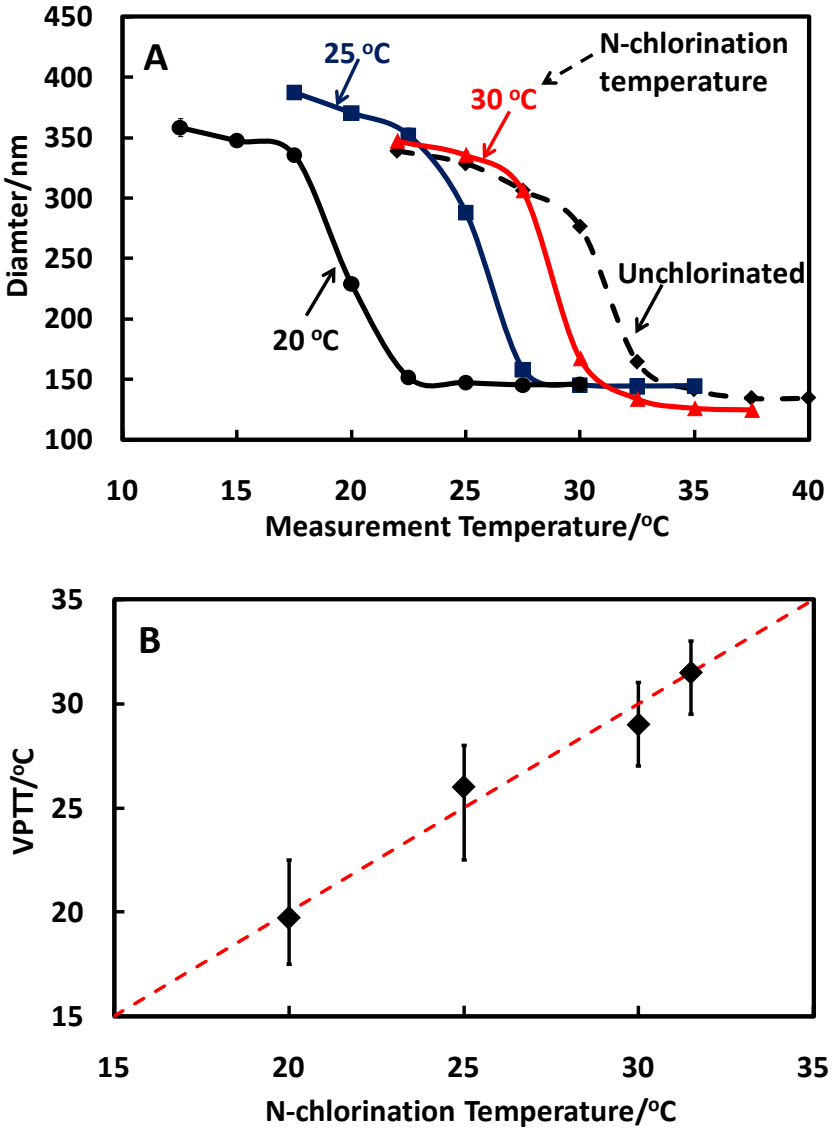

Figure 3. A) Diameters of purified microgels in water were determined by DLS along with measurement temperature. Microgels reacted with NaClO prior to DLS measurement, and the modification recipe was as follow: 0.56 g/L microgels, 20 mM NaClO, pH 10.5 and N-chlorination temperature shown in the figure.

B) Relationship between result VPTT and reaction temperature. The error bars on the VPTTs reflect the temperatures where microgel diameters start decreasing drastically and stop decreasing.

The electrophoretic mobility of purified N-chlorinated microgels in 1 mM NaCl is shown in Figure 4. All microgels were negatively charged. Some N-chlorinated microgels (modified at 25 ^{o}C and 20 ^{o}C) had more surface charges than the unmodified microgels in a shrunken state, which contributed to the slight hydrolysis of amides at high pH.[25] The results of carboxylic content from conductometric titration did not show significant difference between unchlorinated microgels and N-chlorinated microgels (results are not shown in this paper), which suggests limited hydrolysis from N-chlorination reaction. Plus, the pH effect on diameters of the N-chlorinated microgels (VPTT=~26 ^{o}C) in 1 mM NaCl is shown in the Supporting Information (S3). The diameter only increased slightly with pH, which also indicates limited hydrolysis.

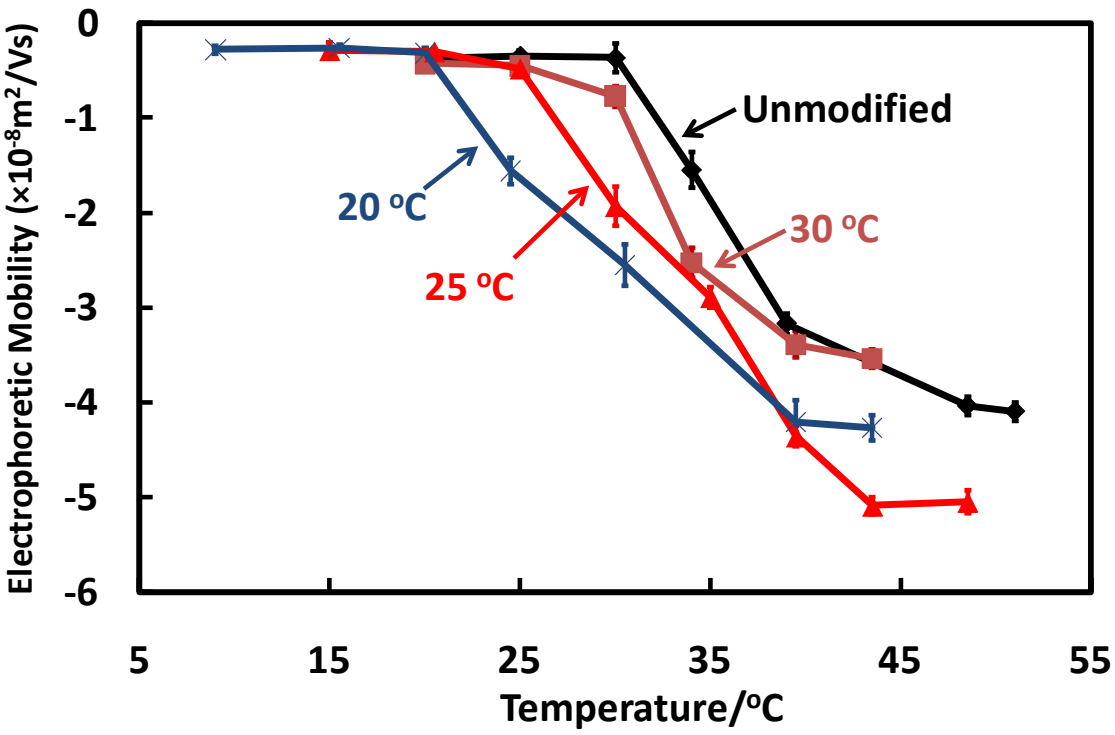

Figure 4 Electrophoretic mobilities of chlorinated microgels after cleaning and dispersion in 1 mM NaCl. Modification condition: 0.56 g/L microgels, 20 mM NaClO, and pH 10.5. The chlorination temperatures are shown in the figure.

The active chlorine content in purified N-chlorinated microgels was determined by iodometric titration. The relationship between VPTT and chlorine content is shown in Figure 5. It is shown that higher active chlorine content led to a lower VPTT. In this

paper, the highest content of 0.8 mmol/g was obtained when a reaction temperature of 20 ^{o}C was used in the chlorination stage.

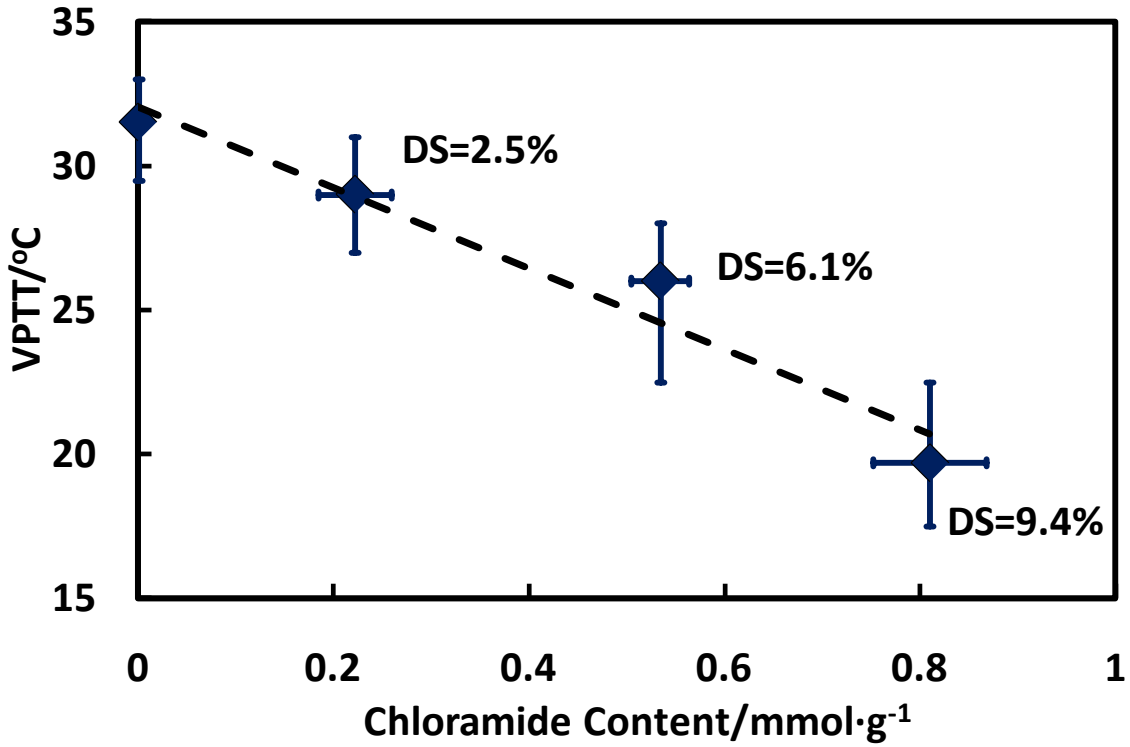

Figure 5 VPTT versus active chlorine content of chlorinated microgels. The error bars in the Y direction are adapted from Figure 3B. The error bars in the X direction is the standard deviations of chloramide content from three repeat measurements. The degree of substitution (DS) is also shown in the figure.

3.3.2 Mechanism for Colloidal Instability

The aggregation of PNIPAM microgels in 20 mM NaClO during N-chlorination was studied in detail in this section. The reaction was monitored by tracking the change of turbidity and particle size as a function of reaction time. The results are shown in Figure 6A. The reaction is divided into four stages and explained by the mechanism as proposed in Figure 6B.

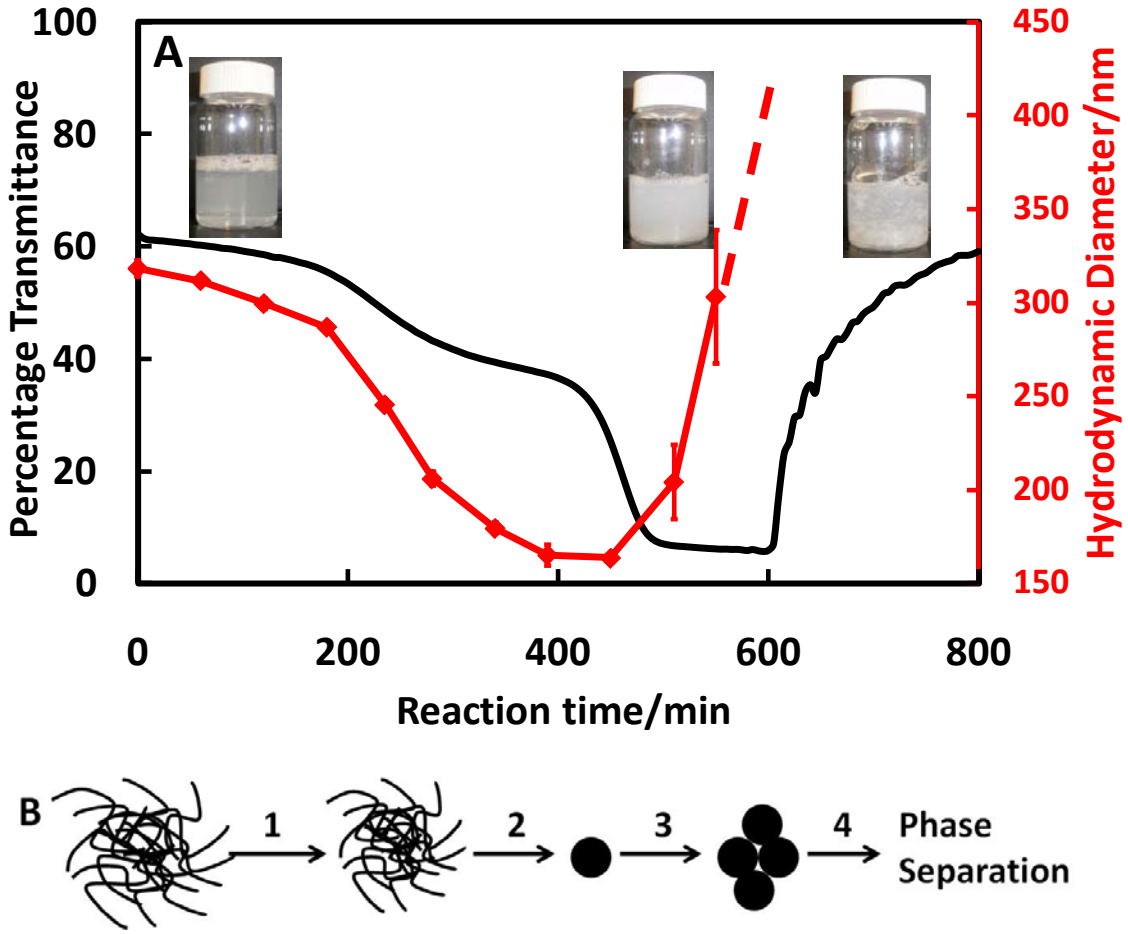

Figure 6 A) Suspension turbidity and hydrodynamic diameter as a function of reaction time (0.56 g/L microgels, 20 mM NaClO, 25 ^{o}C). B) Proposed mechanism

The decreasing suspension transmittance and microgel size up to 400 min reaction time indicated that the microgels were getting smaller but still well-dispersed in 20 mM bleach. This is because PNIPAM microgels became more hydrophobic due to N-chlorination, and the VPTT was decreasing. At about 400 min reaction time, the microgels were completely shrunken. At this point, the VPTT was very close to the reaction temperature. After 400 min reaction time, the measured size increased quickly, with a large uncertainty (shown by the error bars). Therefore the chlorinated microgels were colloidally unstable at the VPTT in 20 mM NaClO Macroscopic separation of microgels in the reaction solution was eventually observed.

3.3.3 NaCl effect on VPTT

Critical flocculation temperatures (CFTs) of purified N-chlorinated microgels in aqueous NaCl were determined as a function of NaCl concentration, as shown in Figure 7. The

CFT was defined as the temperature at which the highest suspension absorbance was obtained. The absorbance vs. temperature data is shown in the Supporting Information. It is shown that microgels with lower VPTT have lower CFT. Furthermore, CFT decreases with NaCl concentration. VPTTs of the N-chlorinated microgels prepared from 20 mM NaClO were close to the CFTs in 100 mM NaCl solution. This is because the electrical conductivity of 20 mM bleach was determined close to that of 100 mM NaCl.

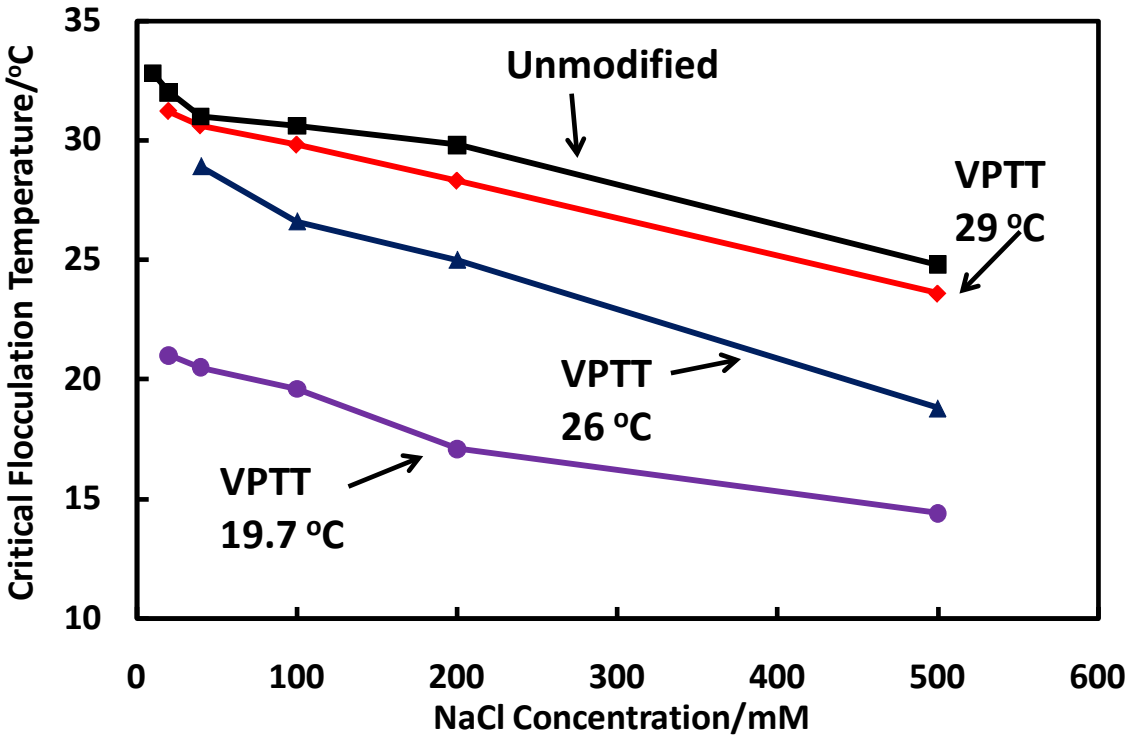

Figure 7 Critical flocculation temperature of chlorinated microgels against NaCl concentration. VPTTs of chlorinated microgels are shown in the figure.

Thus, the CFT decreased by adding extra salt (NaCl) in the reaction solution. The reaction between PNIPAM microgels and bleach was redone but with extra NaCl added into the reaction solution. The resulting N-chlorinated microgels were purified and the diameters in pure water were measured by DLS, as shown in Figure 8. Adding extra NaCl shortened the time for macroscopic separation. Thus, the active chlorine content decreased with increasing NaCl concentration, resulting in higher VPTT.

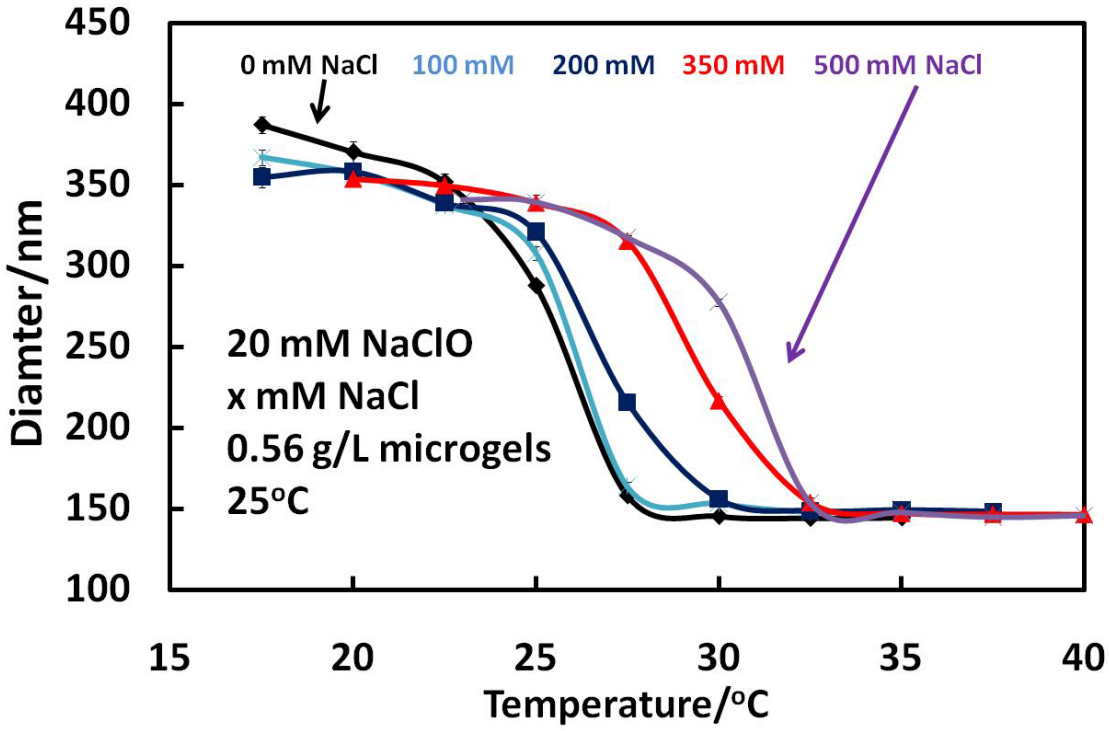

Figure 8 Diameters of purified N-chlorinated microgels in pure water. Modification recipe: 0.56 g/L microgels, 20 mM NaClO, 25 ^{o}C and varied concentration NaCl. The NaCl concentration in the solution during reaction is shown in the figure.

3.3.4 Chlorinated PNIPAM Microgels as a Source of Active Chlorine

It has been shown that linear poly(NIPAM-co-NIPAMCl) is oxidative on reacting with potassium iodine and $Na_2S_2O_3$.[19] Since glutathione (GSH) is present in almost all cells and plays a number of crucial roles[26], the reduction of N-chlorinated PNIPAM microgels with GSH was evaluated. The purified N-chlorinated microgels with a VPTT of about 20 ^{o}C (~0.8 mmol/g active chlorine) were redispersed in 1 mM GSH at a different pH. The concentration of microgels was 0.25 g/L. Thus the active chlorine concentration was 0.2 mM. The changes of mixture transmittance were determined at 25 ^{o}C, and the results are shown in Figure 9. The reaction rate between N-chlorinated microgels and GSH strongly depended on the pH. At a pH above 6, the suspension transmittance increases rapidly, and the reaction was completed in several minutes. At a lower pH, the reaction was much slower.

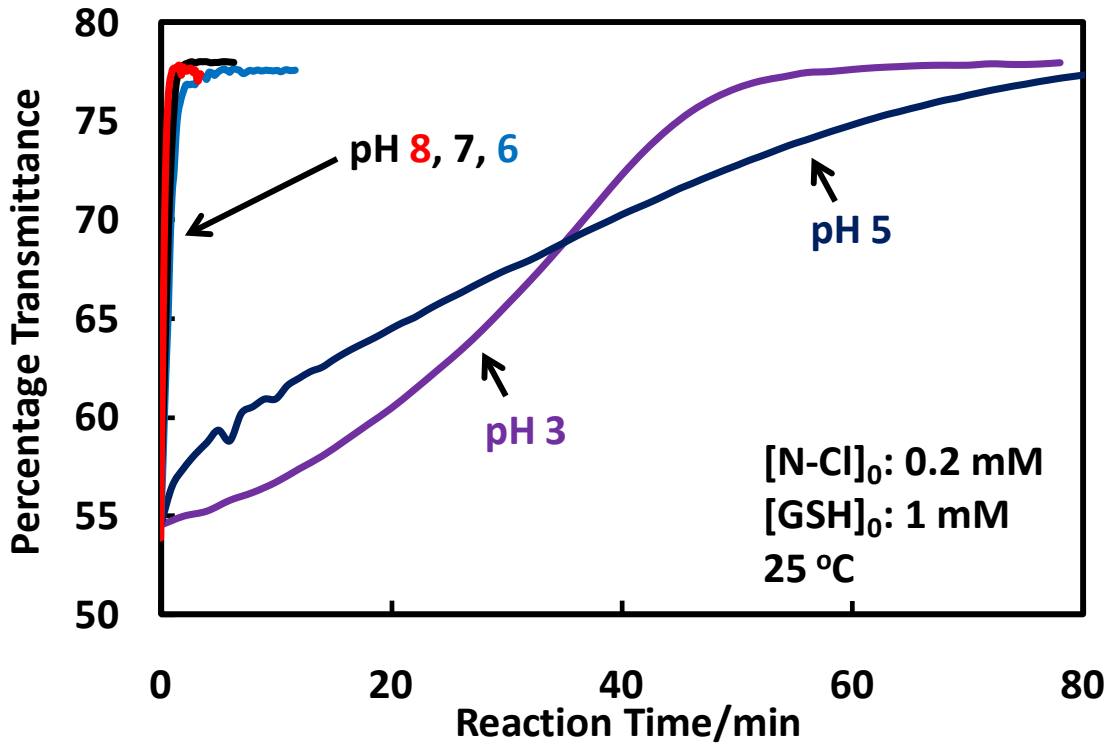

Figure 9 Effect of pH on the transmittance change of N-chlorinated microgels reacting with 1 mM GSH. $[N\text{-}Cl]_0$ and $[GSH]_0$ represent the initial concentrations of N-chloramide and GSH in the solution, respectively.

The GSH concentration effect on the reaction rate at pH 7 was also evaluated. The active chlorine concentration was kept at 0.2 mM, and the GSH concentration was varied from 0.1 mM to 1 mM. The changes of suspension turbidity were recorded as shown in Figure 10**A**. After the reaction was fully completed, the final diameters of reduced microgels were determined as shown in Figure 10B. The final transmittance was around 78% for suspensions with excess GSH (0.5, 0.8, 1 mM). Also the final diameter was around 360 nm, which was close to the swollen size of unmodified microgels (Figure 3A). Both results indicate microgels fully swollen at 25 ^{o}C in suspensions with excess GSH. In suspensions with lower GSH concentration (0.1, 0.2 mM), the final transmittances were lower than 78% and the final diameters were lower than 360 nm. Thus, the microgels were partially swollen in these suspensions.

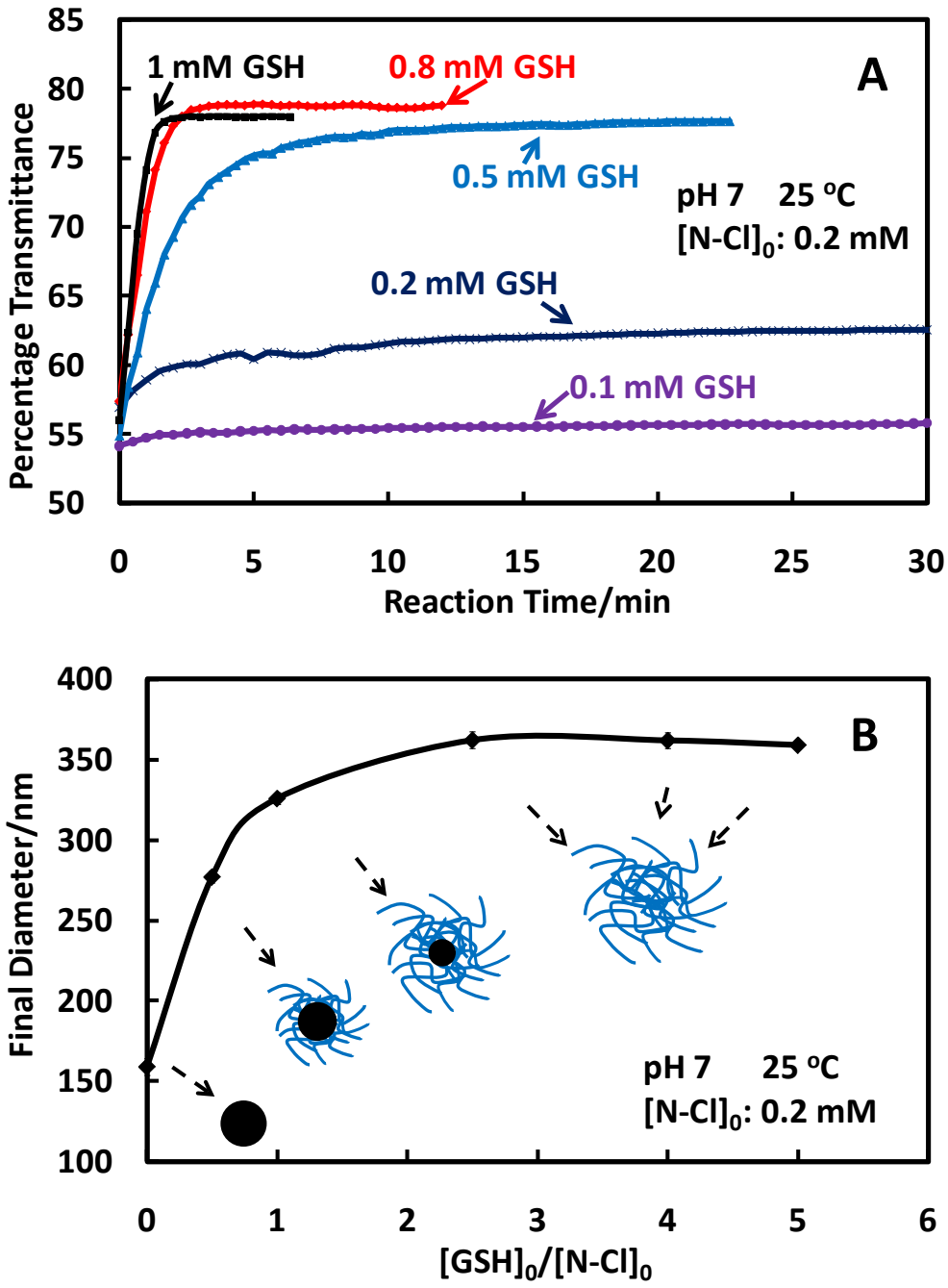

Figure 10 A) Transmittance of N-chlorinated microgels (VPTT= ~20 °C) in glutathione solution with varied concentrations at 25 °C. B) Final diameters of reduced microgels. $[N\text{-}Cl]_0$ and $[GSH]_0$ represent the initial concentrations of N-chloramide and GSH in the solution, respectively.

After reduction with 1 mM GSH, the microgel diameters were determined by DLS as shown in Figure 11. VPTT increased from 20 ^{o}C to 31 ^{o}C after reduction. The increase in VPTT indicates full consumption of the active chlorine. The results also indicate that GSH can react with shrunken N-chlorinated microgels.

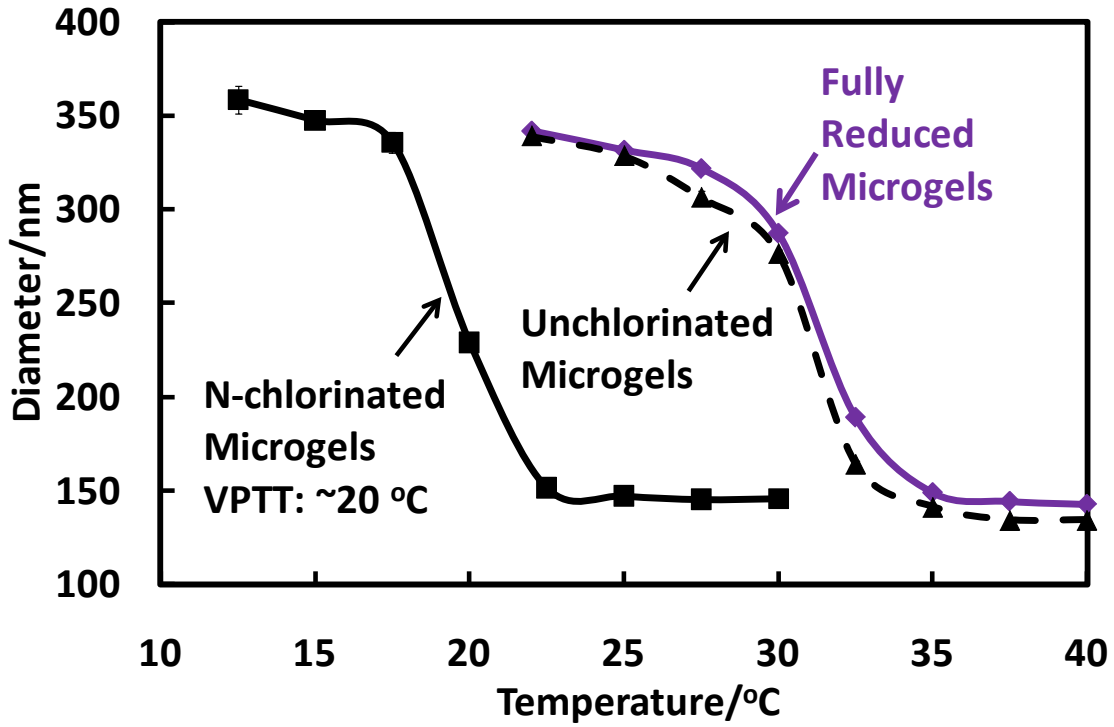

Figure 11 Diameter of unchlorinated, N-chlorinated and fully reduced microgels along with temperature in water.

After partial reduction with 0.1 mM GSH at pH 7, the microgel diameters along with the measurement temperature were determined with DLS. The results are shown in Figure 12**A**. The diameter curve shows a two-stage thermal transition, indicating a core/shell structure. The particle size distributions were narrow and mono-peak at different temperatures, as shown in the Figure 12A. N-chlorinated microgels aggregated in 200 mM NaCl after treatment at 25 ^{o}C for about 1 hr, while reduced microgels (reduced with 0.1 mM GSH) were kept stable. The photographs are shown in Figure 12B. Since chlorinated microgels were shrunken at 25 ^{o}C, aggregation can be observed in 200 mM NaCl. However, partially reduced microgels were still colloidal stable in the NaCl solution. This difference further supports the hypothesis of a core/shell structure of partially reduced microgels.

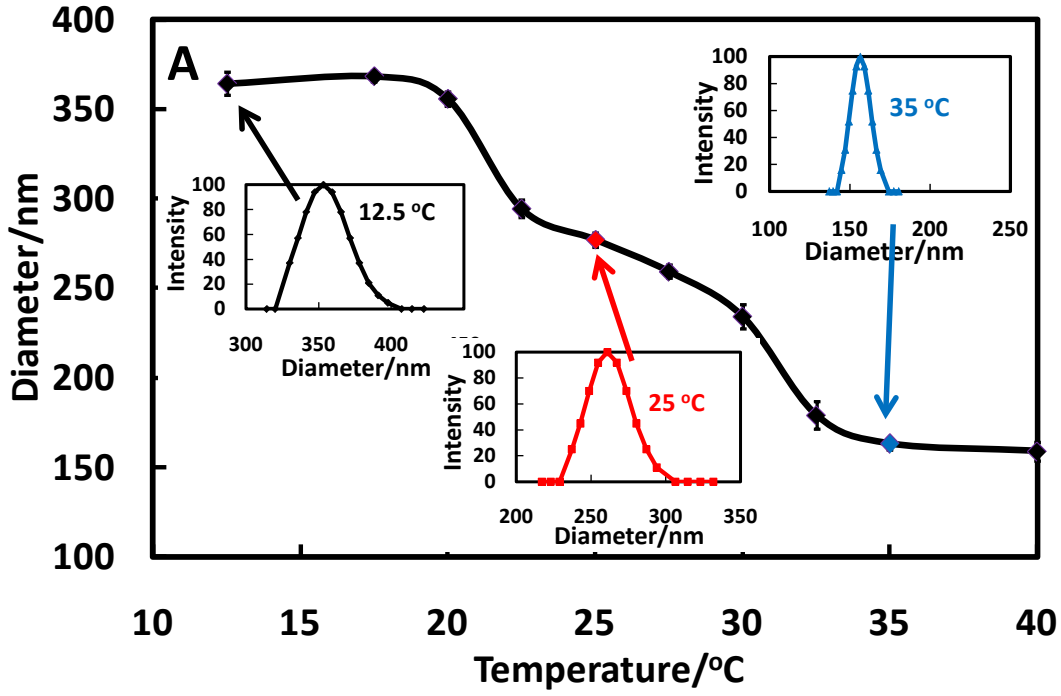

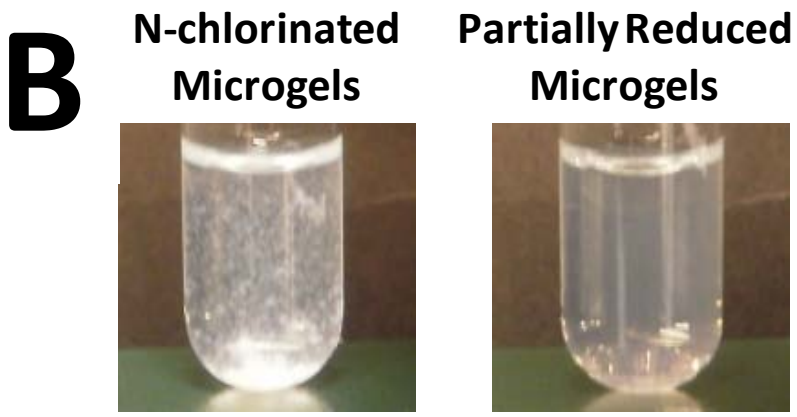

Figure 12 (A) Diameter of N-chlorinated microgels after reduced by 0.1 mM GSH at pH 7. The size distributions at different temperature are also shown. (B) Photographs of N-chlorinated microgels and partially reduced microgels in 200 mM NaCl at 25 ^{o}C for 1 hr.

3.4 Discussion

3.4.1 N-chlorination of PNIPAM Microgels

It has been shown that N-chloramines are more hydrophobic than their parent amines/amides.[27] Hence PNIPAM microgels become more hydrophobic during N-chlorination in bleach at pH 10.5, due to the formation of nitrogen-chlorine bonds. Microgels keep shrinking in bleach, as indicated by a decrease in suspension transmittance and size (Figure 1). Although electrophoretic mobility of N-chlorinated PNIPAM microgels increase slightly (Figure 4), the electrostatic repulsion is completely screened in bleach (20 mM NaClO) due to the high salt concentration. The steric repulsion of swollen PNIPAM chains is the only force keeping microgels dispersed in bleach during the reaction. When the active chlorine content is high enough, microgels are fully shrunken in bleach. As a result, the steric stabilization is suppressed and the van der Waals attraction increases[28-29], leading to aggregation of the N-chlorinated microgels.

At the point of microgels aggregation, the critical flocculation temperature (CFT) of the N-chlorinated microgels is equal to the reaction temperature. The volume phase transition temperature (VPTT) depends on salt concentration. The conductivity of 20 mM NaClO is close to that of 100 mM NaCl. Thus, the VPTT of N-chlorinated microgels is almost identical to its CFT in 20 mM NaClO (Figure 7). Hence, the VPTT of N-chlorinated microgel prepared from 20 mM NaClO is almost identical to its reaction temperature (Figure 3B). However, adding extra NaCl in the 20 mM NaClO decreases the CFT, since higher salt concentration solution is a poorer solvent for PNIPAM. The reaction stops faster, and less active chlorine is formed, with added extra NaCl. As a result, the VPTT of N-chlorinated microgels is higher than its reaction temperature (Figure 8).

Upon macroscopic separation, further N-chlorination on microgels is resisted due to their fully shrunken state. This effect is attributed to the following mechanisms. First, the formation of intrachain hydrogen bonds[30-31] in the shrunken state may prevent the attack of ClO^- to amides. Furthermore, it has been determined that self-diffusion coefficient of water in PNIPAM microgels is 4.3×10^{-10} m^2 s^{-1} in a swollen state, while it decreases to 1.7×10^{-11} m^2 s^{-1} in a shrunken state.[32] It is also reasonable to assume the diffusion of ClO^- is also restrained in a shrunken state, which may further decrease the N-chlorination rate. Besides, the surface charge density (mobility) of the shrunken microgels is higher than that of the swollen microgels (Figure 4), which may further suppress the diffusion of ClO^- into the shrunken microgels. A similar trend was found that the diffusion of Cu^{2+} ions into collapsed microgels was more difficult than the diffusion into the swollen microgels.[33]

In N-chlorinated microgels, the VPTT corresponds to the active chlorine content (Figure 5). Higher active chlorine content, which also means higher hydrophobic species content, leads to a lower VPTT. This is consistent with the results from copolymerization of

NIPAM with hydrophobic comonomers.[34] Since VPTT is controlled by reaction temperature and salt concentration, the active chlorine content is easily tuneable. Besides, PNIPAM microgels eventually aggregate in aqueous bleach, which indicates the end of the reaction. Thus, our method is easier to conduct than copolymerization.

3.4.2 N-chlorinated Microgels Reacting with GSH

The reaction scheme of N-chloramines reacting with GSH is summarised from the literatures[35-36] and shown in Scheme 3. This scheme can explain the pH-dependent on the reaction between N-chlorinated microgels with GSH. At low pH, the formation of HCl is suppressed, which gives low reaction rate.

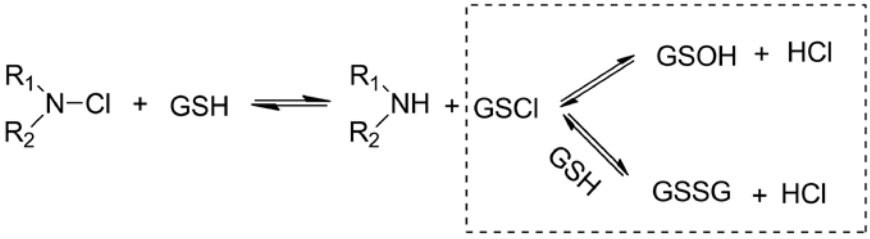

GSH:

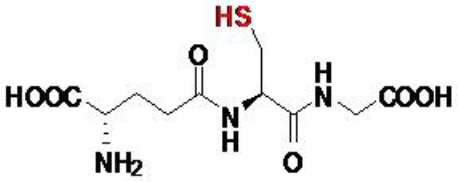

GSCl:

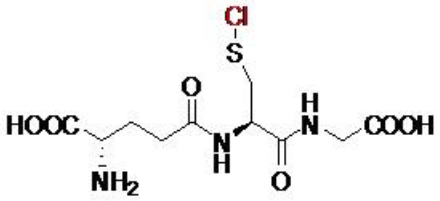

GSOH:

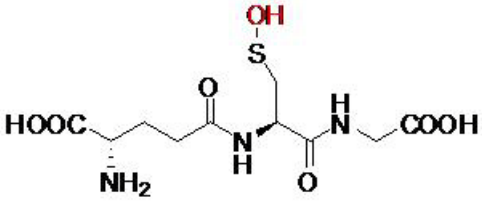

GSSG:

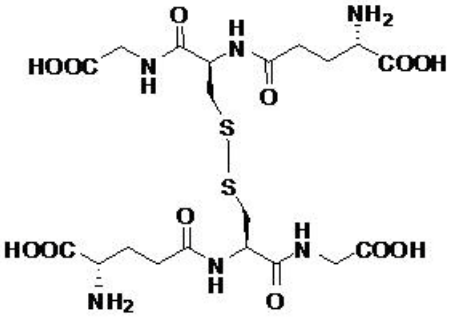

Scheme 3 Proposed reaction scheme between N-chloramines or N-chloramines and GSH.

The reaction rate at pH 7 is very fast, with the reaction complete in a few minutes (Figure 10A). It has been reported that every N-chloramine molecule consumes thiol molecules in a range of 1.6~2.0 when the thiol compound is in excess.[36] In suspensions with 0.2 mM active chlorine content, high GSH concentration (0.5, 0.8, 1 mM) is enough to consume all active chlorine, since the VPTT increases again to 31 ^{o}C after reduction.

With low GSH concentration (0.1, 0.2 mM), only partial active chlorine is consumed. The partially reduced microgels have a core/shell structure. This conclusion is made based on the following arguments. The partially reduced microgels have a two-stage thermo-induced volume transition. Thus, there are only two possible structures: one is the core/shell and the other is a mixture of N-chlorinated microgels and fully reduced microgels. If the latter is the case, the particle size distribution at 25 ^{o}C would not be mono-peak, and part of microgels would aggregate in 200 mM NaCl. However, these are contrary to the results (Figure 12**)**. Thus, it is reasonable to conclude that partially reduced microgels have a core/shell structure. This is consistent to the two-stage thermo-induced transition found for core/shell microgels with PNIPAM cores and poly(N-isopropylmethacrylamide) shells by Berndt and Richtering.[37]

Based on the core/shell structure of partially reduced microgels, it is argued that the reduction between N-chlorinated microgels and GSH is diffusion-controlled. If the reduction is reaction-controlled, the decrease in active chlorine content is uniform. Then there would be only one VPTT for partially reduced microgels. However, only the shell part of the N-chlorinated microgels is reduced with inadequate GSH. Hence it is reasonable to assume that GSH reacts only with the periphery of shrunken microgels, as described in Scheme 4. The reduced area becomes swollen, and GSH can diffuse further into microgels, reacting with the periphery of the unreduced core.

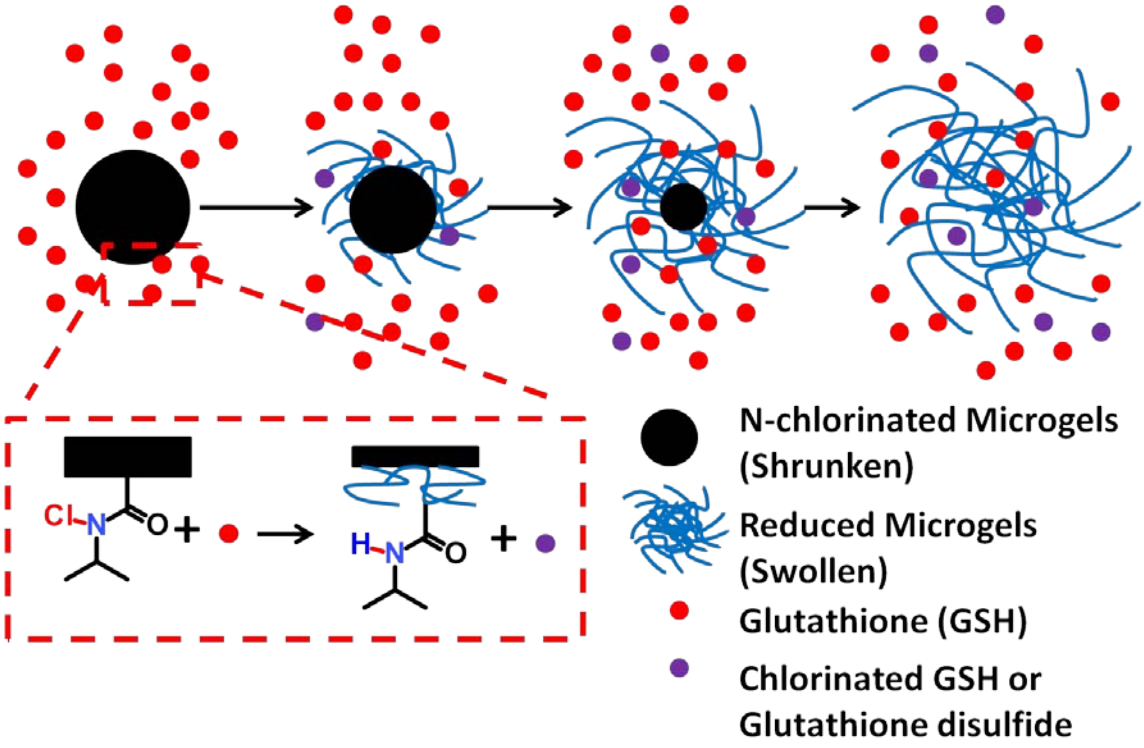

Scheme 4 Schematic description of N-chlorinated microgels reacting with GSH

3.4.3 Potential Applications

The active chlorine content of N-chlorinated microgels can go up to ~0.8 mmol/g, which is much higher than that in compounds with polymeric N-halamines coating. For example, the highest active chlorine content was found about 54.8 μmol/g for hard nanoparticles with a diameter of 11 nm.[17] Thus, N-chlorinated PNIPAM microgels can be used as chlorine-releasing agent with long-term efficacy. N-chlorinated PNIPAM microgels can be dispersed in solution, and also fabricated into monolayers[38] and multilayers[39] coating.

PNIPAM microgels can be coupled to folic acids[40] or proteins[41] for targeting cancer cells. On the other hand, the N-chlorinated microgels react with GSH (Figure 10), and GSH depletion is a potential strategy in cancer therapy[42]. Thus, the N-chlorinated PNIPAM microgels with cell-targeting labels may be useful for killing cancer cells. We propose using the N-chlorinated PNIPAM microgels not only as a drug carrier, but also as the drug itself to destroy the antioxidant systems of cancer cells.

3.5 Conclusion

1. PNIPAM microgels are N-chlorinated by aqueous bleach at high pH (>9), as illustrated by the change of mixture turbidity during the reaction.

2. The volume phase transition temperature (VPTT), which is almost identical to the reaction temperature, decreases with the active chlorine content. Thus, the extent of N-chlorination is easily controlled by adjusting the reaction temperature. Microgels phase separate when the desired reaction extent is reached, indicating suppression of further modification, and the end of the reaction.

3. Although N-chlorinated microgels are slightly more negatively charged, their electrostatic stability is screened in aqueous bleach due to the high ionic strength. The aggregation of microgels in aqueous bleach is triggered by microgels shrinking. As a result, microgels eventually aggregate in bleach, and the VPTT is almost equal to the reaction temperature. Increasing salt concentration, caused by the addition of more NaCl in bleach, leads to faster aggregation of N-chlorinated microgels, with a higher VPTT.

4. After N-chlorinated microgels aggregate in bleach, the further chlorination is inhibited. This effect contributes to the formation of intrachain hydrogen bonds of PNIPAM and lower diffusion coefficient of ClO^- in shrunken microgels.

5. Shrunken N-chlorinated PNIPAM microgels react with glutathione in a diffusion-controlled manner. After full reduction, the VPTT increases again to about 31 ^oC. For partially reduced microgels, a core/shell structure is proposed.

3.6 References

1. Worley, S. D.; Williams, D. E., Halamine Water Disinfectants. *Crc Critical Reviews in Environmental Control* **1988,** 18, (2), 133-175.
2. Qian, L.; Sun, G., Durable and regenerable antimicrobial textiles: Synthesis and applications of 3-methylol-2,2,5,5-tetramethylimidazolidin-4-one (MTMIO). *Journal of Applied Polymer Science* **2003,** 89, (9), 2418-2425.
3. Sun, Y. Y.; Sun, G., Novel refreshable N-halamine polymeric biocides: N-chlorination of aromatic polyamides. *Industrial & Engineering Chemistry Research* **2004,** 43, (17), 5015-5020.
4. Sun, J.; Sun, Y. Y., Acyclic N-halamine-based fibrous materials: Preparation, characterization, and biocidal functions. *Journal of Polymer Science Part a-Polymer Chemistry* **2006,** 44, (11), 3588-3600.
5. Liu, S.; Sun, G., New Refreshable N-Halamine Polymeric Biocides: N-Chlorination of Acyclic Amide Grafted Cellulose. *Industrial & Engineering Chemistry Research* **2009,** 48, (2), 613-618.
6. Sun, Y. Y.; Chen, T. Y.; Worley, S. D.; Sun, G., Novel refreshable N-halamine polymeric biocides containing imidazolidin-4-one derivatives. *Journal of Polymer Science Part a-Polymer Chemistry* **2001,** 39, (18), 3073-3084.
7. Chen, Z. B.; Sun, Y. Y., N-halamine-based antimicrobial additives for polymers: Preparation, characterization, and antimicrobial activity. *Industrial & Engineering Chemistry Research* **2006,** 45, (8), 2634-2640.
8. Kocer, H. B.; Cerkez, I.; Worley, S. D.; Broughton, R. M.; Huang, T. S., N-Halamine Copolymers for Use in Antimicrobial Paints. *ACS Applied Materials & Interfaces* **2011,** 3, (8), 3189-3194.
9. Kocer, H. B.; Cerkez, I.; Worley, S. D.; Broughton, R. M.; Huang, T. S., Polymeric antimicrobial N-halamine epoxides. *ACS Applied Materials & Interfaces* **2011,** 3, (8), 2845-50.
10. Akdag, A.; Okur, S.; McKee, M. L.; Worley, S. D., The stabilities of N-Cl bonds in biocidal materials. *Journal of Chemical Theory and Computation* **2006,** 2, (3), 879-884.
11. Sun, G.; Wheatley, W. B.; Worley, S. D., A New Cyclic N-Halamine Biocidal Polymer. *Industrial & Engineering Chemistry Research* **1994,** 33, (1), 168-170.
12. Chen, Z.; Luo, J.; Sun, Y., Biocidal efficacy, biofilm-controlling function, and controlled release effect of chloromelamine-based bioresponsive fibrous materials. *Biomaterials* **2007,** 28, (9), 1597-1609.
13. Ahmed, A. E. S. I.; Hay, J. N.; Bushell, M. E.; Wardell, J. N.; Cavalli, G., Optimizing Halogenation Conditions of N-Halamine Polymers and Investigating Mode of Bactericidal Action. *Journal of Applied Polymer Science* **2009,** 113, (4), 2404-2412.
14. Kocer, H. B.; Worley, S. D.; Broughton, R. M.; Acevedo, O.; Huang, T. S., Effect of Phenyl Derivatization on the Stabilities of Antimicrobial N-Chlorohydantoin Derivatives. *Industrial & Engineering Chemistry Research* **2010,** 49, (22), 11188-11194.

15. Cerkez, I.; Kocer, H. B.; Worley, S. D.; Broughton, R. M.; Huang, T. S., N-Halamine Biocidal Coatings via a Layer-by-Layer Assembly Technique. *Langmuir* **2011,** 27, (7), 4091-4097.
16. Padmanabhuni, R. V.; Luo, J.; Cao, Z. B.; Sun, Y. Y., Preparation and Characterization of N-Halamine-Based Antimicrobial Fillers. *Industrial & Engineering Chemistry Research* **2012,** 51, (14), 5148-5156.
17. Jang, J.; Kim, Y., Fabrication of monodisperse silica-polymer core-shell nanoparticles with excellent antimicrobial efficacy. *Chemical Communications* **2008**, (34), 4016-4018.
18. Heskins, M.; Guillet, J. E., solution properties of poly(N-isopropylacrylamide). *Journal of Macromolecular Science: Part A - Chemistry* **1968,** A2, (8), 1441-1455.
19. Wang, Z.; Pelton, R., Chloramide Copolymers From Reacting Poly(N-isopropylacrylamide) with Bleach. *Submitted* **2012**.
20. Pelton, R. H.; Chibante, P., Preparation of Aqueous Lattices with N-Isopropylacrylamide. *Colloids and Surfaces* **1986,** 20, (3), 247-256.
21. Pelton, R., Temperature-sensitive aqueous microgels. *Advances in Colloid and Interface Science* **2000,** 85, (1), 1-33.
22. Wirsen, A.; Ohrlander, M.; Albertsson, A. C., Bioactive heparin surfaces from derivatization of polyacrylamide-grafted LLDPE. *Biomaterials* **1996,** 17, (19), 1881-1889.
23. Mcphee, W.; Tam, K. C.; Pelton, R., Poly(N-Isopropylacrylamide) Latices Prepared with Sodium Dodecyl-Sulfate. *Journal of Colloid and Interface Science* **1993,** 156, (1), 24-30.
24. Wang, Z.; Pelton, R., Chloramide Copolymers From Reacting Poly (N-isopropylacrylamide) with Bleach. *European Polymer Journal* **2013,** 49, (8), 2196-2201.
25. Hoare, T.; Pelton, R., Functional group distributions in carboxylic acid containing poly(N-isopropylacrylamide) microgels. *Langmuir* **2004,** 20, (6), 2123-2133.
26. Pompella, A.; Visvikis, A.; Paolicchi, A.; De Tata, V.; Casini, A. F., The changing faces of glutathione, a cellular protagonist. *Biochemical Pharmacology* **2003,** 66, (8), 1499-1503.
27. MacCrehan, W. A.; Jensen, J. S.; Helz, G. R., Detection of sewage organic chlorination products that are resistant to dechlorination with sulfite. *Environmental Science & Technology* **1998,** 32, (22), 3640-3645.
28. Routh, A. F.; Vincent, B., Salt-induced homoaggregation of poly(N-isopropylacrylamide) microgels. *Langmuir* **2002,** 18, (14), 5366-5369.
29. Rasmusson, M.; Routh, A.; Vincent, B., Flocculation of microgel particles with sodium chloride and sodium polystyrene sulfonate as a function of temperature. *Langmuir* **2004,** 20, (9), 3536-3542.
30. Wang, X.; Qiu, X.; Wu, C., Comparison of the Coil-to-Globule and the Globule-to-Coil Transitions of a Single Poly(N-isopropylacrylamide) Homopolymer Chain in Water. *Macromolecules* **1998,** 31, (9), 2972-2976.
31. Zhou, K.; Lu, Y.; Li, J.; Shen, L.; Zhang, G.; Xie, Z.; Wu, C., The Coil-to-Globule-to-Coil Transition of Linear Polymer Chains in Dilute Aqueous Solutions: Effect of Intrachain Hydrogen Bonding. *Macromolecules* **2008,** 41, (22), 8927-8931.

32. Sierra-Martin, B.; Romero-Cano, M. S.; Cosgrove, T.; Vincent, B.; Fernandez-Barbero, A., Solvent relaxation of swelling PNIPAM microgels by NMR. *Colloids and Surfaces a-Physicochemical and Engineering Aspects* **2005,** 270, 296-300.
33. Yin, J.; Guan, X.; Wang, D.; Liu, S., Metal-Chelating and Dansyl-Labeled Poly(N-isopropylacrylamide) Microgels as Fluorescent Cu2+ Sensors with Thermo-Enhanced Detection Sensitivity. *Langmuir* **2009,** 25, (19), 11367-11374.
34. Zhang, Q. S.; Zha, L. S.; Ma, J. H.; Liang, B. R., Synthesis and characterization of novel, temperature-sensitive microgels based on N-isopropylacrylamide and tert-butyl acrylate. *Journal of Applied Polymer Science* **2007,** 103, (5), 2962-2967.
35. Prutz, W. A., Consecutive halogen transfer between various functional groups induced by reaction of hypohalous acids: NADH oxidation by halogenated amide groups. *Archives of Biochemistry and Biophysics* **1999,** 371, (1), 107-114.
36. Peskin, A. V.; Winterbourn, C. C., Kinetics of the reactions of hypochlorous acid and amino acid chloramines with thiols, methionine, and ascorbate. *Free Radical Biology and Medicine* **2001,** 30, (5), 572-579.
37. Berndt, I.; Richtering, W., Doubly temperature sensitive core-shell microgels. *Macromolecules* **2003,** 36, (23), 8780-8785.
38. Singh, N.; Bridges, A. W.; Garcia, A. J.; Lyon, L. A., Covalent tethering of functional microgel films onto poly(ethylene terephthalate) surfaces. *Biomacromolecules* **2007,** 8, (10), 3271-3275.
39. Serpe, M. J.; Jones, C. D.; Lyon, L. A., Layer-by-layer deposition of thermoresponsive microgel thin films. *Langmuir* **2003,** 19, (21), 8759-8764.
40. Nayak, S.; Lee, H.; Chmielewski, J.; Lyon, L. A., Folate-mediated cell targeting and cytotoxicity using thermoresponsive microgels. *Journal of the American Chemical Society* **2004,** 126, (33), 10258-10259.
41. Das, M.; Mardyani, S.; Chan, W. C. W.; Kumacheva, E., Biofunctionalized pH-responsive microgels for cancer cell targeting: Rational design. *Advanced Materials* **2006,** 18, (1), 80-83.
42. Trachootham, D.; Alexandre, J.; Huang, P., Targeting cancer cells by ROS-mediated mechanisms: a radical therapeutic approach? *Nature Reviews Drug Discovery* **2009,** 8, (7), 579-591.

3.7 Appendix: Supporting Information for Chapter 3

Here the reason using ethylene glycol dimethacrylate (EGDMA) for crosslinkers in this paper, instead of *N*,*N'*-methylenebisacrylamide (MBA) the most common crosslinking agent, is demonstrated. Poly(N-isopropylmethacrylamide), PNIPMAM, microgels were prepared with different crosslinkers: NIPMAM-EGDMA and NIPMAM-MBA. The change of turbidity of these microgels in bleach at pH 10.5 is shown in Figure S1. The transmittance of NIPMAM-EGDMA microgels was almost unchanged with reaction time, while transmittance of NIPMAM-MBA microgels kept increasing with time. The significant increase in the transmittance of NIPMAM-MBA in bleach at pH 10.5 contributes to the decrosslinking of MBA. Thus, EGDMA was used instead of MBA in our work.

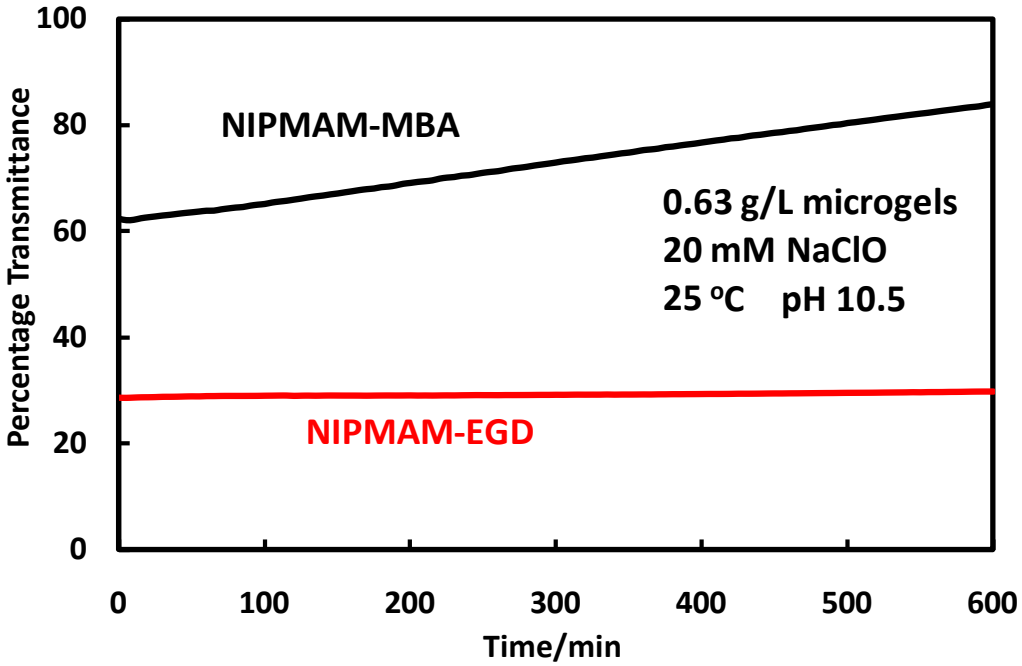

S1 Effect of crosslinker on the transmittance of PNIPAM microgels in 20 mM NaClO.

Microgels chlorinated at 20 °C

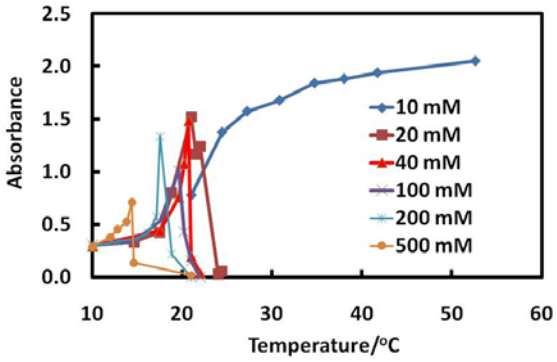

Microgels chlorinated at 25 °C

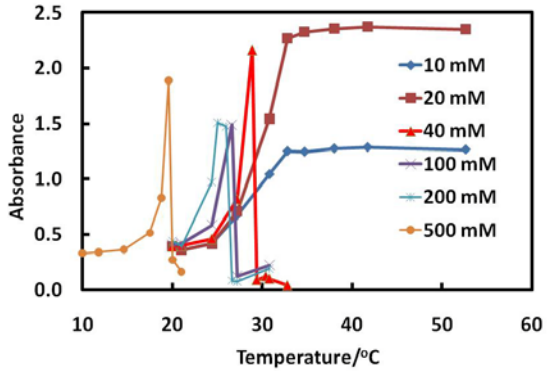

Microgels chlorinated at 30 °C

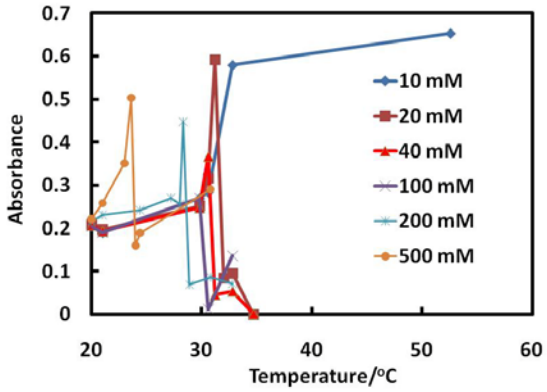

Unmodified

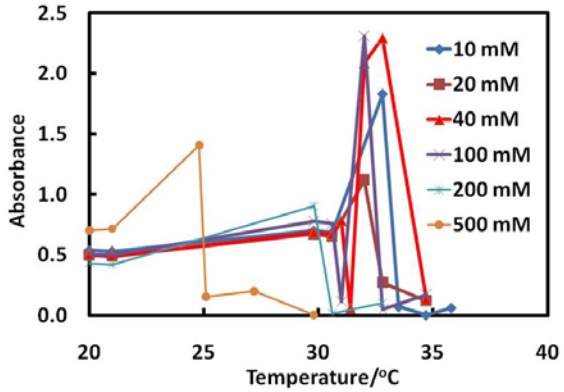

S2 Raw absorbance data for critical flocculation temperature determine. The measurements were conducted at a wavelength of 500 nm.

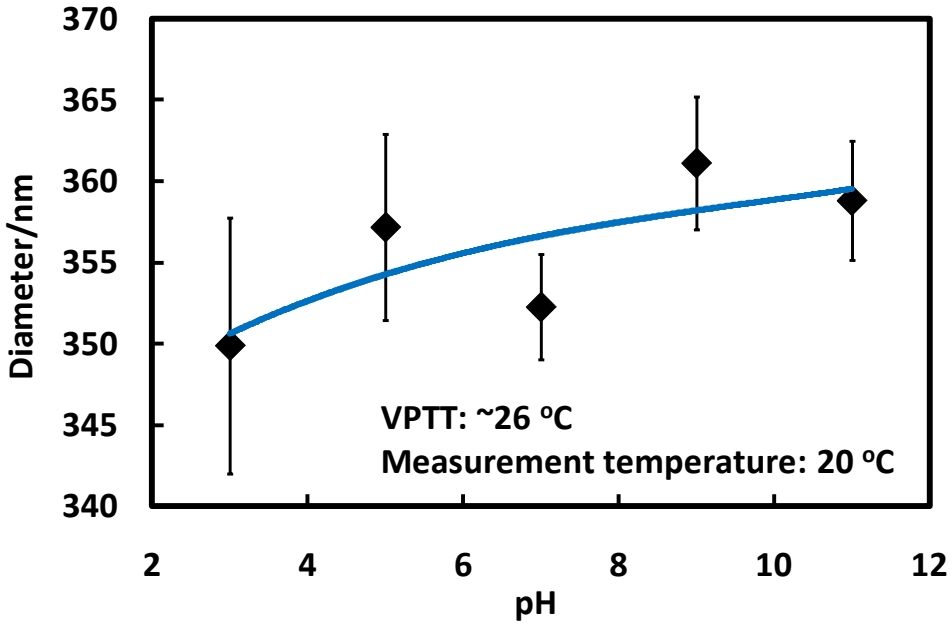

S3 pH effect on diameter of N-chlorinated microgels at 20 °C. The N-chlorinated microgels have VPTT around 26 °C.

Chapter 4 Poly(N-isopropyl*meth*acrylamide) Microgels Resist N-chlorination in Alkaline Bleach

In chapter 4, all experiments were initialized and conducted by myself. I plotted the experiment data and wrote the first draft. Dr. Pelton helped the data analysis and revised the first draft.

Poly(N-isopropyl*meth*acrylamide) Microgels Resist N-chlorination in Alkaline Bleach

Zuohe Wang and Robert Pelton*

Department of Chemical Engineering, McMaster University, Hamilton, Canada, 1280 Main Street, West Hamilton, Ontario, Canada, L8S 4L7.

* Corresponding author email: peltonrh@mcmaster.ca

Abstract

This paper presents the results of comparative studies of N-chlorination of poly(N-isopropylacrylamide) (PNIPAM) microgels and poly(N-isopropyl*meth*acrylamide) (PNIPMAM) microgels in aqueous bleach at pH 10.5. The active chlorine content of N-chlorinated PNIPMAM microgels was about one-tenth of that of N-chlorinated PNIPAM microgels under the same chlorination condition, which led little change in volume phase transition temperature (VPTT) of PNIPMAM microgels before and after N-chlorination. Core/shell microgels with PNIPAM cores and poly(NIPAM-co-NIPMAM) shells showed improved colloidal stability after N-chlorination, comparing with N-chlorinated PNIPAM microgels. Furthermore, the VPTT gap between cores and shells can be easily controlled via N-chlorination. The low reactivity of PNIPMAM in bleach is attributed to the stronger electron-donating power of methyl group than that of α–hydrogen.

4.1 Introduction

N-chloramines, which are defined as compounds with nitrogen-chlorine covalent bonds, exhibit superior antimicrobial activities.[1] Many efforts have been invested to preparing polymeric N-chloramines, due to their easy rechargeability.[2-11] Polymeric N-chloramines show antibacterial activities against both gram-negative bacteria (e.g. *E. coli*) and gram-positive bacteria (e.g. *S. aureus*). It has been shown that polymeric N-chloramines kill microbial in a combined mode of direct contact, active chlorine releasing and active chlorine transferring.[12-13]

Recently, polymeric N-chloramines based on PNIPAM microgels have been prepared by reacting PNIPAM microgels with aqueous bleach at pH 10.5 in our lab.[14] The nitrogen-hydrogen bonds of the amides in PNIPAM are chlorinated into nitrogen-chlorine bonds, giving a new polymeric N-chloramines poly(NIPAM-co-NIPAMCl).[15] The active chlorine content can be controlled by the reaction temperature. An active chlorine content of about 0.8 mmol/g can be obtained when a reaction temperature of 20 ^{o}C was used.[14] It is noted that the highest active chlorine content in polymeric N-chloramines coated silica nanoparticles (with a diameter of ~11 nm) was 54.8 μmol/g.[5] Therefore N-chlorinated microgels may offer long-term biocidal efficacy due to the high active content. We have also shown that the N-chlorinated microgels can efficiently react with reducing agents (e.g. glutathione, KI and $Na_2S_2O_3$), which makes the N-chlorinated microgels as a delivery vehicle of active chlorine. However, the critical flocculation temperature (CFT) of N-chlorinated PNIPAM microgels is fairly low in concentrated NaCl solution.[14] Taking microgels with active chlorine content of 0.8 mmol/g as an example, the CFT is about 20 ^{o}C in 100 mM NaCl. Thus, the applications of N-chlorination PNIPAM microgels as a delivery vehicle of active chlorine in solutions with high salt concentration (e.g. waste water and blood) are limited because of microgel coagulation.

Poly(N-isopropyl*meth*acrylamide), PNIPMAM, is an alternative to PNIPAM with methyl groups on the backbone instead of α–hydrogens (Scheme 1). PNIPMAM has a higher lower critical solution temperature (LCST, 44 ^{o}C) than PNIPAM (32 ^{o}C).[16] Microgels based on PNIPMAM[17] and core/shell microgels based on PNIPAM and PNIPMAM[18-19] can also be prepared via aqueous precipitation polymerization. The core/shell microgels show a two-stage thermal transition corresponding to PNIPAM and PNIPMAM, respectively.[18] Despite their similar chemical structures, the following paragraphs will show that PNIPMAM microgels and PNIPAM microgels differ significantly from each other in regard to N-chlorination in alkaline bleach.

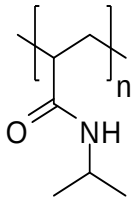

PNIPAM

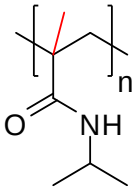

PNIPMAM

Scheme 1. Chemical structure of PNIPAM and PNIPMAM

Herein, the results of N-chlorination of PNIPMAM microgels and PNIPAM microgels in aqueous bleach at pH 10.5 are compared. Under the same reaction conditions, the active chlorine content of N-chlorinated PNIPMAM microgels is about one-tenth of (or less than) that in N-chlorinated PNIPAM microgels. As a result, the decrease in volume phase transition temperature (VPTT) of PNIPMAM microgels is limited after chlorination. Core/shell microgels are prepared in a one-pot manner, with PNIPAM as cores and poly(NIPAM-co-NIPMAM) as shells. N-chlorination of core/shell microgels leads to chlorinated cores and less chlorinated shells. Therefore, the VPTT gap between core and shell can be easily controlled. Furthermore, the shell gives N-chlorinated core/shell microgels with improved colloidal stability in phosphate buffered saline solution at 37 ^{o}C. Finally, a preliminary mechanism is proposed to explain the difference between the reactivity of PNIPMAM and PNIPAM in alkaline bleach.

4.2 Experiments

Materials. All chemicals were purchased from Sigma-Aldrich (Canada). N-isopropylacrylamide (NIPAM, 97%) and N-isopropylmethacrylamide (NIPMAM, 97%) was purified from re-crystallization with a mixture of toluene and hexane (60:40). Ethylene glycol dimethacrylate (EGDMA, 98%), sodium dodecyl sulfate (SDS, 99%), ammonium persulfate (APS, 98%) and sodium hypochlorite (NaClO, 10-15%) were used as received. Type I water (with a resistivity of 18.2 MΩ·cm) from a Barnstead Nanopure Diamond system was used in all experiments. The concentration of NaClO was determined by iodometric titration.

Synthesis of Microgels. Microgels were prepared via precipitation polymerization.[20] Typically, 1.40 g NIPAM (or 1.56 g NIPMAM), 0.13 g EGDMA and 0.05 g SDS were added to 150 mL water in a 250 mL flask reactor. The flask was equipped with a mechanical stirrer, a nitrogen inlet/outlet and a condenser. After deoxygenation of the solution with nitrogen for 30 min at 70 ^{o}C, 0.025 g APS (dissolved in 5 mL water) was added. The polymerization was conducted at 70 ^{o}C under nitrogen atmosphere for another 6 hours. After polymerization, microgels were purified by ultracentrifugation (Beckman

L-80 XP), decantation and suspension in water for several cycles until the conductivity of the supernatant was less than 5 μS/cm. Microgels were then lyophilized for storage.

Synthesis of Core/Shell Microgels. Core/Shell microgels were synthesized in a one-pot manner. First, the core microgels were prepared using the same procedure for PNIPAM microgels, as described above. NIPMAM was then added after the core reaction was conducted for 1 hour. The polymerization was conducted for another 6 hours. After polymerization, microgels were purified by ultracentrifugation (Beckman L-80 XP), decantation and suspension in water for several cycles until the conductivity of the supernatant was less than 5 μS/cm. Microgels were lyophilized for storage. The recipe for preparation of core/shell microgels is shown in Table 1.

Table 1 Recipe for Preparation of Core/Shell Microgels

Core					Shell*	
NIPAM/g	EGDMAMA/g	SDS/g	APS/g	Water/mL	NIPMAM/g	Water/mL
1	0.13	0.05	0.025	150	1	40

*Shell solution was deoxygenated by bubbling with nitrogen and then added after 1 hour reaction for core solution

N-Chlorination of Microgels. The procedure used here was similar to the one developed for PNIPAM microgels.[14] A suspension (20 mL) with 0.56 g/L PNIPAM (or 0.63 g/L PNIPMAM, or 0.56 g/L core/shell) microgels and NaClO (20 mM) was prepared in a beaker. The suspension pH was then adjusted to 10.5 by adding 1 M HCl. The beaker was placed in a water bath with the desired reaction temperature (20, 25, 30 ^{o}C). The reaction was conducted until the microgels phase-separated. For reactions with PNIPMAM and core/shell microgels, the same reaction condition (temperature and time) was applied without observation of aggregation. Then the suspension was diluted with water (about 200 mL) for dialysis in cellulose membrane tubes against water for one day. The resulting microgels were collected by ultracentrifugation and stored at 4 ^{o}C.

Some experiments were conducted in a spectrophotometer to record the turbidity changes. Typically, 1 mL microgel suspension was mixed with 1mL NaClO (40 mM) in a polystyrene cuvette. After adjusting pH to the desired value, transmittance at 500 nm was measured at 25 ^{o}C with a DU800 visible-UV spectrophotometer (Beckman Coulter) using water as a blank.

Iodometric Titration. The active chlorine content in chlorinated microgels was determined by iodometric titration. About 5 mg chlorinated PNIPAM microgels (20 mg

for PNIPMAM microgels) were dissolved in water to make a 1 g/L solution. An excess amount of KI (100 mg) was added to the solution. The solution pH was adjusted to 3. Then 2 mL of starch indicator (1%) was added. The solution was titrated with sodium thiosulfate (10 mM) until the solution turned colorless. The substitution degree (DS) of N-chlorinated microgels was calculated by the following equation:

$$DS\% = \frac{[Cl]}{[Cl] + \frac{1 - [Cl] * M_{Cl}}{M_P * 1000}} * 100 \quad (1)$$

where [Cl] was the active chlorine content of the microgels; M_{Cl} was the molecular weight of repeat unit of chlorinated polymers (147.5 g/mol for chlorinated PNIPAM; 161.5 g/mol for chlorinated PNIPMAM; 152.4 g/mol for chlorinated core/shell microgels); and M_p was the molecular weight of unchlorinated repeat unit (113 g/mol for PNIPAM; 127 g/mol for PNIPMAM; 118 g/mol for core/shell microgels). The calculation was made based on the assumption that the crosslinker EGDMA content in microgels was negligible.

Dynamic Light Scattering (DLS). Hydrodynamic diameters of microgels were measured by DLS with a detection angle of 90°. The laser source was a Melles Griot HeNe laser with a wavelength of 633 nm. The scattering intensity was between 100 and 250 kcps for all measurements. Each sample was measured for at least three runs with 2 min for each run. Every sample was kept under the measurement temperature for at least 30 min before started the measurement.

Transmission Electron Microscopy (TEM). A single drop (~5 μL) of a dilute microgel suspension was dropped on a Formvar-coated copper TEM grid and dried overnight. TEM image was obtained using a JEOL 1200EX TEMSCAN microscope operating at 80 kV.

Nuclear Magnetic Resonance (NMR). ^{1}H NMR spectra were recorded on Bruker AV-200 spectrometers (200 MHz) with samples dissolved in $CDCl_3$.

4.3 Results

PNIPAM and PNIPMAM microgels were prepared with EGDMA as crosslinkers, since EGDMA is more stable than N,N'-methylenebisacrylamide in bleach at pH 10.5.[14] The N-chlorination on PNIPAM or PNIPMAM microgels is shown in Scheme 2.

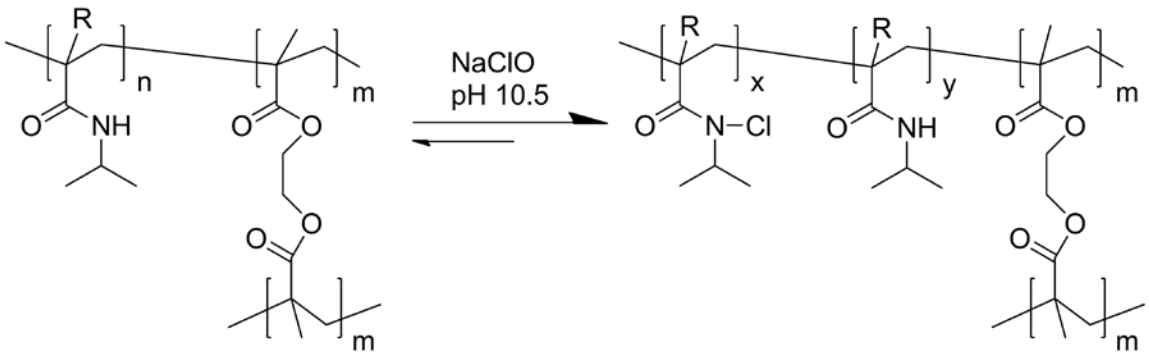

Scheme 2. N-chlorination of PNIPAM microgels and PNIPMAM microgels. R=H: PNIPAM microgels; R=CH_3: PNIPMAM microgels. The reaction on PNIPMAM microgels is much slower (y>>x), as shown in Figure 8.

Suspensions consisting of PNIPAM or PNIPMAM microgels and bleach were prepared at pH 10.5. The suspension turbidity was recorded as a function of time at 25 ^{o}C. The results in Figure 1 show little change in turbidity for PNIPMAM microgel suspension. By contrast, the PNIPAM microgel suspension slowly became more turbid, and ultimately phase-separated giving visible precipitates. Both kinds of microgels were then purified after N-chlorination for further characterization.

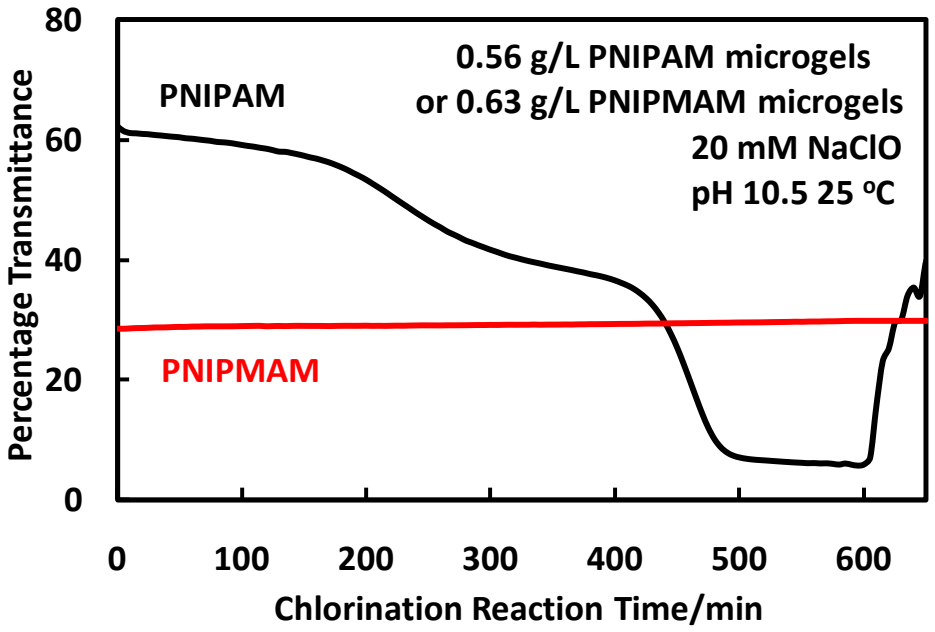

Figure 1 Suspension transmittances of PNIPAM microgels and PNIPMAM microgels in 20 mM NaClO with pH 10.5 at 25 ^{o}C along with reaction time.

DLS was used to determine the size of purified microgels after N-chlorination, and the results are shown in Figure 2. Volume phase transition temperature (VPTT) of PNIPAM microgels decreased from 31 ^{o}C to 26 ^{o}C after 10 hours N-chlorination at 25 ^{o}C. However, the results show little change in VPTT of PNIPMAM microgels after N-chlorination under the same reaction condition, which stayed at 44 ^{o}C.

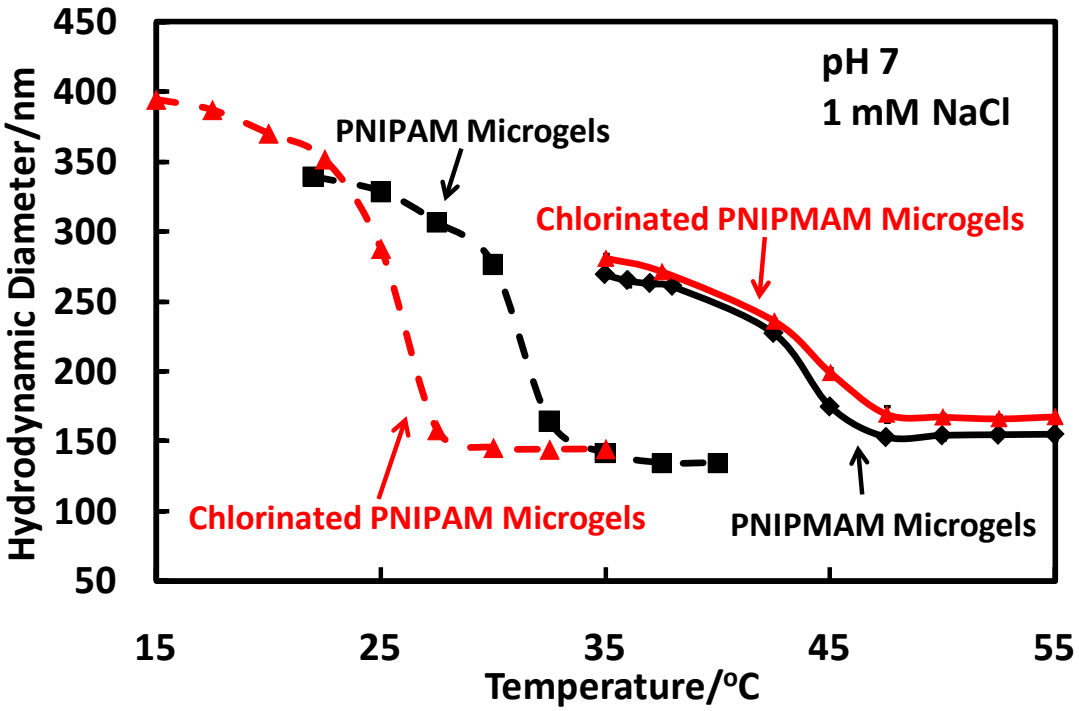

Figure 2. Diameters of purified PNIPAM microgels and PNIPMAM microgels before and after chlorination. The chlorinated microgels were treated with 20 mM NaClO at pH 10.5 for 10 hours at 25 ^{o}C, prior to the DLS measurements.

Core/shell microgels with PNIPAM cores and PNIPMAM shells were prepared in a one-pot manner, as described in the experimental section. NIPAM monomers and EGDMA crosslinkers were added to water with SDS as surfactant, and the reaction was initialized by adding APS. After 1 hour reaction, NIPMAM monomers were added. The reaction was conducted for further 6 hours. The particle morphology was observed by TEM, and the image is shown in Figure 3. The microgels were fairly uniform in a dry state, which indicated the absent of secondary nucleation. Furthermore, the core/shell microgels were stable in phosphate buffered saline (PBS) solution at 37 ^{o}C. The molar ratio between PNIPAM and PNIPMAM was calculated as 1.9 in the core/shell microgels from the NMR spectrum (Figure 4). A sample calculation is given in Supporting Information. It should

be noted that the calculation was based on the assumption that the EGDMA content in resulting core/shell microgels was limited.

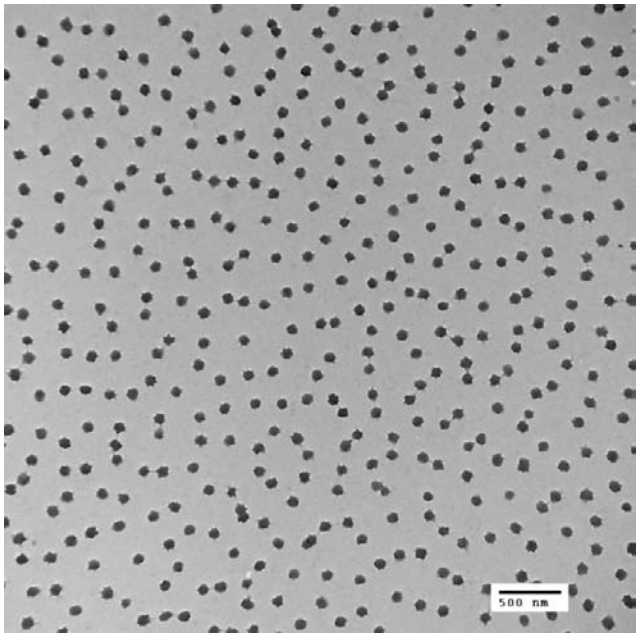

Figure 3 TEM image of core/shell microgels

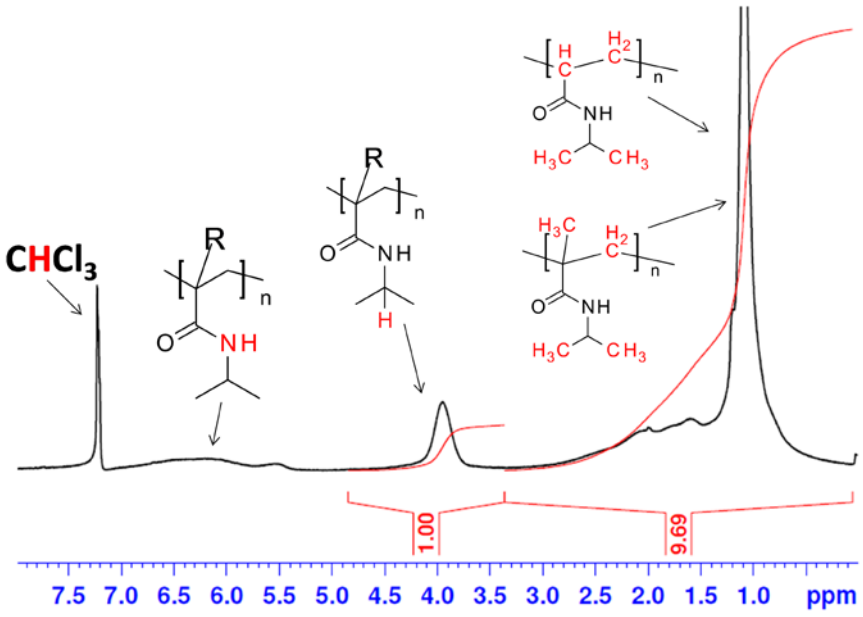

Figure 4 ^{1}H-NMR spectrum of core/shell microgels in CDCl3.

In a parallel experiment, naked core microgels were prepared. The polymerization was conducted for 1 hour and then stopped by adding excess amount of hydroquinone without the addition of NIPMAM. The hydrodynamic diameters of purified naked core microgels and core/shell microgels were determined in 1 mM NaCl at pH 7 by DLS. The results in Figure 5A indicate core/shell microgels possessed a two-stage thermo-induced transition, which further support the core/shell morphology. The first transition was at 31 ^{o}C, attributed to the transition of cores (PNIPAM). The other transition, corresponding to shell, was at 42 ^{o}C. The shell VPTT is lower than the VPTT of PNIPMAM microgels (44 ^{o}C). Thus the shell should be poly(NIPAM-co-NIPMAM) instead of pure PNIPMAM. This is probably because NIPAM monomers are not fully consumed when NIPMAM monomers are added. A random copolymer with 40% NIPAM and 60% NIPMAM has a LCST of 42 ^{o}C[21], which suggests the shell is consisted of ~40% NIPAM and ~60% NIPMAM. The core and shell sizes in core/shell microgels were calculated from comparison of sizes of naked core microgels and core/shell microgels. A sample calculation is given in Supporting Information. It is noticeable that the calculation based on DLS can only provide rough results.[22] The diameter of core domain is about 100 nm at shrunken state and 220 nm at swollen state, while the shell thickness is 15 nm at shrunken state and 50 nm at swollen state, as schematic described in Figure 5B. Note that the core diameter in fully swollen core/shell microgels was calculated as about 220 nm, which is smaller than that of naked core microgels (~260 nm). This is probably because the cores were compressed by the shells in core/shell microgels, as demonstrated by Jones and Lyon.[23]

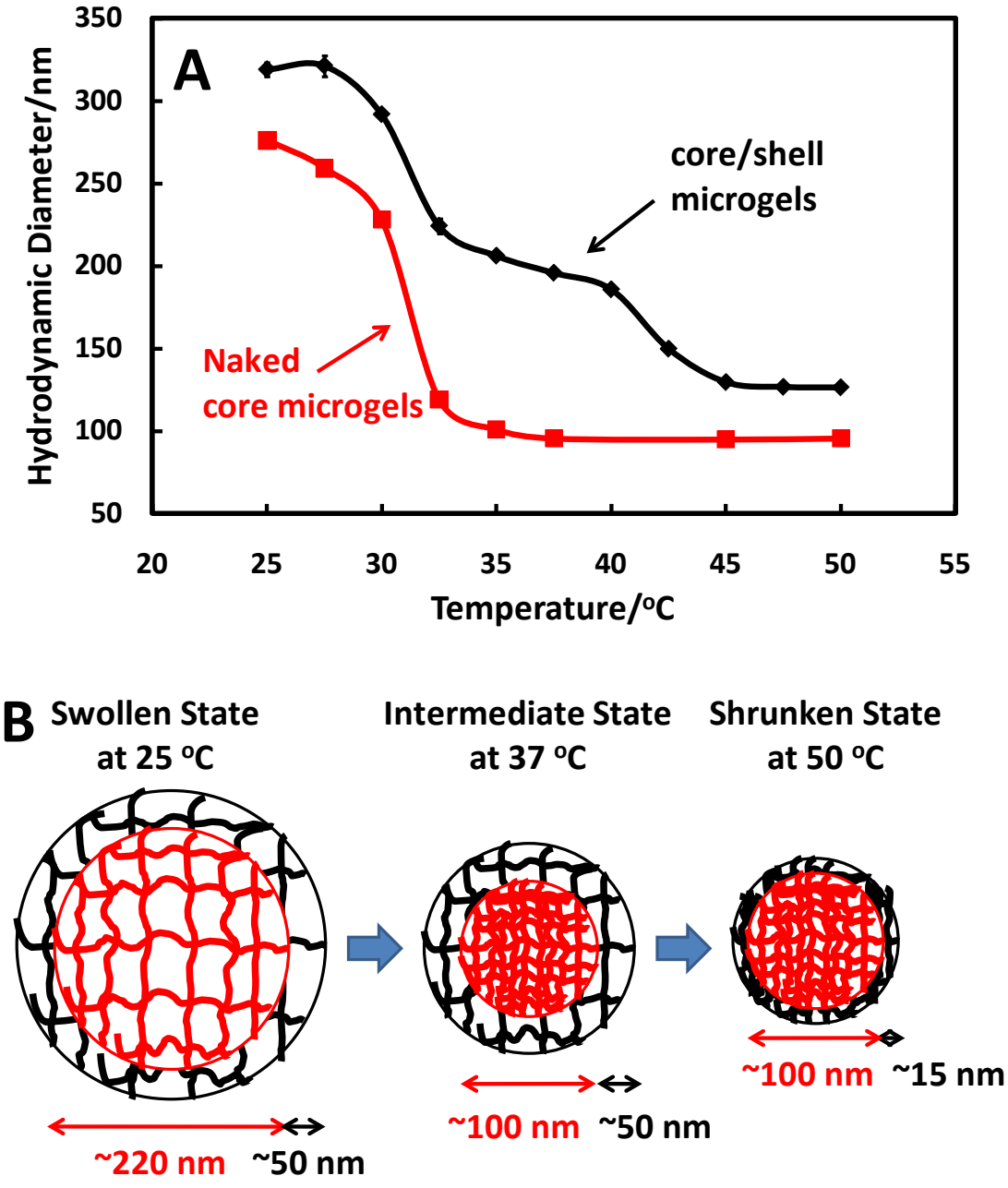

Figure 5 A) Diameters of purified naked core microgels and core/shell microgels in 1 mM NaCl at pH 7. B) Schematic description of sizes of core domain and shell domain in core/shell microgels.

Purified core/shell microgels were treated with bleach at pH 10.5. The reaction was conducted for 2 hours at 30 °C, for 10 hours at 25 °C and for 24 hours at 20 °C. These conditions were the same as those applied for PNIPAM microgels.[14] Under these conditions, PNIPAM microgels phase-separated from bleach, while core/shell microgels were colloidally stable throughout. The size of N-chlorinated core/shell microgels in 1mM NaCl at pH 7 was determined by DLS, and the results are shown in Figure 6. The diameter curve also shows a two-stage transition of N-chlorinated microgels. After N-chlorination, the core VPTT decreased significantly, and the final core VPTT was almost identical to the reaction temperature. The decrease in shell VPTT with chlorination was much less than the decrease in core VPTT. Taking the reaction at 20 °C as an example, the core VPTT decreased by 11 °C, while the shell VPTT only decreased by 2 °C. Therefore, the VPTT gap between cores and shells increased from 11 °C to 20 °C. The photographs in Figure 7 indicate that the N-chlorinated core/shell microgels are stable in PBS solution at 37 °C. By contrast, the N-chlorinated microgels with a VPTT of 20 °C macroscopically separated in PBS solution at 37 °C in a few minutes.

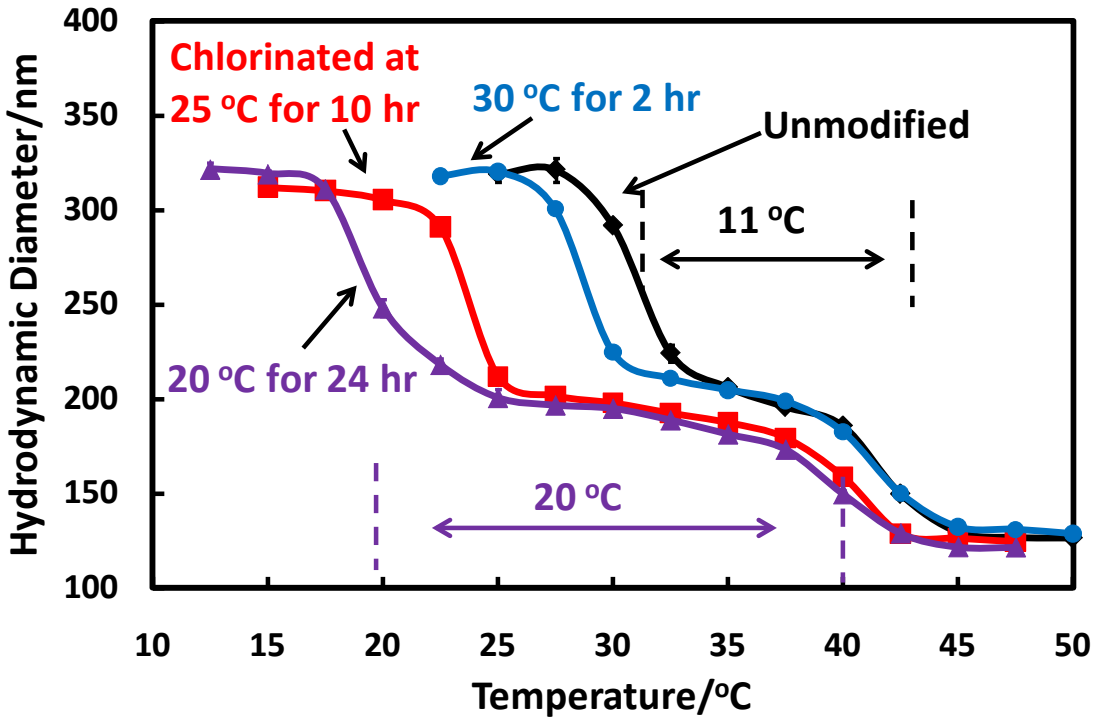

Figure 6. Diameters of purified core/shell microgels before and after chlorination. The chlorinated microgels were treated with 20 mM NaClO with pH 10.5, prior to the DLS measurements. The reaction temperature and time were varied: 2 hours at 30 °C, 10 hours at 25 °C and 24 hours at 20 °C.

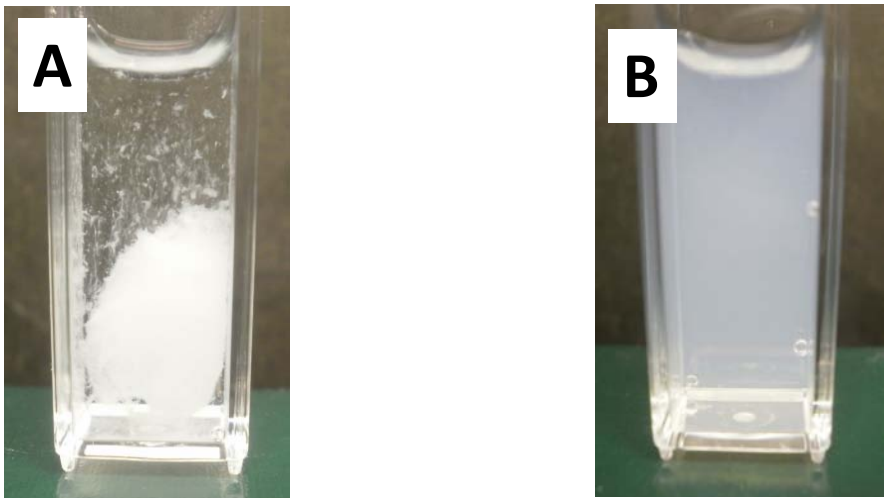

Figure 7. Photographs of microgels in PBS solution at 37 ^{o}C for 12 hours. A) N-chlorinated PNIPAM microgels with a VPTT of 20 ^{o}C. B) N-chlorinated core-shell microgels with a core VPTT of 20 ^{o}C and a shell VPTT of 40 ^{o}C.

The substitution degree of chlorinated microgels was calculated from the active chlorine content determined via iodometric titration, and the results are shown in Figure 8. The calculation was made on the assumption that the content of EGDMA in the core/shell microgels is negligible. Under the same reaction condition (temperature, time, and concentration), N-chlorinated PNIPAM microgels had the highest substitution degree, and PNIPMAM microgels had the lowest content. This difference also indicates that PNIPMAM is more stable than PNIPAM in alkaline bleach. The substitution degrees of PNIPAM in the core/shell microgels were also calculated by subtracting the active chlorine content of PNIPMAM in the core/shell microgels with that in PNIPMAM microgels. The calculation was made based on the assumption that the N-chlorination rate of PNIPMAM was similar in both PNIPMAM microgels and core/shell microgels. The results show the substitution degree of PNIPAM in N-chlorinated core/shell microgels is higher than that in PNIPAM microgels under the same reaction condition. This effect may contribute to the following reason. PNIPAM microgels shrunk when the extent of N-chlorination was high enough, which inhibited further chlorination.[14] However, the shells in core/shell microgels were always swollen during N-chlorination, due to the presence of PNIPMAM. As a result, PNIPAM in shells can be further chlorinated compared with PNIPAM microgels under the same reaction condition.

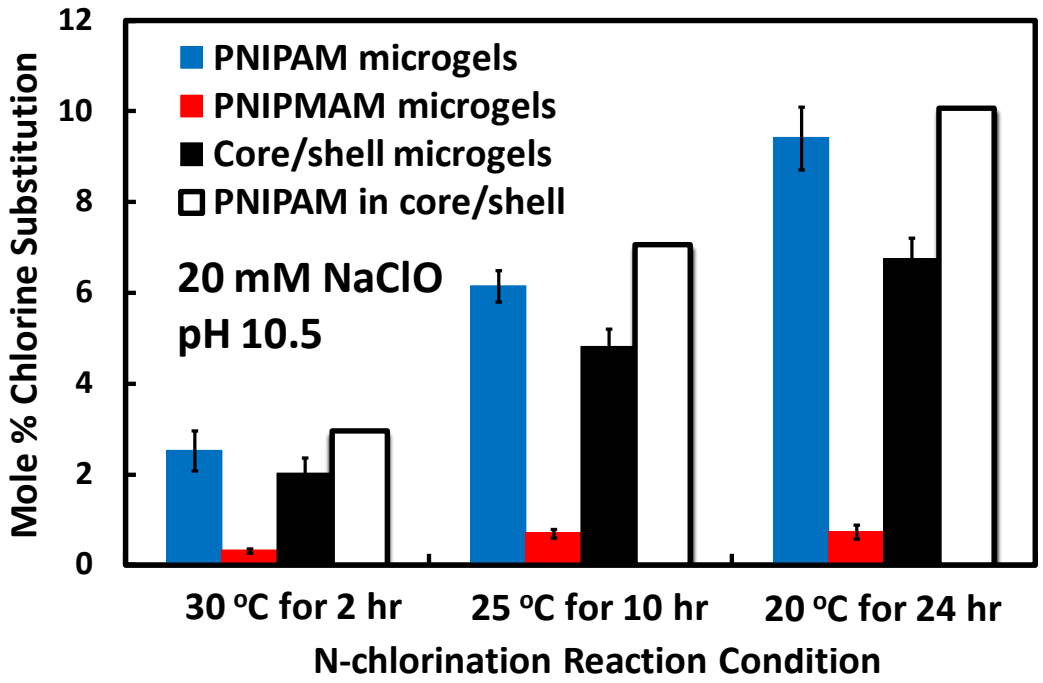

Figure 8. Molar percentage chlorination of N-chlorinated microgels under varying reaction conditions. The blank columns represent the degree of substitution of PNIPAM in core/shell microgels, which is calculated based on the assumption that the N-chlorination of PNIPMAM in core/shell microgels is the same as that in PNIPMAM microgels.

4.4 Discussion

Both turbidity and DLS results indicate that PNIPMAM microgels are more stable than PNIPAM microgels in bleach at pH 10.5. The active chlorine content of N-chlorinated PNIPMAM microgels is only one-tenth of the content of N-chlorinated PNIPAM microgels under the same reaction condition, which leads to little decrease in suspension turbidity and VPTT. Thus, we believe that PNIPMAM microgels have potential applications as support particles for reactions in alkaline bleach, such as TEMPO-mediated oxidation[24] and Hofmann degradation[25].

Core/shell microgels with PNIPAM cores and poly(NIPAM-co-NIPMAM) shells were prepared, followed by N-chlorination via alkaline bleach. N-chlorinated core/shell microgels have a tuneable two-stage transition. The core VPTT decreases significantly after N-chlorination, while the decrease in shell VPTT is limited under the same reaction condition. Hence the VPTT gap of core/shell microgels can be easily varied. Also, it has been shown that the VPTT of N-chlorinated PNIPAM microgels increases again to about 32 ^{o}C after reduction.[14] Therefore, the VPTT gap of N-chlorinated core/shell microgels

can be reduced back by reacting with reducing agents (e.g. glutathione). Thus N-chlorination offers a simple and facile method for the construction of microgels with complicated thermal-responsive properties.

Another advantage of N-chlorinated core/shell microgels over N-chlorinated PNIPAM microgels is improved colloidal stability. The N-chlorinated core/shell microgels are colloidal stable in PBS solution at 37 ^{o}C, since the shells have a VPTT higher than 37 ^{o}C even after N-chlorination. Thus the N-chlorinated core/shell microgels can act as active chlorine vehicle which releases active chlorine slowly in solutions with high salt concentration (e.g. waste water) for antimicrobial purpose. The reason why PNIPMAM is much more stable than PNIPAM in alkaline bleach is discussed in the following paragraph.

Thomm and Wayman reported the substituent effect on reaction rate of N-chlorination of secondary amides.[26] They found that alkane substituent with longer chain gave lower N-chlorination rate, as the order shown in Scheme 3. They argued that alkane substituent with longer chain had a stronger electron-donating power, which led to a higher electron density of nitrogen atoms in amides. As a result, amides with longer alkane substituent have stronger nitrogen-hydrogen bonds, and therefore a lower N-chlorination rate. PNIPMAM has methyl groups on the backbone compared with α–hydrogens in PNIPAM. The electron-donating power of methyl group is stronger than hydrogen. Thus, we attribute the difference between the reactivity of PNIPMAM and PNIPAM in alkaline bleach to difference between electron-donating power of methyl group and hydrogen.

N-chlorination of Secondary Amides

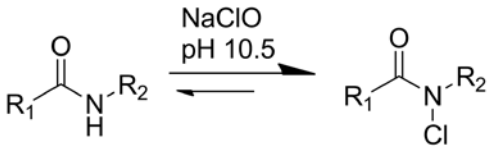

Substituent Effect on N-chlorination rate

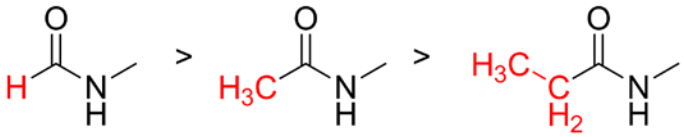

Rate Constant ($M^{-1}s^{-1}$): 2.1×10^{-1} 1.8×10^{-2} 9.2×10^{-3}

Scheme 3 Substituent effect on N-chlorination rate of secondary amides by reacting with NaClO at pH 10.5.[26]

4.5 Conclusions

1. The active chlorine content of N-chlorinated PNIPMAM microgels are only about one-tenth of that of N-chlorinated PNIPAM microgels under the same reaction conditions, which suggests PNIPMAM microgels can act as support particles in reactions involving alkaline bleach.

2. N-chlorinated core/shell microgels with highly N-chlorinated PNIPAM cores and much less N-chlorinated poly(NIPAM-co-NIPMAM) shells are prepared. The shells prevent aggregation of N-chlorinated PNIPAM cores in PBS solution at 37 ^{o}C, which extends the application of N-chlorinated microgels in high salt solutions.

3. The observation that PNIPMAM is less susceptible to chlorination with bleach compared to PNIPAM is consistent with the behaviour of small molecule analogues, described in the literature[26], where it was proposed that the lower reactivity was due to the stronger electron-donating power of methyl groups, in comparison with that of α–hydrogens.

4.6 References

1. Worley, S. D.; Williams, D. E., Halamine Water Disinfectants. *Crc Critical Reviews in Environmental Control* **1988,** 18, (2), 133-175.
2. Sun, G.; Wheatley, W. B.; Worley, S. D., A New Cyclic N-Halamine Biocidal Polymer. *Industrial & Engineering Chemistry Research* **1994,** 33, (1), 168-170.
3. Sun, Y. Y.; Chen, T. Y.; Worley, S. D.; Sun, G., Novel refreshable N-halamine polymeric biocides containing imidazolidin-4-one derivatives. *Journal of Polymer Science Part a-Polymer Chemistry* **2001,** 39, (18), 3073-3084.
4. Chen, Z. B.; Sun, Y. Y., N-halamine-based antimicrobial additives for polymers: Preparation, characterization, and antimicrobial activity. *Industrial & Engineering Chemistry Research* **2006,** 45, (8), 2634-2640.
5. Jang, J.; Kim, Y., Fabrication of monodisperse silica-polymer core-shell nanoparticles with excellent antimicrobial efficacy. *Chemical Communications* **2008**, (34), 4016-4018.
6. Dickerson, M. B.; Lyon, W.; Gruner, W. E.; Mirau, P. A.; Slocik, J. M.; Naik, R. R., Sporicidal/Bactericidal Textiles via the Chlorination of Silk. *ACS Applied Materials & Interfaces* **2012,** 4, (3), 1724-1732.
7. Cerkez, I.; Worley, S. D.; Broughton, R. M.; Huang, T. S., Rechargeable antimicrobial coatings for poly(lactic acid) nonwoven fabrics. *Polymer* **2013,** 54, (2), 536-541.
8. Liu, S.; Sun, G., New Refreshable N-Halamine Polymeric Biocides: N-Chlorination of Acyclic Amide Grafted Cellulose. *Industrial & Engineering Chemistry Research* **2009,** 48, (2), 613-618.
9. Kocer, H. B.; Cerkez, I.; Worley, S. D.; Broughton, R. M.; Huang, T. S., Polymeric antimicrobial N-halamine epoxides. *ACS Applied Materials & Interfaces* **2011,** 3, (8), 2845-50.
10. Cerkez, I.; Kocer, H. B.; Worley, S. D.; Broughton, R. M.; Huang, T. S., N-Halamine Biocidal Coatings via a Layer-by-Layer Assembly Technique. *Langmuir* **2011,** 27, (7), 4091-4097.
11. Kocer, H. B.; Cerkez, I.; Worley, S. D.; Broughton, R. M.; Huang, T. S., N-Halamine Copolymers for Use in Antimicrobial Paints. *ACS Applied Materials & Interfaces* **2011,** 3, (8), 3189-3194.
12. Chen, Z.; Luo, J.; Sun, Y., Biocidal efficacy, biofilm-controlling function, and controlled release effect of chloromelamine-based bioresponsive fibrous materials. *Biomaterials* **2007,** 28, (9), 1597-1609.
13. Ahmed, A. E. S. I.; Hay, J. N.; Bushell, M. E.; Wardell, J. N.; Cavalli, G., Optimizing Halogenation Conditions of N-Halamine Polymers and Investigating Mode of Bactericidal Action. *Journal of Applied Polymer Science* **2009,** 113, (4), 2404-2412.
14. Wang, Z.; Pelton, R.; Lam, W. Y., N-Chlorinated Poly(N-isopropylacrylamide) Microgels. *Submitted* **2013**.
15. Wang, Z.; Pelton, R., Chloramide Copolymers From Reacting Poly (N-isopropylacrylamide) with Bleach. *European Polymer Journal* **2013,** 49, (8), 2196-2201.

16. Tang, Y. C.; Ding, Y. W.; Zhang, G. Z., Role of methyl in the phase transition of poly(N-isopropylmethacrylamide). *Journal of Physical Chemistry B* **2008,** 112, (29), 8447-8451.
17. Duracher, D.; Elaissari, A.; Pichot, C., Preparation of poly(N-isopropylmethacrylamide) latexes kinetic studies and characterization. *Journal of Polymer Science Part a-Polymer Chemistry* **1999,** 37, (12), 1823-1837.
18. Berndt, I.; Richtering, W., Doubly temperature sensitive core-shell microgels. *Macromolecules* **2003,** 36, (23), 8780-8785.
19. Hu, X. B.; Tong, Z.; Lyon, L. A., Multicompartment Core/Shell Microgels. *Journal of the American Chemical Society* **2010,** 132, (33), 11470-11472.
20. Mcphee, W.; Tam, K. C.; Pelton, R., Poly(N-Isopropylacrylamide) Latices Prepared with Sodium Dodecyl-Sulfate. *Journal of Colloid and Interface Science* **1993,** 156, (1), 24-30.
21. Iwai, K.; Matsumoto, N.; Niki, M.; Yamamoto, M., Fluorescence Probe Studies of Thermosensitive N-Isopropylacrylamide Copolymers in Aqueous Solutions. *Molecular Crystals and Liquid Crystals Science and Technology Section a-Molecular Crystals and Liquid Crystals* **1998,** 315, 53-58.
22. Berndt, I.; Pedersen, J. S.; Richtering, W., Structure of multiresponsive "intelligent" core-shell microgels. *Journal of the American Chemical Society* **2005,** 127, (26), 9372-9373.
23. Jones, C. D.; Lyon, L. A., Shell-restricted swelling and core compression in poly(N-isopropylacrylamide) core-shell microgels. *Macromolecules* **2003,** 36, (6), 1988-1993.
24. Kitaoka, T.; Isogai, A.; Onabe, F., Chemical modification of pulp fibers by TEMPO-mediated oxidation. *Nordic Pulp & Paper Research Journal* **1999,** 14, (4), 279-284.
25. Wirsen, A.; Ohrlander, M.; Albertsson, A. C., Bioactive heparin surfaces from derivatization of polyacrylamide-grafted LLDPE. *Biomaterials* **1996,** 17, (19), 1881-1889.
26. Thomm, E.; Wayman, M., N-chlorination of secondary amides. II. Effects of substituents on rates of N-chlorination. *Canadian Journal of Chemistry* **1969,** 47, (18), 3289-3297.

4.7 Appendix: Supporting Information for Chapter 4

Calculation 1: Molar ratio between PNIPAM and PNIPMAM in core/shell microgels calculated from NMR spectrum (Figure 4).

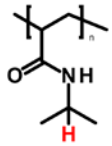	H_1
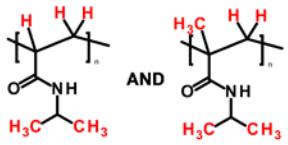	H_2

The number of H_1 hydrogen in one PNIPAM and PNIPMAM repeat unit is 1.

The number of H2 hydrogen in one PNIPAM repeat unit is 9, and in one PNIPMAM repeat unit is 11.

From NMR spectrum:

Peak area of H_1: $S_{H1}=1$

Peak area of H_2: $S_{H2}=9.69$

Assume the molar of PNIPAM and PNIPMAM repeat units in core/shell microgels as n_{AM} and n_{AM}, respectively.

Then, $n_{AM}+n_{MAM}=S_{H1}$ and $9n_{AM}+11n_{MAM}=S_{H2}$

Solve the equations, $n_{AM}=0.655$; $n_{MAM}=0.345$.

Thus the molar ratio between PNIPAM and PNIPMAM is $\frac{n_{AM}}{n_{MAM}}=1.9$

Calculation 2: The size of core domain and shell domain in core/shell microgels calculated from Figure 5A.

Assume the diameter of core domain in core/shell microgels is $\mathbf{d_1}$ at shrunken state, and $\mathbf{d_2}$ at swollen state.

Assume the thickness of shell domain is core/shell microgels is $\mathbf{H_1}$ at shrunken state, and $\mathbf{H_2}$ at swollen state.

1. At 50 ^{o}C, both cores and shells are in shrunken state. The diameter of naked core microgels is 100 nm and the diameter of core/shell microgels is 130 nm.

Thus we have $\mathbf{d_1}$=100 nm and $\mathbf{d_1}$+ 2$\mathbf{H_1}$=130 nm.

Solve the equations, $\mathbf{H_1}$ =15 nm.

2. At 37 ^{o}C, cores are still shrunken, while the shells are swollen. The diameter of core/shell microgels at 37 ^{o}C is 200 nm. Thus, $\mathbf{d_1}$+ 2$\mathbf{H_2}$=200 nm.

Then $\mathbf{H_2}$=50 nm.

3. At 25 ^{o}C, both cores and shells are swollen. The diameter of core/shell microgels is 320 nm.

4. Thus, $\mathbf{d_2}$+ 2$\mathbf{H_2}$=320 nm.

5. Then $\mathbf{d_2}$=220 nm.

The results are summarized in Figure 5B. However, it should be noted that the calculations only give rough results at temperatures of 37 ^{o}C and 25 ^{o}C. Berndt et al. showed that the swollen shell forces the shrunken core apart at the intermediate stage[1], which gives a larger core size in core/shell microgels than the size of naked core microgels at 37 ^{o}C. Thus the shell thickness at 37 ^{o}C is smaller than 50 nm, and the core diameter at 25 ^{o}C is bigger than 220 nm. However, the differences should be slight, since only about 3 nm increasing for shrunken cores with diameter of 40 nm as shown in the literature.[1]

1. Berndt, I.; Pedersen, J. S.; Richtering, W., Structure of multiresponsive "intelligent" core-shell microgels. *Journal of the American Chemical Society* **2005,** 127, (26), 9372-9373.

Chapter 5 Synthesis of Primary Amine-containing Poly(N-isopropylmethacrylamide) Microgels via Hofmann Rearrangement

In chapter 5, all experiments were conducted by me, Miles Montgomery, Wing Yan Lam and Kyle Lefebvre, who worked as summer students. I plotted the experiment data and wrote the first draft. Dr. Pelton helped the data analysis and revised the first draft.

Synthesis of Primary Amine-containing Poly(N-isopropyl*meth*acrylamide) Microgels via Hofmann Rearrangement

Zuohe Wang, Robert Pelton*, Miles Montgomery, Wing Yan Lam and Kyle Lefebvre

Department of Chemical Engineering, McMaster University, Hamilton, Canada, 1280 Main Street, West Hamilton, Ontario, Canada, L8S 4L7.

* Corresponding author email: peltonrh@mcmaster.ca

Abstract

The Hofmann rearrangement of poly(N-isopropylmethacrylamide) (PNIPMAM)/methacrylamide (MAM) copolymer microgels carried out in alkaline bleach (NaClO) at room temperature resulted in primary amine-containing microgels. The formed amines were converted from the unsubstituted amides in MAM. The amine content increased with Hofmann rearrangement time, and a content of 0.4 mmol/g was achieved after 60 min reaction. Primary amines offered microgels with positive charges, pH sensitivity and conjugation sites. The method was easily extended for preparation of amphoteric microgels containing both primary amines and carboxyls. The resulting amphoteric microgels exhibited zwitterionic behaviour. The isoelectric point of amphoteric microgels, corresponding to the molar ratio of primary amines to carboxyls, was controlled by Hofmann rearrangement time.

5.1 Introduction

Thermosensitive microgels based on poly(N-isopropylacrylamide) (PNIPAM)[1] have applications in many fields: such as drug delivery[2], nanocomposite[3-4], biosensing[5-6], optical devices[7-8], and separation[9]. Most applications require PNIPAM-based microgels incorporated with functional groups, other than PNIPAM homogenous microgels. Many efforts have been made to prepare functionalized PNIPAM microgels with various functional groups, including phenylboronic[5], carboxyl[10], "clickable" groups (azido and terminal alkyne)[11], glycidyl[12], and N-chloramide[13], etc. These groups offer either additional stimuli-responsive property, reactivity or conjugation sites for further modification.

Primary amine is extremely important in chemistry, material science and biology. The most used method for preparing PNIPAM (or poly(N-isopropyl*meth*acrylamide), PNIPMAM) microgels with primary amines is precipitation copolymerization of NIPAM (or NIPMAM) with amine-containing comonomers. The comonomers can be 2-aminoethylmethacrylate hydrochloride[14], N-(3-aminopropyl)methacrylamide hydrochloride[15] or allylamine[16]. This copolymerization method is one step and simple. However, several issues have been considered during precipitation polymerization with such comonomers. First, the electrostatic interaction during polymerization is critical, since these co-monomers are positively charged under reaction conditions. Therefore the salt concentration has to be considered during polymerization. Second, the location of primary amines in microgels is difficult to control, due to the difference in the reactivity ratios between NIPAM (or NIPMAM) and comonomers.

Primary amine-containing microgels can also be prepared by post-modification strategies, generating primary amines from uncharged precursors. A hydrolysis method has been developed in our laboratory.[17] PNIPAM microgels incorporated with *N*-vinylformamide were prepared via precipitation polymerization in a semibatch manner, followed by hydrolysis of *N*-vinylformamide at pH 1.5 giving the primary amines. Recently, Saunders et al. applied a similar method for preparation of polyvinylamine microgels.[18] Poly(N-vinylformamide) microgels were synthesized via non-aqueous dispersion polymerization. Polyvinylamine microgels were then obtained by hydrolysis of poly(N-vinylformamide) microgels in NaOH (1 M) at 80 ^{o}C. This hydrolysis method requires complicated polymerization strategies and harsh conditions for hydrolysis.

Other than hydrolysis of formamide, Hofmann rearrangement of unsubstituted amides also generates primary amines, following the path shown in Scheme 1. Although side reactions (formation of carboxylic acid and urea RNHCONHR[19]) are involved, the Hofmann rearrangement has been applied in polymer chemistry for preparation of primary amine-containing polymers from polyacrylamide[19-20] or polymethacrylamide[21]. Shiroya et al. applied Hofmann rearrangement in preparation of PNIPAM microgels containing primary amines.[22] PNIPAM microgels were prepared with acrylamide as

comonomers via precipitation polymerization, and the unsubstituted amides of acrylamide were then converted into primary amines by reacting with alkaline bleach at 4°C. Horecha et al. prepared PNIPAM microgels containing primary amines with a similar method by conducting Hofmann rearrangement with diacetoxyiodobenzene in water/acetonitrile solution at 0 °C for 4 hour.[23] However, both methods require low temperature and/or organic solvents.

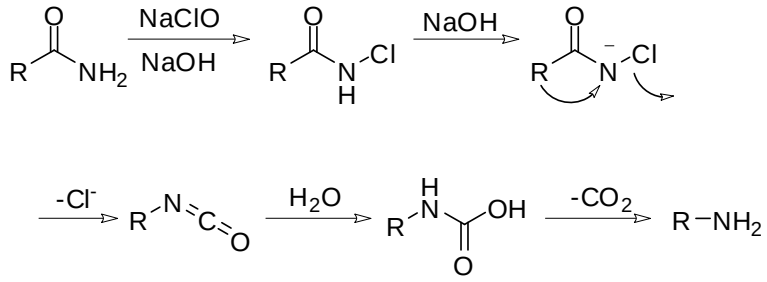

Scheme 1. Hofmann rearrangement of unsubstituted amides with NaClO/NaOH.

The Hofmann rearrangement can also be conducted in alkaline bleach at room temperature.[24-25] The attempted Hofmann rearrangement of PNIPAM microgels (copolymerized with acrylamides) in alkaline bleach at room temperature was unsuccessful, however, since both PNIPAM and bisacrylamide crosslinker are chemically unstable in alkaline bleach.[13, 26] On the other hand, we have shown that PNIPMAM microgels crosslinked by ethylene glycol dimethacrylate resist N-chlorination and degradation in alkaline bleach at room temperature[27], which can be used as supporting particles in reactions involving alkaline bleach.

In this paper, we show that primary amine-containing microgels can be prepared via the Hofmann rearrangement of PNIPMAM/methacrylamide copolymer microgels in alkaline bleach at room temperature. The primary amine content in the resulting microgels was tuneable by Hofmann rearrangement time, and a content of 0.4 mmol/g was achieved after a 60 min reaction, which corresponds to a 50% conversion of MAM.

Amphoteric microgel based on PNIPAM has been getting more attentions, due to its special pH-induced swelling property.[28-34] Here we also show this Hofmann rearrangement can be easily extended to prepare amphoteric microgels containing both primary amines and carboxyls. The molar ratio of primary amines to carboxyls can be controlled by Hofmann rearrangement time, which offers a simple way to tune isoelectric point.

5.2 Experiments

Materials. All chemicals were purchased from Sigma-Aldrich (Canada), and used without further purification except for N-isopropyl*meth*acrylamide (NIPMAM). NIPMAM (97%) was purified from re-crystallization with mixture of toluene and hexane (60:40) prior to use. Fluorescein isothiocyanate (FITC, ≥90%) were used directly as received. Type I water with a resistivity of 18.1 MΩ·cm from a Barnstead Nanopure Diamond system was used in all experiments. The concentration of sodium hypochlorite (bleach, NaClO, 10-15%) was determined by iodometeric titration prior to use. The details can be found elsewhere.[24]

Synthesis of Microgels. PNIPMAM Microgels were prepared according to the literature[35] with minor modifications. The recipe is shown in Table 1. The procedure is described as following. A 250 mL three-neck flask reactor was equipped with a mechanical stirrer, a nitrogen inlet/outlet, and a condenser. In the reactor, 1.56 g NIPMAM, 0.13 g ethylene glycol dimethacrylate (EGDMA, 98%), 0.3 g methacrylamide (MAM, 98%), 0.1 g sodium dodecyl sulfate (SDS, 99%), and 150 mL water were added. The solution was deoxygenated with nitrogen for 30 min at 70 ^{o}C, before 0.025 g ammonium persulfate (APS, 98%) dissolved in 5 mL water was added. The polymerization was conducted at 70 ^{o}C under nitrogen atmosphere for another 6 hour. After polymerization, microgels were purified by ultracentrifugation (Beckman L-80 XP), decantation and suspension in water for several cycles until the conductivity of supernatant was less than 5 μS/cm. Microgels were then lyophilized for storage. Microgels with MAM without Hofmann rearrangement are referred as AMI microgels; microgels without MAM are referred as CON microgels; and microgels with both MAM and carboxyls are referred as AMP microgels.

Table 1. Recipes for Preparation of Starting Microgels

Microgels*	NIPMAM/g	MAM/g	AA/g	EGDMA/g	SDS/g	APS/g	Water/mL
CON-0	1.56	0	0	0.13	0.1	0.025	150
AMI-0	1.56	0.3	0	0.13	0.1	0.025	150
AMP-0	1.56	0.3	0.03	0.13	0.1	0.025	150

* CON-120 microgels are CON-0 microgels after treated (Hofmann rearrangement) for 120 min.

AMI-0.4 microgels are AMI microgels with 0.4 mmol/g amines after Hofmann rearrangement.

Hofmann Rearrangement of Microgels. Amines were converted from amide groups in NaClO solution via a modified Hofmann rearrangement process. The procedure is briefly described as follows, which can also be found in literatures.[24-25] A beaker with 10 mL water was kept in an ice bath, and 0.286 mL NaClO (1.4 M) was added into the beaker. Next, 1 mL NaOH (1 M) was added in a drop-wise fashion into the beaker under vigorous stirring. In addition, 113 mg of microgels were dispersed in 10 mL of water. The microgel suspension was subsequently added to the 10 mL NaClO solution in the ice bath which was then well mixed. Adjust the stirring speed to a proper value and increase temperature to 25 ^{o}C to start the reaction. After a certain time (10 min, 30 min, or 60 min), 60 mg sodium thiosulfate (98%) was added to stop the reaction. The resultant microgels were purified via ultracentrifugation, followed by freeze-drying, as described in the previous section.

Fluorescence Labelling. The presence of primary amines in AMI microgels after Hofmann rearrangement was confirmed by FITC labelling. AMI microgels with 0.4 mmol/g primary amines (AMI-0.4) were added to 10 mL borate buffer (pH 9) to make a 1 mg/mL suspension. Then the suspension was added with 0.1 mL FITC solution in DMSO (1 mg/mL). The reaction was conducted for 12 hour at 4 ^{o}C with moderate magnetic stirring, and then quenched by mixing with 0.26 mL NH_4Cl (2 M) for 2 hour. The result microgels were purified by ultracentrifugation until the conductivity of supernatant was less than 5 μS/cm. In a parallel experiment, AMI-0 reacted with FITC as control.

Dynamic Light Scatterings (DLS). Microgels were dispersed in 1 mM NaCl, and the pH was adjusted with 1 mM HCl and NaOH. Hydrodynamic diameters of microgels were measured by DLS with a detection angle at 90^{o}. The laser source is a Melles Griot HeNe laser with a wavelength of 633 nm. The scattering intensity was between 100 and 250 kcps for all measurements. Each sample was measured for three runs with 2 min for each run.

Electrophoretic Mobility. Electrophoretic mobility was measured using a ZetaPlus analyzer (Brookhaven Instruments Corp.), operating in phase analysis light scattering (PALS) mode. Microgels were dissolved in 1 mM NaCl, and the microgels concentration was 1 g/L for all measurements. For each measurement, 10 runs (15 cycles each) were carried out.

Titration. Amine content of microgels was measured by conductometric titration. The titration was performed using a Burivar-I2 Buret Module (ManTech Associates) with PC-Titrate software (version 2.0.0.79). Samples were prepared by adding lypholyzied microgels (25 mg) in 50mL NaCl (1mM) in a beaker of well-controlled temperature. The beaker was installed with an overhead stirrer, a pH electrode, a conductivity electrode and a thermometer (connected with the computer). NaOH (0.1 M, LabChem Inc.) was uses as titrant. The samples were purged with nitrogen for 30 min to remove dissolved CO_2. The

sample pH was then adjusted to 3 before starting the measurement. The interval between two drops was set to 300 sec.

Nuclear Magnetic Resonance (NMR). The content of amide groups in microgels before Hofmann rearrangement was estimated from ^{1}H NMR. Microgels after being freeze-dried were dissolved in deuterated methanol to obtain a suspension with a concentration of about 20 g/L. The spectrum was acquired in a Bruker AV200 NMR spectrometer (200 MHz).

UV-vis Absorbance. FITC-labelled microgels and control samples were dissolved in phosphate buffered saline at pH 7.4. UV-vis absorbances of microgels were measured at 25 ^{o}C with a UV-vis spectrophotometer (Beckman Coulter DU800). The control samples include unlabelled AMI microgels and CON microgels before and after react with FITC.

5.3 Results

5.3.1 Hofmann Rearrangement of AMI microgels

Primary amine-containing microgels were prepared in two consequent steps: 1. The starting microgels, PNIPMAM microgels with MAM, were prepared via the precipitation polymerization; 2. Primary amines were converted from unsubstituted amides (MAM) by reacting the microgels with alkaline bleach at ambient temperature (Hofmann rearrangement, Scheme 2).

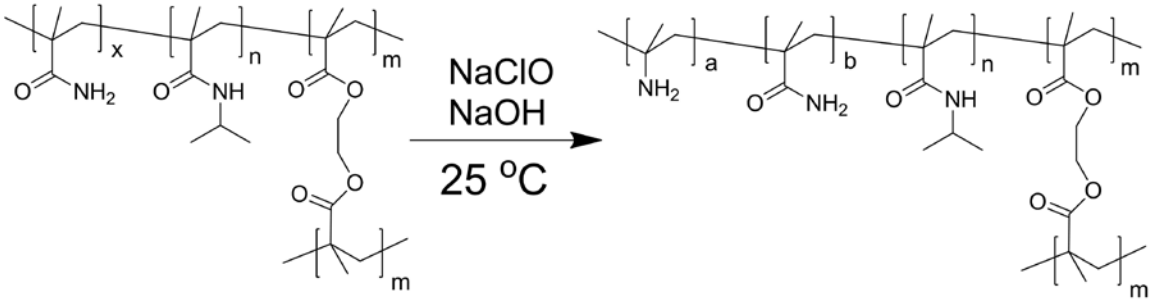

Scheme 2. Scheme description of Hofmann rearrangement of AMI-0 microgels

Table 1 shows the recipes for the preparation of the starting microgels. PNIPMAM microgels without MAM were used as control sample, which was labelled as CON-0. After treated under Hofmann rearrangement condition for 120 min, CON-0 is designated CON-120. AMI-0 microgels were PNIPMAM microgels with MAM, and AMI-0.4 microgels were AMI microgels with 0.4 mmol/g amines after Hofmann rearrangement.

The microgel containing MAM and AA without Hofmann rearrangement was labelled as AMP-0.

The content of unsubstituted amides in AMI-0 microgels was determined prior to the Hofmann rearrangement. The ^{1}H NMR spectrum of AMI-0 microgels is shown in Figure 1. The unsubstituted amide content was then calculated based on Figure 1, following the method described in the literature.[36] The content of unsubstituted amides in AMI-0 microgels was determined as 0.76 mmol/g (w/w 6.5%), which is lower than the content of MAM in the monomer feed (15.8% from Table 1). This unexpected difference was also found in the preparation of PNIPAM microgels with acrylamide.[36] Although the data of reactivity ratios between methacrylamide and PNIPMAM is lacking, it is expected that the reactivity ratios are close, since acrylamide and NIPAM have similar reactivity ratios close to 1.[37] Hence the molar ratio between NIPMAM and MAM should be close to the ratio in the monomer feed. Although the reason for the difference remains unknown, the Hofmann rearrangement of AMI-0 microgels can be conducted without difficulty.

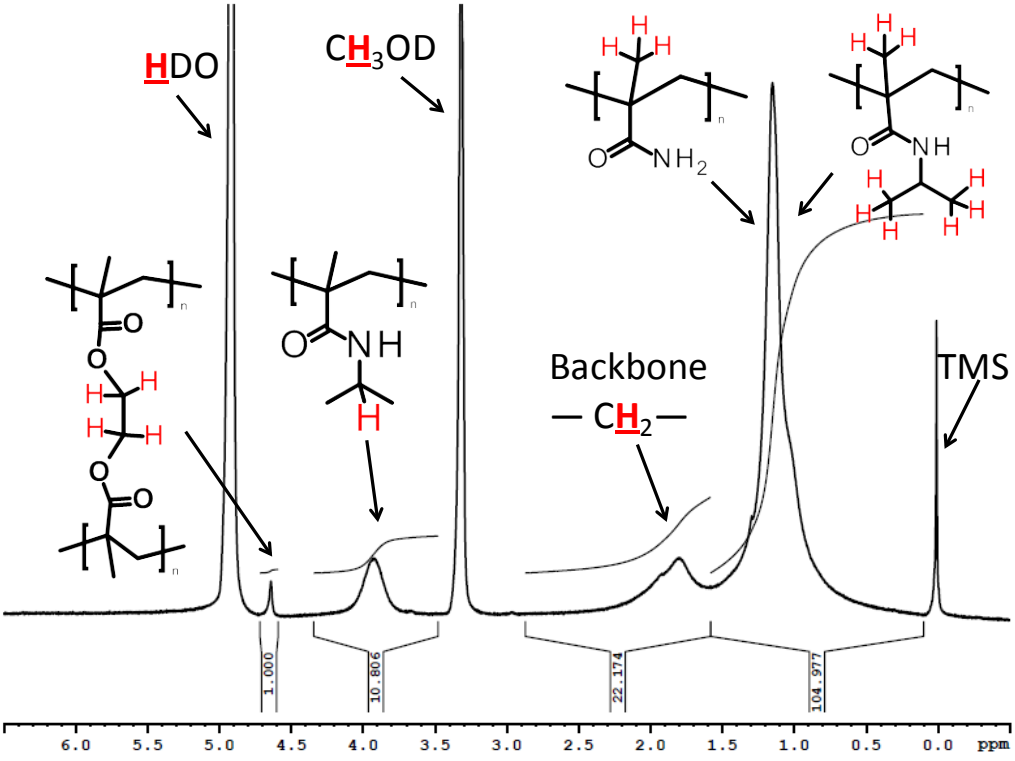

Figure 1. ^{1}H-NMR Spectrum of AMI-0 Microgel.

The Hofmann rearrangement of AMI-0 microgels was conducted in a mixture of NaClO and NaOH at 25 ^{o}C. After purification, the amine contents of AMI microgels after Hofmann rearrangement were determined via conductometric titration, and the results are

shown in Figure 2. Typical titration curves are shown in supporting information. The amine content in AMI microgels increased with Hofmann rearrangement time. The amine content of 0.4 mmol/g (AMI-0.4 microgels) was found with 60 min Hofmann rearrangement, which corresponds to 53% conversion of unsubstituted amides in the starting microgels (AMI-0).

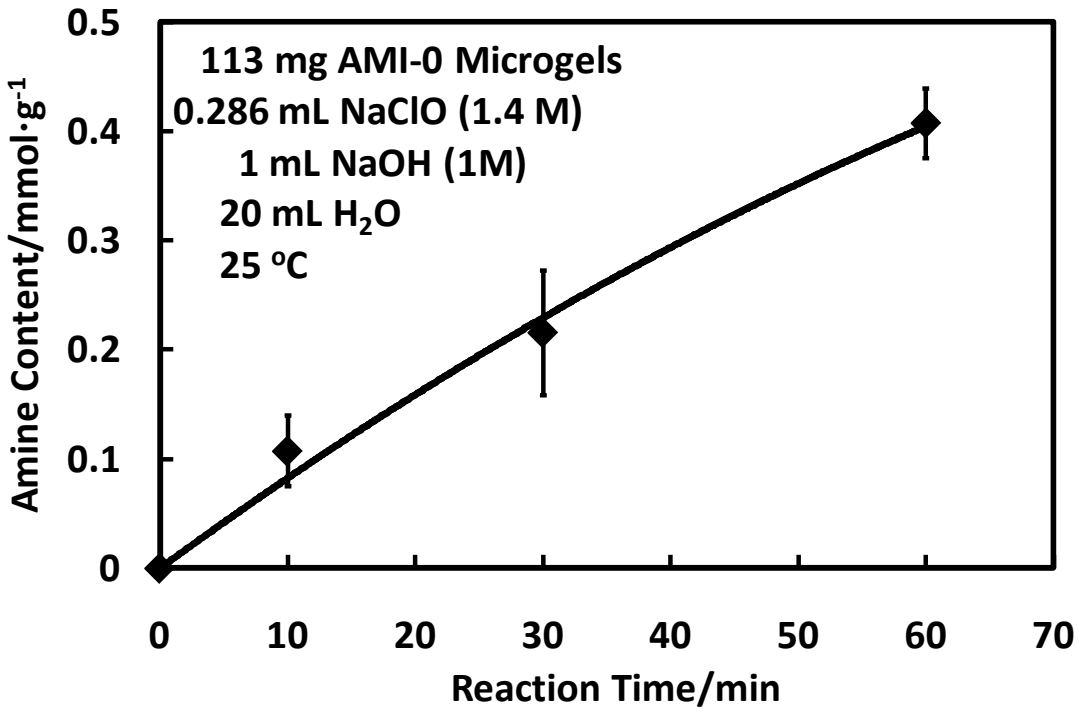

Figure 2. Amine contents in AMI microgels after Hofmann rearrangement determined via conductometric titration. The amine content corresponding to 100% conversion of methacrylamide groups is 0.76 mmol/g. The error bars were calculated from duplicated measurements. Dash line is drawn as an eye guideline.

The conjugation ability of AMI microgels was shown by labelling of AMI-0.4 microgels with FITC. The UV-absorbance spectrum of FITC-labelled microgels and control samples in phosphate buffered solution at 25 ^{o}C are shown in Figure 3. It is shown that AMI-0.4 microgels exhibit an absorption peak at 495 nm after labelled with FITC, which corresponds to the absorption maximum wavelength of FITC molecules. There was no peak observed at 495 nm for control samples. Hence the results show AMI microgels obtained from Hofmann rearrangement can be used as supporting particle for bioconjugation. The results also indicate the formation of primary amines after Hofmann rearrangement, since FITC can only form stable products with primary amines.[38]

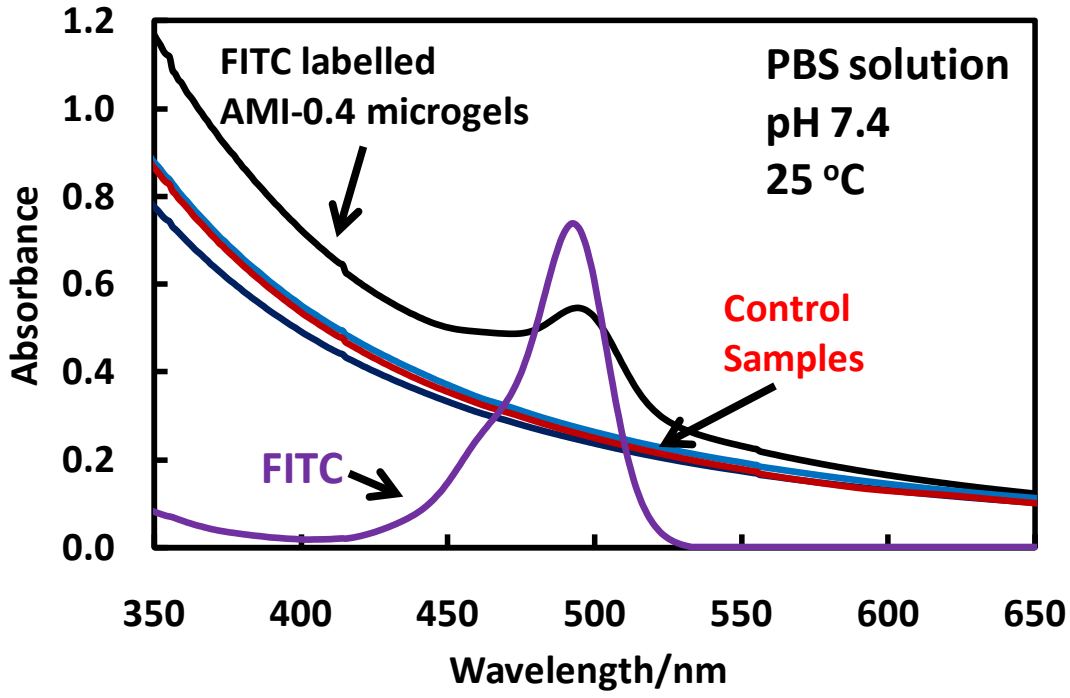

Figure 3 Absorbance of FITC-labelled AMI-0.4 microgels. The control samples include unlabelled AMI-0.4 microgels and AMI-0 microgels before and after react with FITC.

5.3.2 Effect of pH on AMI microgels

Mobility and particle diameter of AMI microgels were measured as a function of pH, and the results are shown in Figure 4. The measurements were conducted in 1 mM NaCl, and the pH was adjusted with 1 mM HCl and NaOH. AMI-0 microgels were slightly negatively charged as shown in Figure 4A, due to sulfate ester groups from initiators.[35] After Hofmann rearrangement, the resulting microgels were positively charged and the mobility increased with the amine content. For microgels with a specific amine content, the mobility decreased with increasing pH. The effect of pH on particle size of AMI microgels at 25 ^{o}C is shown in Figure 4B. Hydrodynamic diameters of AMI microgels decreased with pH after Hofmann rearrangement, and increased with amine content at specific pH value. A pH-induced swelling ratio (d_{pH4}/d_{pH10}) was 1.5 found for AMI-0.4 microgels. CON-0 microgels were also treated under the same Hofmann rearrangement condition for 120 min as control. The mobility and particle size of CON microgels before and after Hofmann rearrangement are shown in Supporting Information. Little change was observed for both mobility and particle size of CON microgels before and after Hofmann rearrangement.

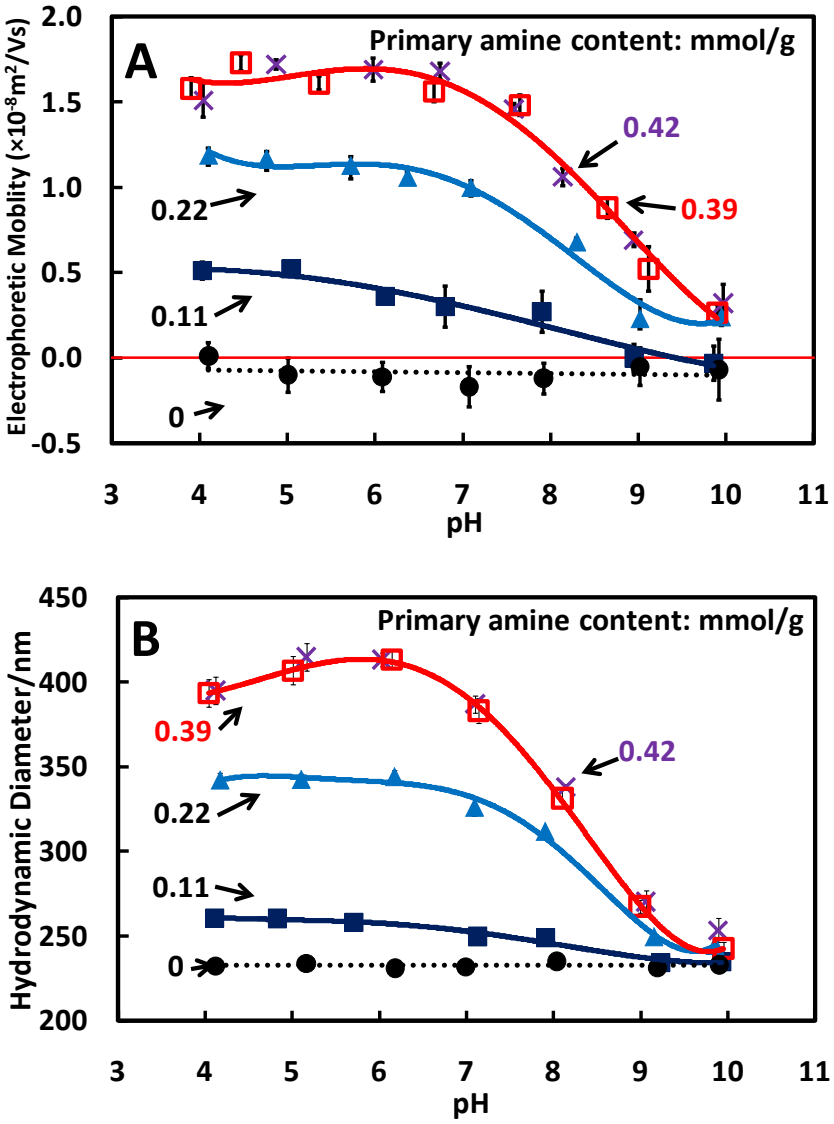

Figure 4 Effect of pH on (A) electrophoretic mobility and (B) hydrodynamic diameter of AMI microgels before and after Hofmann rearrangement. The measurement was conducted in 1 mM NaCl. The primary amine contents in microgels are shown in the figure. The error bars were calculated from three repeat measurements. Dash lines are drawn as eye guidelines.

5.3.3 Temperature Effect on AMI Microgels

Effect of temperature on diameter of AMI microgels at pH4 and pH 10 is shown in Figure 5. The volume phase transition temperature (VPTT) of CON microgels was determined

around 43 ^{o}C (Supporting Information). However, no definable volume phase transition was observed both at pH 4 and pH 10 in the range of 25 ^{o}C to 50 ^{o}C. The decrease on diameter was highly suppressed at pH 4 along with temperature. At pH 4, microgels with higher amine content showed less thermosensitivity. The temperature-induced swelling ratio ($d_{25^{o}C}/d_{50^{o}C}$) was 1.14 for AMI-0.4 microgels. While at pH 10, most amines were de-ionized. Microgels showed similar thermosensitivity before and after Hofmann rearrangement. The swelling ratio ($d_{25^{o}C}/d_{50^{o}C}$) of AMI-0.4 microgels was 1.26 at pH10.

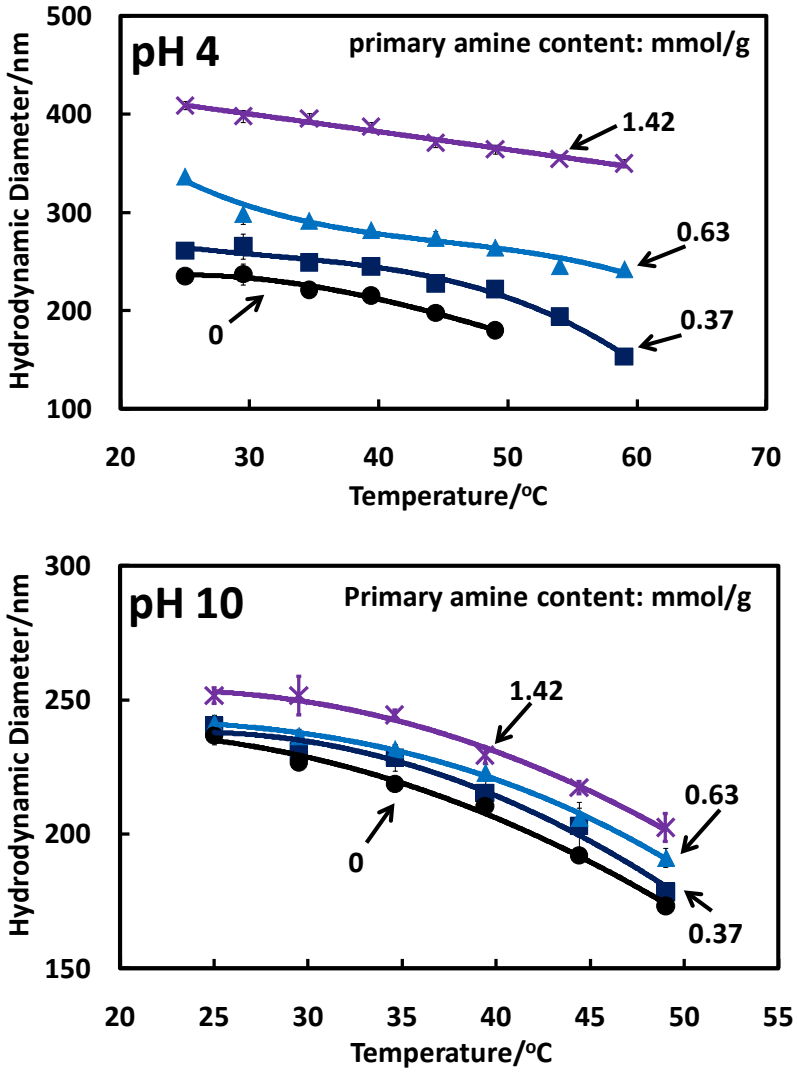

Figure 5. Temperature effect on diameters of AMI microgels before and after Hofmann rearrangement at pH 4 and pH 10. The measurements were conducted in 1 mM NaCl. The error bars were calculated from three repeat measurements. Dash lines are drawn as eye guidelines.

5.3.4 Amphoteric Microgels

The Hofmann rearrangement was extended to prepare of amphoteric microgels (AMP microgels). First, AMP-0 microgels were prepared via copolymerization of NIPMAM, MAM and acrylic acid, following the recipe in Table 1. Second, Hofmann rearrangement of AMP-0 microgels resulted in amphoteric microgels containing primary amines and carboxyls, as schematic described in Scheme 3.

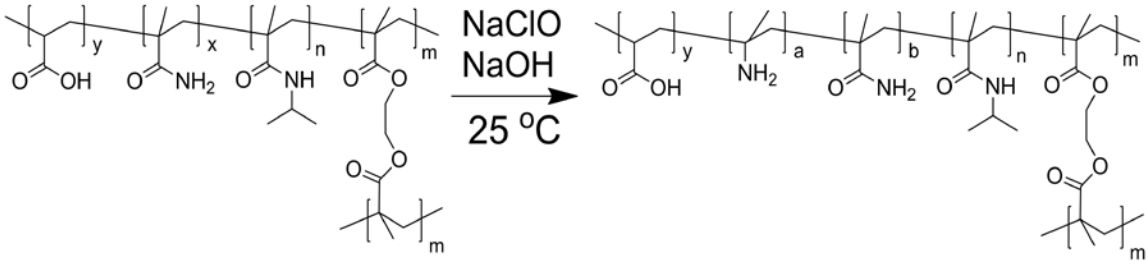

Scheme 3 Preparation of amphoteric microgels via Hofmann rearrangement from AMP-0 microgels.

The molar ratio between total amines and total carboxyls, regardless of degree of ionization, was abbreviated as $[NH_2]_T/[COOH]_T$. The $[NH_2]_T/[COOH]_T$ ratio was determined via conductometric titration, and the results are shown in Figure 6. Since both carboxyls and amines contribute to a conductometric endpoint, we do not attempt to separate the contributions of carboxyls and amines here. Therefore the calculation of $[NH_2]_T/[COOH]_T$ was based on the assumption that the formation of COOH during Hofmann rearrangement was negligible, which will be discussed in next section. The $[NH_2]_T/[COOH]_T$ ratio increased with Hofmann rearrangement time, due to the formation of primary amines.

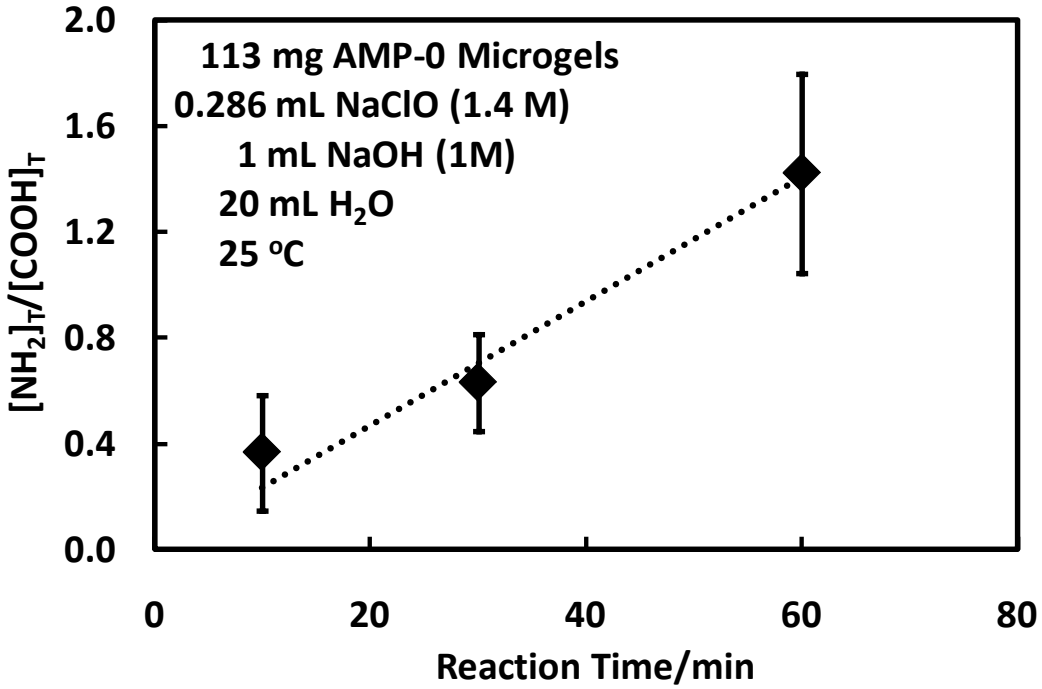

Figure 6. The $[NH_2]_T/[COOH]_T$ ratio in amphoteric microgels as a function of Hofmann rearrangement time. Dash line is drawn as an eye guideline.

The pH effect on mobility and diameter of AMP microgels before and after Hofmann rearrangement is shown in Figure 7. AMP-0 microgels were negatively charged in the range of pH 3 to pH 10, and the diameter increased with pH. After Hofmann rearrangement, the mobility of AMP microgels changed from positive to negative with increased pH. The diameter curves of AMP microgels were U-shape after Hofmann rearrangement. Both mobility and diameter results indicated zwitterionic behaviour of AMP microgels after Hofmann rearrangement.

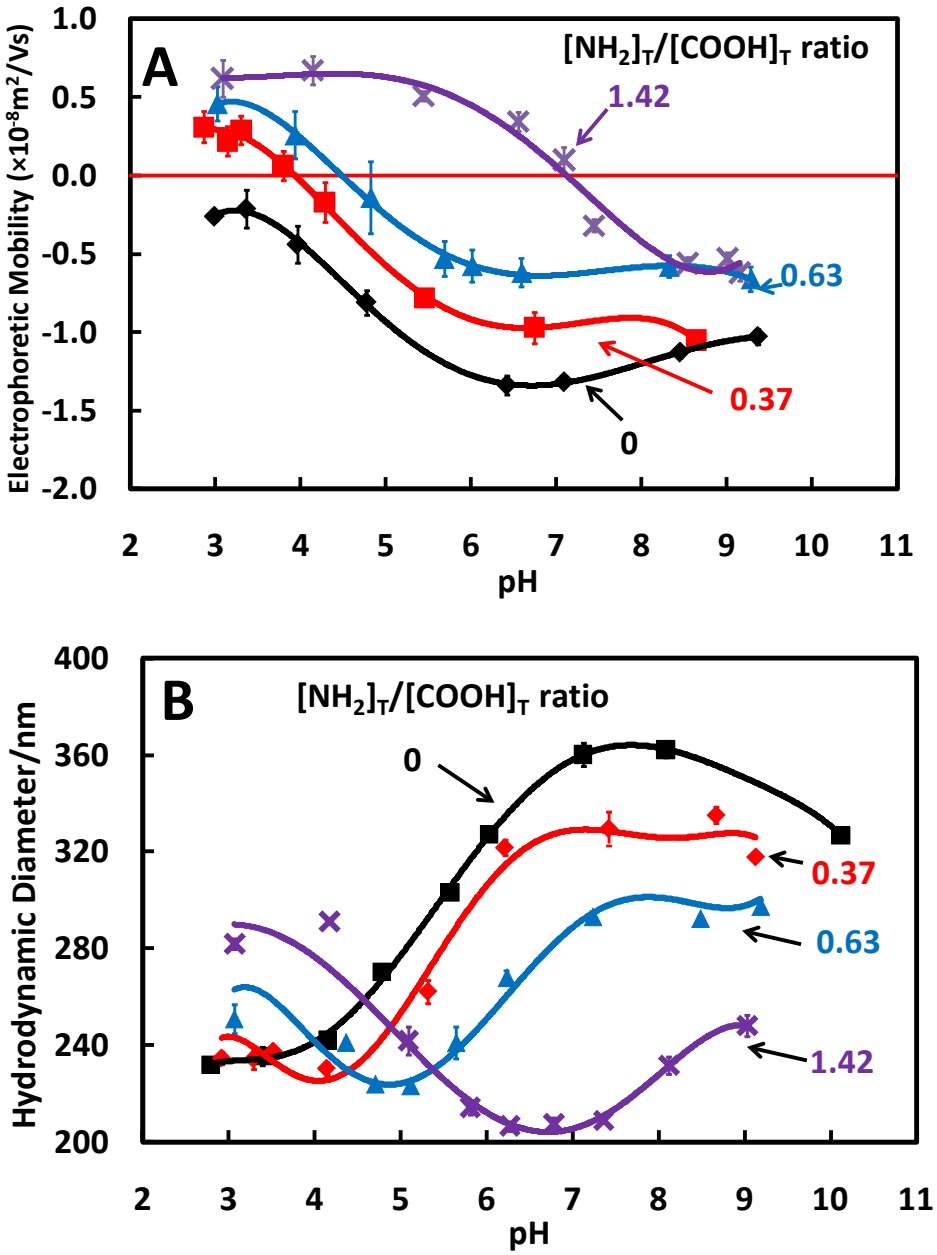

Figure 7 Effect of pH on (A) mobility and (B) diameter of AMP microgels before and after Hofmann rearrangement. The $[NH_2]_T/[COOH]_T$ ratios are shown in the figures. The error bars were calculated from three repeat measurements. Dash lines are drawn as eye guidelines.

The isoelectric point (IEP) was determined from mobility and diameter results. With mobility results, the IEP is defined as the pH value where the mobility equals to 0; while with diameter results the IEP is defined as the pH value where the smallest size is

achieved. The relationship between IEP and $[NH_2]_T/[COOH]_T$ ratio are shown in Figure 8. It is shown that higher $[NH_2]_T/[COOH]_T$ ratio gives higher IEP.

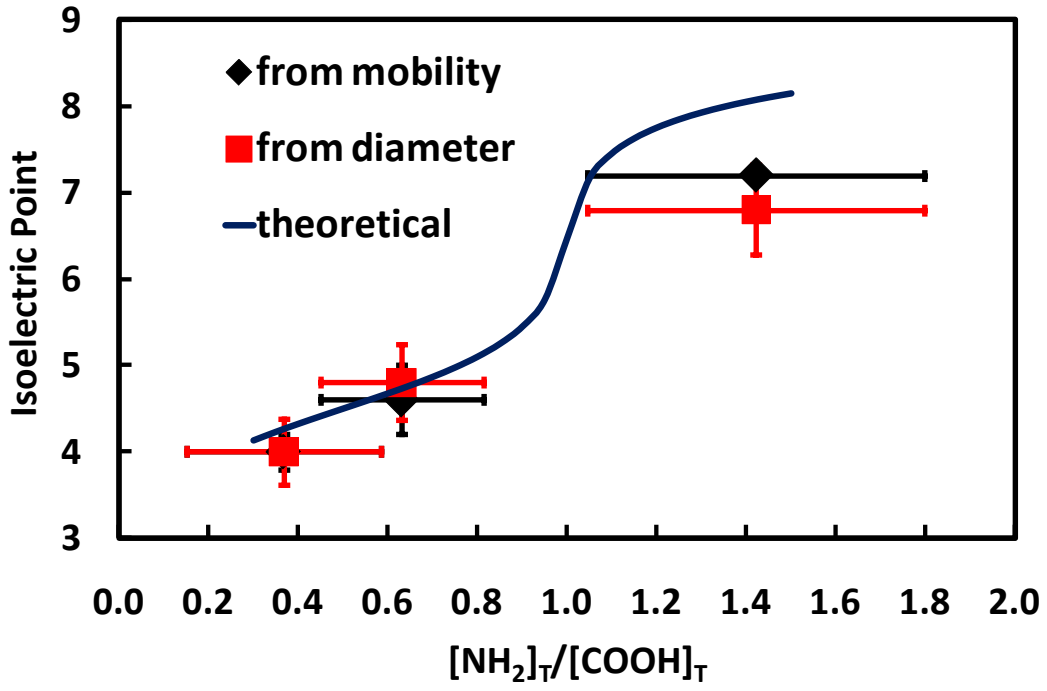

Figure 8. Isoelectric point of amphoteric microgels as a function of $[NH_2]_T/[COOH]_T$ ratio. The isoelectric points were independently determined from mobility results (Figure 7A) and DLS results (Figure 7B). The error bars in x axial were adopted from Figure 6. The error bars in y axial were determined from Figure 7. The solid curve was calculated according to Eq. 2.

5.4 Discussion

5.4.1 Advantages of the Hofmann Rearrangement

Primary amine-containing PNIPMAM microgels have been successfully prepared via the Hofmann rearrangement, since PNIPMAM resists the N-chlorination reaction in alkaline bleach.[27] Although it can not be extended to PNIPAM microgels, due to the instability of PNIPAM microgels in alkaline bleach[13], this method still exhibits several advantages in preparing primary amine-containing microgels, which may be industrially attractive.

First, the reaction is conducted by simply mixing reactants in aqueous solution at ambient temperature. Hence this method is simple and less cost comparing with the conventional Hofmann rearrangement used in the literatures.[22-23] In the conventional Hofmann

rearrangement, the reaction is conducted at low temperature (e.g. 4 ^{o}C) and/or in organic solvents.

Second, this method is fast and efficient. The amine content is controlled by the Hofmann rearrangement time. A primary amine content of 0.4 mmol/g, which corresponds to 50% conversion of MAM, can be achieved after 60 min reaction. The formed primary amines can be used as bioconjugation sites, as shown by the FITC labelling experiment.

Third, the side reaction introducing carboxyls is insignificant. Wirsen et al. showed that the ratio of carboxyl to amine was 10% after Hofmann rearrangement at ambient temperature.[24] However, we argued that the carboxyl content in AMI microgels after Hofmann rearrangement is limited in this paper. This argument is made based on the mobility and DLS results as shown in Figure 4. After Hofmann rearrangement, the mobility of AMI microgels is still positive and the particle size does not turn up at high pH (e.g. pH 10). Hence the amine content in AMI microgels and AMP microgels was determined by conductometric titration directly as shown in Results section, based on the assumption that the formation of carboxyls is negligible during the Hofmann rearrangement.

Fourth, this method does not involve the complications of primary amine-containing comonomers during polymerization. Primary amines can react with peroxide initiators (ammonium persulfate or *tert*-butyl hydroperoxide)[39-40], which may lead side reactions during polymerization when cationic comonomers are used. The utilization of MAM instead of amine-containing comonomers can avoid such side reactions. Besides, the incorporation of functional comonomers in resulted microgels is strongly affected by several factors, such as the reactivity ratios[36], the chemistry of comonomers[10], and reaction solution properties[15]. Since MAM is non-ionic and has a similar chemical structure to NIPMAM, it is easier to control the comonomers distribution by using MAM, so as the distribution of amines after Hofmann rearrangement, in comparison with cationic comonomers.

5.4.2 Preparation of Amphoteric Microgels

The Hofmann rearrangement can be easily extended to amphoteric (AMP) microgels containing both primary amines and carboxyls. IEP of AMP increases with $[NH_2]_T/[COOH]_T$ ratio, as shown in Figure 8. This shift can be explained that more base (OH^-) is required to consume the excess of NH_3^+ groups, as proposed for PNIPAM amphoteric microgels containing carboxyls and imidazole groups by Das et al.[30] Since the primary amine content is affected by Hofmann rearrangement time, the $[NH_2]_T/[COOH]_T$ ratio in AMP microgels is varied with Hofmann rearrangement time. Therefore the IEP of microgels, which corresponds to $[NH_2]_T/[COOH]_T$ ratio, is tuneable via Hofmann rearrangement time.

The theoretical IEP curve shown in Figure 8 is calculated based on the model presented by Ehrlich and Doty for prediction of polyampholyte IEP.[41] The model is shown as Equation 1.

$$\frac{\left(1+10^{pK_a-pI}\right)}{\left(1+10^{pI-pK_b}\right)}=\frac{\left[NH_2\right]_T}{\left[COOH\right]_T}=R \qquad (1)$$

where pK_a and pK_b are the dissociation constants of primary amine and carboxylic acid, respectively; pI is isoelectric point; R is the molar ratio of amines to carboxylic acid in microgel. And an analytic solution was obtained by Patrickios, as shown by Equation 2.[42]

$$pI = pK_b + \log\left\{\frac{1}{2}\left[\frac{1-R}{R}+\sqrt{\left(\frac{1-R}{R}\right)^2+\left(\frac{4}{R}\right)10^{pK_a-pK_b}}\right]\right\} \qquad (2)$$

In the calculation, the effective dissociation constant of primary amine (pK_a) is 8.45, which was determined for polyvinylamine.[43] The effective dissociation constant of carboxylic acid (pK_b) is 4.5, as for polyacrylic acid.[44]

Theory and experiment show reasonable agreement at low $[NH_2]_T/[COOH]_T$ ratio and large discrepancies at high $[NH_2]_T/[COOH]_T$ ratio. This model was developed for linear polyampholytes. Hence an intrinsic hypothesis in this model is that the distribution of both amines and carboxyls is uniform. The large discrepancies at high $[NH_2]_T/[COOH]_T$ ratio is probably due to the uneven distribution of amines and carboxyls in AMP microgels, which is caused by the difference of the reactivity ratios between NIPMAM and comonomers.[10]

Other than the ability to easily control the IEP, this method shows other advantages in preparation of amphoteric microgels. Since MAM is uncharged prior to Hofmann rearrangement, the colloidal stability during polymerization is enhanced, due to absence of the interaction between ionic comonomers and cationic comonomers. Furthermore, amphoteric microgels with complicated distribution of functional groups (e.g. core/shell[45-46]) could be achieved with this method.

5.5 Conclusions

1. By replacing the α-hydrogen atoms in NIPAM with methyl groups, it is possible to generate amine groups by the Hofmann rearrangement with minimum side reactions. This paper shows that Hofmann rearrangement of PNIPMAM microgels

with unsubstituted amides can be conducted in the solution of NaClO and NaOH at ambient temperature, resulting primary amine-containing microgels.

2. The amine contents of microgels can be controlled by controlling the Hofmann rearrangement time. A content of 0.4 mmol/g was achieved after 60 min reaction. The resulting microgels are positively charged and highly pH-sensitive. However, no definable volume phase transition was found up to 50 ^{o}C.

3. This method can be easily extended for preparation of amphoteric microgels containing both primary amines and carboxyls. The resulting amphoteric microgels are positively charged at low pH and negatively charged at high pH. The microgels display U-shape diameter curves as function of pH. The isoelectric point can be tuned via Hofmann rearrangement time.

5.6 References

1. Pelton, R., Temperature-sensitive aqueous microgels. *Advances in Colloid and Interface Science* **2000,** 85, (1), 1-33.
2. Oh, J. K.; Drumright, R.; Siegwart, D. J.; Matyjaszewski, K., The development of microgels/nanogels for drug delivery applications. *Progress in Polymer Science* **2008,** 33, (4), 448-477.
3. Zhang, J. G.; Xu, S. Q.; Kumacheva, E., Polymer microgels: Reactors for semiconductor, metal, and magnetic nanoparticles. *Journal of the American Chemical Society* **2004,** 126, (25), 7908-7914.
4. Bai, S.; Nguyen, T. L.; Mulvaney, P.; Wang, D. Y., Using Hydrogels to Accommodate Hydrophobic Nanoparticles in Aqueous Media via Solvent Exchange. *Advanced Materials* **2010,** 22, (30), 3247-+.
5. Hoare, T.; Pelton, R., Engineering glucose swelling responses in poly(N-isopropylacrylamide)-based microgels. *Macromolecules* **2007,** 40, (3), 670-678.
6. Su, S. X.; Ali, M.; Filipe, C. D. M.; Li, Y. F.; Pelton, R., Microgel-based inks for paper-supported biosensing applications. *Biomacromolecules* **2008,** 9, (3), 935-941.
7. Tsuji, S.; Kawaguchi, H., Colored thin films prepared from hydrogel microspheres. *Langmuir* **2005,** 21, (18), 8439-8442.
8. Sorrell, C. D.; Serpe, M. J., Reflection Order Selectivity of Color-Tunable Poly(N-isopropylacrylamide) Microgel Based Etalons. *Advanced Materials* **2011,** 23, (35), 4088-+.
9. Parasuraman, D.; Serpe, M. J., Poly (N-Isopropylacrylamide) Microgels for Organic Dye Removal from Water. *ACS Applied Materials & Interfaces* **2011,** 3, (7), 2732-2737.
10. Hoare, T.; Pelton, R., Highly pH and temperature responsive microgels functionalized with vinylacetic acid. *Macromolecules* **2004,** 37, (7), 2544-2550.
11. Meng, Z. Y.; Hendrickson, G. R.; Lyon, L. A., Simultaneous Orthogonal Chemoligations on Multiresponsive Microgels. *Macromolecules* **2009,** 42, (20), 7664-7669.
12. Suzuki, D.; Kawaguchi, H., Hybrid microgels with reversibly changeable multiple brilliant color. *Langmuir* **2006,** 22, (8), 3818-3822.
13. Wang, Z.; Pelton, R.; Lam, W. Y., N-Chlorinated Poly(N-isopropylacrylamide) Microgels. *Submitted* **2013**.
14. Meunier, F.; Elaissari, A.; Pichot, C., Preparation and Characterization of Cationic Poly(N-Isopropylacrylamide) Copolymer Latexes. *Polymers for Advanced Technologies* **1995,** 6, (7), 489-496.
15. Hu, X. B.; Tong, Z.; Lyon, L. A., Synthesis and physicochemical properties of cationic microgels based on poly(N-isopropylmethacrylamide). *Colloid and Polymer Science* **2011,** 289, (3), 333-339.
16. Huang, G.; Hu, Z. B., Phase behavior and stabilization of microgel arrays. *Macromolecules* **2007,** 40, (10), 3749-3756.

17. Xu, J. J.; Timmons, A. B.; Pelton, R., N-Vinylformamide as a route to amine-containing latexes and microgels. *Colloid and Polymer Science* **2004,** 282, (3), 256-263.
18. Thaiboonrod, S.; Berkland, C.; Milani, A. H.; Ulijn, R.; Saunders, B. R., Poly (vinylamine) microgels: pH-responsive particles with high primary amine contents. *Soft Matter* **2013,** 9, (15), 3920-3930.
19. Elachari, A.; Coqueret, X.; Lablachecombier, A.; Loucheux, C., Preparation of Polyvinylamine from Polyacrylamide - a Reinvestigation of the Hofmann Reaction. *Makromolekulare Chemie-Macromolecular Chemistry and Physics* **1993,** 194, (7), 1879-1891.
20. Tanaka, H., Hofmann Reaction of Polyacrylamide - Relationship between Reaction Condition and Degree of Polymerization of Polyvinylamine. *Journal of Polymer Science Part a-Polymer Chemistry* **1979,** 17, (4), 1239-1245.
21. Arcus, C., The hofmann reaction with polymethacrylamide. *Journal of Polymer Science* **1952,** 8, (4), 365-370.
22. Shiroya, T.; Tamura, N.; Yasui, M.; Fujimoto, K.; Kawaguchi, H., Enzyme Immobilization on Thermosensitive Hydrogel Microspheres. *Colloids and Surfaces B-Biointerfaces* **1995,** 4, (5), 267-274.
23. Horecha, M.; Senkovskyy, V.; Synytska, A.; Stamm, M.; Chervanyov, A. I.; Kiriy, A., Ordered surface structures from PNIPAM-based loosely packed microgel particles. *Soft Matter* **2010,** 6, (23), 5980-5992.
24. Wirsen, A.; Ohrlander, M.; Albertsson, A. C., Bioactive heparin surfaces from derivatization of polyacrylamide-grafted LLDPE. *Biomaterials* **1996,** 17, (19), 1881-1889.
25. Xu, Z. K.; Yang, Q.; Tian, J.; Dai, Z. W.; Hu, M. X., Novel photoinduced grafting-chemical reaction sequence for the construction of a glycosylation surface. *Langmuir* **2006,** 22, (24), 10097-10102.
26. Wang, Z.; Pelton, R., Chloramide Copolymers From Reacting Poly (N-isopropylacrylamide) with Bleach. *European Polymer Journal* **2013,** 49, (8), 2196-2201.
27. Wang, Z.; Pelton, R., Poly(N-isopropylmethacrylamide) Microgels Resist N-chlorination in Alkaline Bleach. *unpulished* **2013**.
28. Ito, S.; Ogawa, K.; Suzuki, H.; Wang, B. L.; Yoshida, R.; Kokufuta, E., Preparation of thermosensitive submicrometer gel particles with anionic and cationic charges. *Langmuir* **1999,** 15, (12), 4289-4294.
29. Ogawa, K.; Nakayama, A.; Kokufuta, E., Preparation and characterization of thermosensitive polyampholyte nanogels. *Langmuir* **2003,** 19, (8), 3178-3184.
30. Das, M.; Kumacheva, E., From polyelectrolyte to polyampholyte microgels: comparison of swelling properties. *Colloid and Polymer Science* **2006,** 284, (10), 1073-1084.
31. Li, X.; Zuo, J.; Guo, Y. L.; Cai, L. B.; Tang, S.; Yang, W. B., Volume phase transition temperature tuning and investigation of the swelling-deswelling oscillation of responsive microgels. *Polymer International* **2007,** 56, (8), 968-975.
32. Kumacheva, E.; Das, M.; Sanson, N., Zwitterionic Poly(betaine-N-isopropylacrylamide) Microgels: Properties and Applications. *Chemistry of Materials* **2008,** 20, (22), 7157-7163.

33. Hoare, T.; Pelton, R., Charge-switching, amphoteric glucose-responsive microgels with physiological swelling activity. *Biomacromolecules* **2008,** 9, (2), 733-740.
34. Nayak, S. P. Design, Synthesis and Characterization of Multiresponsive Microgels. Georgia Institute of Technology, Atlanta, 2004.
35. Mcphee, W.; Tam, K. C.; Pelton, R., Poly(N-Isopropylacrylamide) Latices Prepared with Sodium Dodecyl-Sulfate. *Journal of Colloid and Interface Science* **1993,** 156, (1), 24-30.
36. Hoare, T.; Pelton, R., Functional group distributions in carboxylic acid containing poly(N-isopropylacrylamide) microgels. *Langmuir* **2004,** 20, (6), 2123-2133.
37. Mumick, P. S.; McCormick, C. L., Water-soluble Copolymers. 54. N-Isopropylacrylamide-co-acrylamide Copolymers in Drag Reduction - Synthesis, Characterization, and Dilute-solution Behavior. *Polymer Engineering and Science* **1994,** 34, (18), 1419-1428.
38. Hermanson, G. T., *Bioconjugate Techniques*. 2nd ed.; Academic Press: London, 2008; p 402.
39. Li, P.; Zhu, J. M.; Sunintaboon, P.; Harris, F. W., New route to amphiphilic core-shell polymer nanospheres: Graft copolymerization of methyl methacrylate from water-soluble polymer chains containing amino groups. *Langmuir* **2002,** 18, (22), 8641-8646.
40. Xu, K.; Tan, Y.; Chen, Q.; An, H. Y.; Li, W. B.; Dong, L. S.; Wang, P. X., A novel multi-responsive polyampholyte composite hydrogel with excellent mechanical strength and rapid shrinking rate. *Journal of Colloid and Interface Science* **2010,** 345, (2), 360-368.
41. Ehrlich, G.; Doty, P., Macro-ions. III. The Solution Behavior of a Polymeric Ampholyte. *J. Am. Chem. Soc.* **1954,** 76, (14), 3764-3777.
42. Patrickios, C. S., Polypeptide Amino-Acid-Composition and Isoelectric Point. 1. A Closed-form Approximation. *Journal of Colloid and Interface Science* **1995,** 175, (1), 256-260.
43. Kobayashi, S.; Suh, K. D.; Shirokura, Y., Chelating Ability of Poly(vinylamine); Effects of Polyamine Structure on Chelation. *Macromolecules* **1989,** 22, (5), 2363-2366.
44. Michaels, A. S.; Morelos, O., Polyelectrolyte Adsorption by Kaolinite. *Industrial & Engineering Chemistry* **1955,** 47, (9), 1801-1809.
45. Christodoulakis, K. E.; Vamvakaki, M., Amphoteric Core-Shell Microgels: Contraphilic Two-Compartment Colloidal Particles. *Langmuir* **2010,** 26, (2), 639-647.
46. Schachschal, S.; Balaceanu, A.; Melian, C.; Demco, D. E.; Eckert, T.; Richtering, W.; Pich, A., Polyampholyte Microgels with Anionic Core and Cationic Shell. *Macromolecules* **2010,** 43, (9), 4331-4339.

5.7 Appendix: Supporting Information for Chapter 5

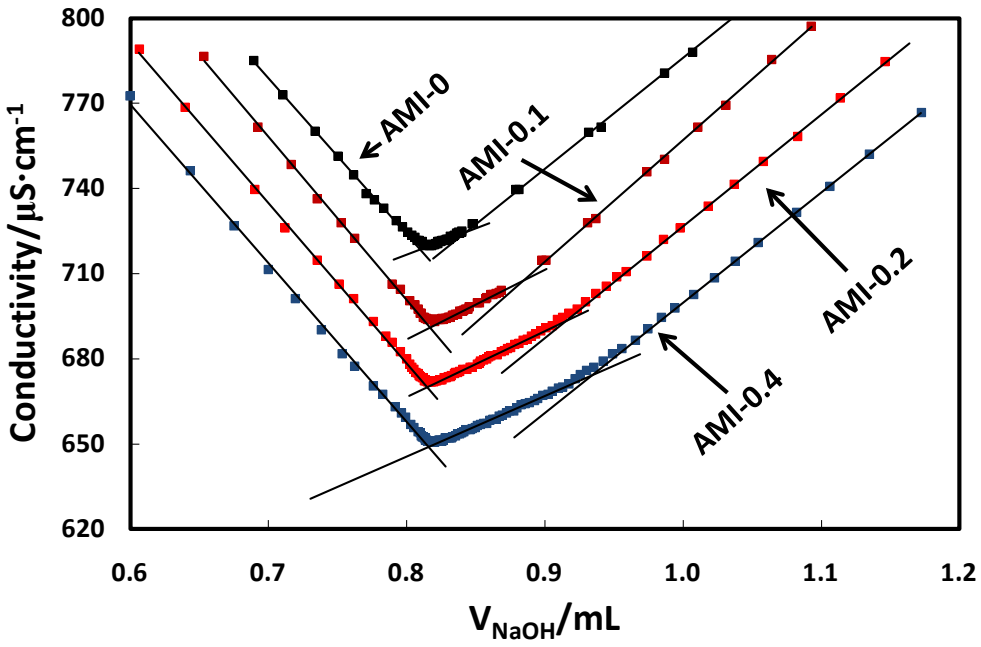

S1 Typical titration curves of AMI microgels before and after Hofmann rearrangement. Typical titration curves are shown in supporting information. It should be noticed that the suspension of AMI-0 microgels also consumed NaOH, which may contribute to residual carboxyl groups formed from the hydrolysis of ammonium persulfate initiator[35]. Hence the amine contents were obtained by subtracting titration results from the result of AMI-0 microgels.

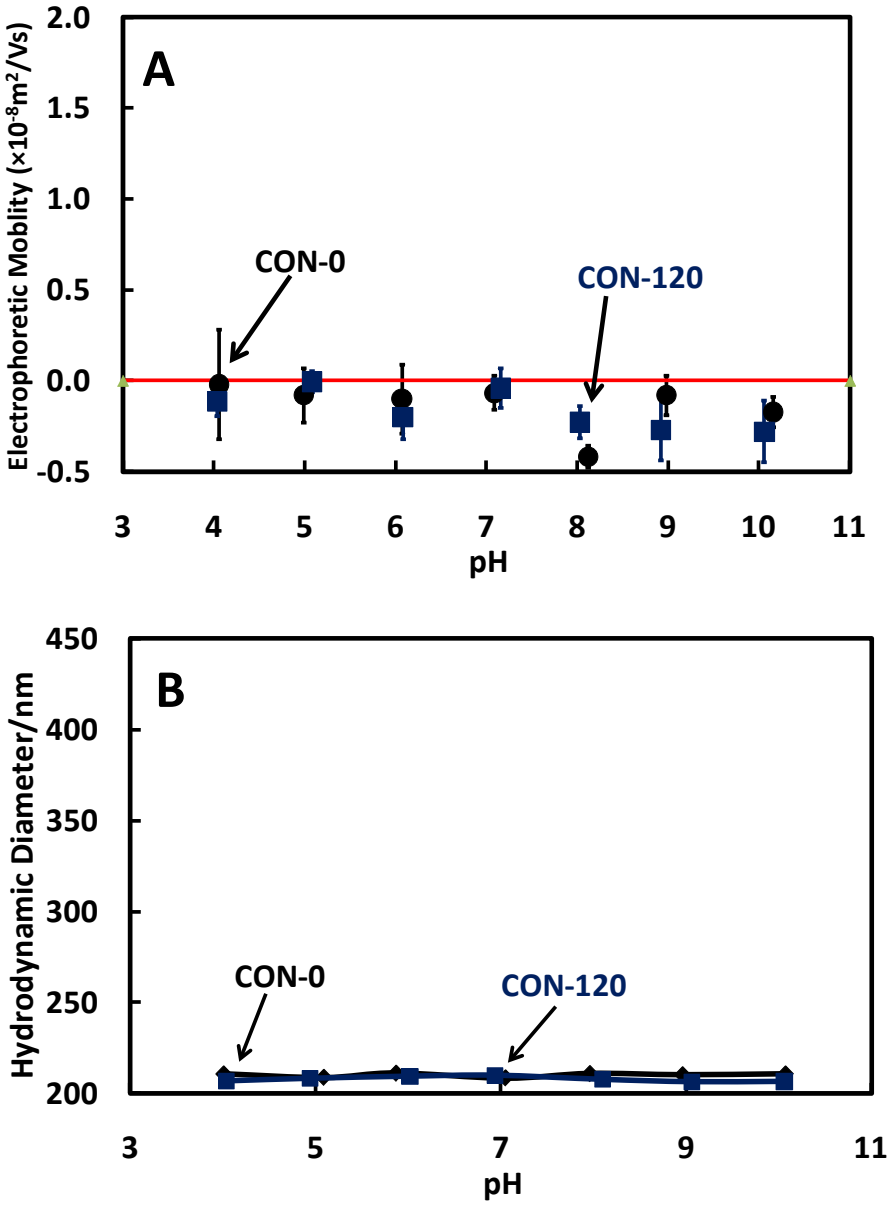

S2. pH effect on (A) mobility and (B) diameter of CON microgels before (CON-0) and after (CON-120) Hofmann rearrangement. The measurements were conducted in 1 mM NaCl. The scales of Y axis are adjusted in consistent with Figure 4A and Figure 4B, respectively.

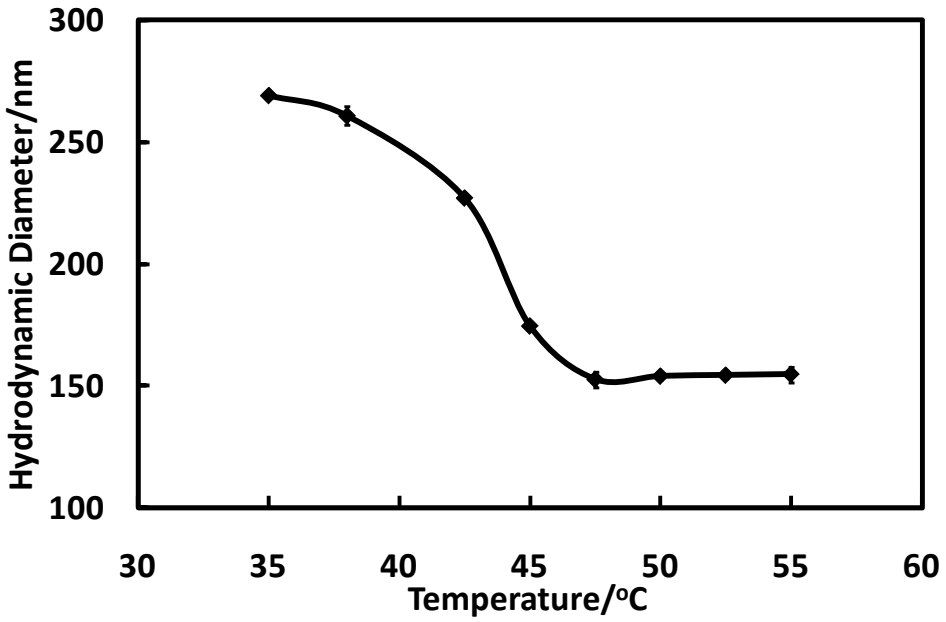

S3 Effect of temperature on diameter of PNIPMAM-EGDMA microgels

Chapter 6 Concluding Remarks

This work reveals a simple and facile pathway to functionalize PNIPAM/PNIPMAM microgels using bleach. The chlorinated PNIPAM microgels have potential application in anti-microbial and cancer therapy, while the primary amine-containing PNIPMAM microgels are a proper candidate as substrate for bio-conjugation. The major contributions of this work are given as follows:

1. Bleach-induced chlorination of PNIPAM was performed, resulting in a new copolymer. The chemical structure was determined as poly(NIPAM-co-NIPAMCl) via ^{1}H-NMR and mass spectrometry. A desirable pH range ($\geq$10) has been found to avoid chain scission during N-chlorination.

2. The phase transition temperature of PNIPAM was lowered after N-chlorination, which can be almost identical to the reaction temperature. The relationship between the phase transition temperature and chloride substitution was given, suggesting a simple method to control the extent of chlorination with temperature. A lowest CPT, corresponding to a 13% DS, was achieved at the reaction temperature of 15 ^{o}C.

3. The chlorinated PNIPAM can be reduced by reducing agents, such as $Na_2S_2O_3$ and KI. The reduced polymer had a phase transition temperature ~34 ^{o}C.

4. PNIPAM microgels crosslinked by EGDMA were chlorinated with the same method applied for linear PNIPAM. A mechanism was proposed to explain the change of microgel size and suspension turbidity during N-chlorination.

5. Both reaction temperature and salt concentration affect the phase transition temperature and the reaction extent of the resulted microgels. Either lower reaction temperature or lower salt concentration resulted in microgels with lower phase transition temperature and higher active chlorine content.

6. The reaction between chlorinated microgels and GSH was studied by DLS and turbidity measurements. The reaction was much faster at pH higher than 6, in comparison with the rate at pH 5 and 3. Upon reacting with insufficient GSH at pH 7, a core-shell structure was found for the resulting microgels, with reduced shells and chlorinated cores. Hence the reaction was proposed as diffusion controlled.

7. PNIPMAM microgels were observed to be fairly stable in alkaline bleach, in comparison with PNIPAM microgels. The active chlorine content in chlorinated PNIPMAM microgels was about one-tenth of the content in PNIPAM microgels under the same N-chlorination conditions.

8. Core-shell microgels with PNIPAM cores and Poly(NIPAM-co-NIPMAM) shells were prepared in a one-pot manner. The copolymer shells enhanced the colloidal stability even after N-chlorinated. The core-shell microgels with a core VPTT 20 ^{o}C were well dispersed in PBS buffer at 37 ^{o}C.

9. A simple method to prepare primary amine-containing PNIPMAM microgels was developed. The Hofmann rearrangement converted unsubstituted amides into primary amines in bleach at room temperature. This method can be easily applied to prepare amphoteric microgels with both carboxyls and primary amines.